Phase A Concept Study Report

Solar-B XRT

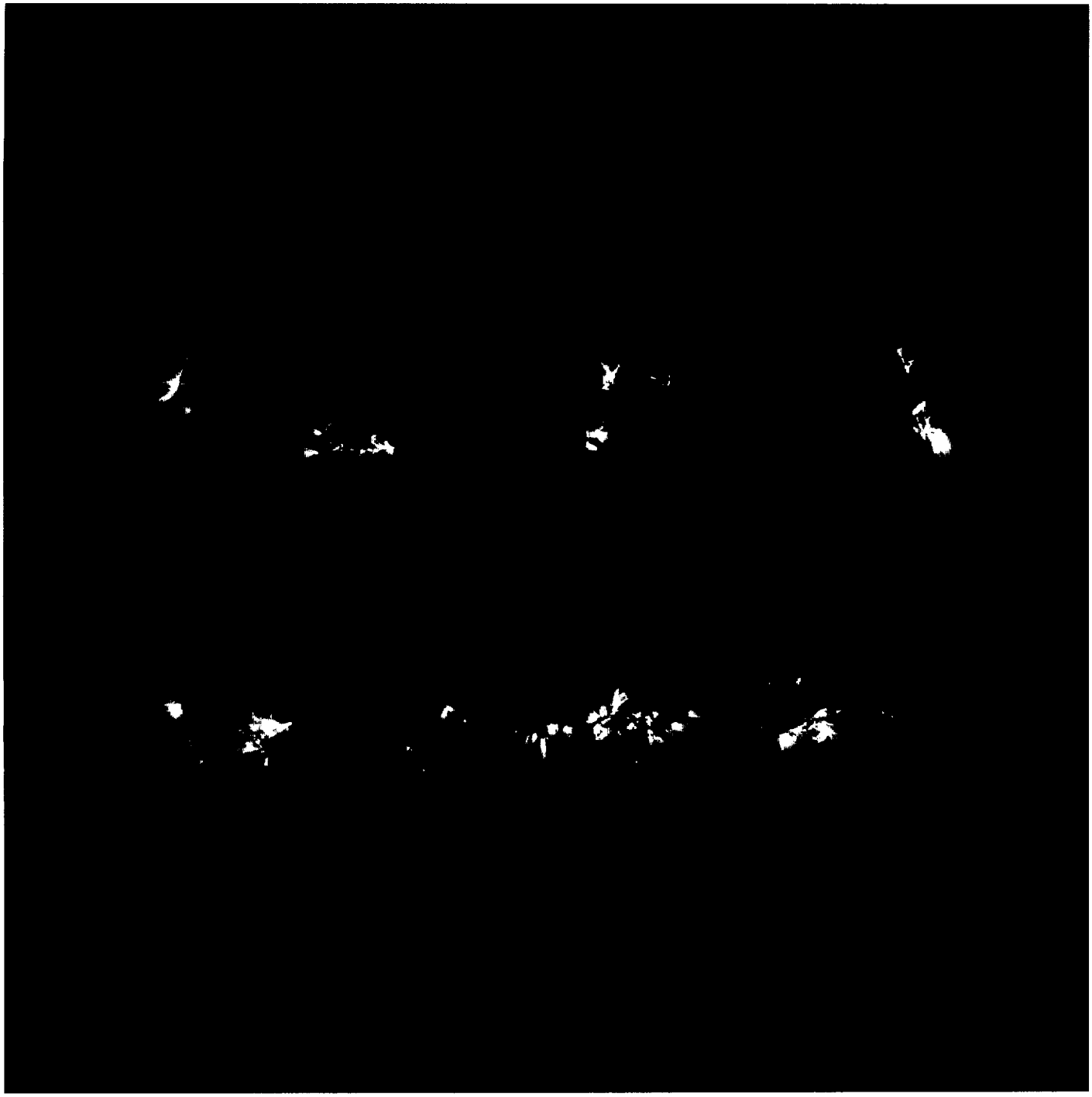

Smithsonian Astrophysical Observatory

REPORT DOCUMENTATION PAGE

Form Approved
OMB No. 0704-0188

1. AGENCY USE ONLY (*Leave blank*)	2. REPORT DATE	3. REPORT TYPE AND DATES COVERED
	October 29, 1999	Concept Study Report/ Phase A

4. TITLE AND SUBTITLE

Solar-B X-ray Telescope (XRT) Concept Study Report

5. FUNDING NUMBERS

NAS8-99099

6. AUTHOR(S)

Dr. Leon Golub

7. PERFORMING ORGANIZATION NAME(S) AND ADDRESS(ES)

Smithsonian Astrophysical Observatory
60 Garden Street, Cambridge MA 02138

8. PERFORMING ORGANIZATION REPORT NUMBER

XRT-PM-99-002

9. SPONSORING/MONITORING AGENCY NAME(S) AND ADDRESS(ES)

National Aeronautics and Space Administration
Marshall Space Flight Center, AL3 5812

10. SPONSORING/MONITORING AGENCY REPORT NUMBER

NASA/DRD 867MA-001

11. SUPPLEMENTARY NOTES

12a. DISTRIBUTION/AVAILABILITY STATEMENT

Unclassified-Unlimited
Subject Category Distribution: Standard or Nonstandard
Availability: NASA CASI (301) 621-0390

12b. DISTRIBUTION CODE

13. ABSTRACT (*Maximum 200 words*)

Phase A Concept Study Report (DRD No. 867MA-001) for the XRT Instrument on Solar-B.

14. SUBJECT TERMS

15. NUMBER OF PAGES
177

16. PRICE CODE

17. SECURITY CLASSIFICATION OF REPORT	18. SECURITY CLASSIFICATION OF THIS PAGE	19. SECURITY CLASSIFICATION OF ABSTRACT	20. LIMITATION OF ABSTRACT
Unclassified	Unclassified	Unclassified	

CONTENTS

Executive Summary 1

Table of Contents 2

Science Investigation 3

EPO/SDB Plan 4

Technical Approach 5

Data Requirements 6

Management Plan 7

Definition and Development 8

Cost Plan 9

Appendices 10

XRT Executive Summary

The X-ray observations from the Yohkoh SXT provided the greatest step forward in our understanding of the solar corona in nearly two decades. Expanding on the accomplishments of *Yohkoh,* we believe that the scientific objectives of the Solar-B mission are achieved with a significantly improved X-ray telescope (XRT) similar to the SXT. The Solar-B XRT will have twice the spatial resolution and a broader temperature response, while building on the knowledge gained from the successful *Yohkoh* mission. We present the scientific justification for this view, discuss the instrumental requirements that flow from the scientific objectives, and describe the instrumentation to meet these requirements. We then provide a detailed discussion of the design activities carried out during Phase A, noting the conclusions that were reached in terms of their implications for the detailed design activities which are now commencing. Details of the instrument that have changed as a result of the Phase A studied are specifically noted, and areas of concern going into Phase B are highlighted.

XRT is a grazing-incidence (GI) modified Wolter I X-ray telescope, of 35cm inner diameter and 2.7m focal length. The 2048x2048 back-illuminated CCD (now an ISAS responsibility) has 13.5 micron pixels, corresponding to 1.0 arcsec and giving full Sun field of view. This will be the highest resolution GI X-ray telescope ever flown for Solar coronal studies, and it has been designed specifically to observe both the high and low temperature coronal plasma. A small optical telescope provides visible light images for co-alignment with the Solar-B optical and EUV instruments.

The XRT science team is working in close cooperation with our Japanese colleagues in the design and construction of this instrument. All of the expertise and resources of the High Energy and Solar/Stellar Divisions of the Center for Astrophysics are being made available to this program, and our team will carry its full share of responsibility for mission operations, data reduction and education and public outreach.

All aspects of the XRT design were reviewed during Phase A. The study focussed particularly on those aspects that have the greatest affect on instrument performance and extended lifetime, on the image quality error budget, and on the camera (mechanical and electrical) interface and the instrument mounting interfaces.

The present instrument design differs in some details from that originally proposed. Selection of the XRT for Phase A study was contingent upon the removal of the camera and its associated electronics, and the acceptance of a stringent cost cap. The removal of the electronics left the XRT without control electronics for the instrument mechanisms. A mechanism controller was therefore added. The removal of the camera resulted in major complications to the integration and test plan. After many discussions, it was decided that the system would be less expensive, and the risk of unacceptable performance lower, if we include a focus mechanism. The remainder of the XRT design baseline matches the proposed configuration.

Data requirements for the XRT are driven by the science plans, which are based on the physical processes in the solar outer atmosphere. Discussions to date of the XRT observing plan, both alone and in conjunction with the other Solar-B instruments, shows that the XRT needs 2 Gbits of on-board storage, at least one circulating buffer of 640 Mbits, and twelve 10-minute downlinks per day in order to carry out its required programs.

Table of Contents

Executive Summary	
Table of Contents	
Science Investigation	1
EPO/SDB Plan	19
Technical Approach	25
Data Requirements	105
Management Plan	108
Definition and Development	119
Cost Plan	122
Appendices	127

TABLE OF CONTENTS: SCIENCE INVESTIGATION

1 SCIENCE INVESTIGATION 2

1.1 CORONAL HEATING 4
1.2 THE NANOFLARE MODEL 5
1.3 SPECIFIC OBJECTIVES 6
1.3.1 Flares & CMEs *6*
1.3.2 Coronal Shock Waves. *8*
1.3.3 Flare and CME Energetics. *9*
1.3.4 Global-Scale Reconnection and the Solar Dynamo *9*
1.3.5 Coordination with the OT& EIS. *10*
1.3.6 Magnetic Field Models & Coronal Structure. *11*
1.3.7 Specific Program *12*
1.4 COALIGNMENT OF X-RAY TO OPTICAL. 12
1.5 FLOW-DOWN SCIENCE REQUIREMENTS 12
1.5.1 Level 1 Science Requirements *13*

1 SCIENCE INVESTIGATION

The X-ray observations from the *Yohkoh* satellite, a small ISAS spacecraft launched in August 1991, provided the greatest step forward in our understanding of the solar corona in nearly two decades. *Yohkoh* was conceived as a flare mission, but also proved capable of pioneering observations of the active non-flare corona. Among the major advances brought about by *Yohkoh* SXT data is the observation of dynamic structures which appear to be caused by MHD instabilities and by reconnection of magnetic fields in the corona.

However, the SXT observations have also raised unexpected difficulties to understanding the causes of variability and dynamics in the solar atmosphere. The corona is seen to consist of two fundamental components: high-temperature (5--10 MK) transient sources (Shimizu & Tsuneta, 1997) and low-temperature (1--5 MK) persistent sources (Kano, 1997). The transient components have clear loop or cusp structures, while the persistent components have unresolved structures. There is essentially no correlation between the X-ray intensity and the derived temperature (Yoshida *et al.* 1995, Yoshida & Tsuneta 1996), with high temperature material also observed well outside of active regions, in the "quiet corona."

An X-ray telescope for Solar-B needs to have a wide temperature sensitivity that covers all of these component structures in order to understand the coronal heating problem, but must also maintain temperature discrimination capability in order to differentiate the components. X-ray loops are seen to vary on a wide range of time scales. Transient brightenings with durations of a few minutes have been observed in active regions (Shimizu *et al.* 1992). These brightenings show a great variety in X-ray morphology, often involving multiple loops (Shimizu *et al.* 1994). Short-timescale variability of emission is seen almost everywhere in the active-region corona (Sheeley & Golub 1979), and this variability is believed to be a manifestation of coronal heating by numerous nanoflare events (Shimizu & Tsuneta 1997). Falconer *et al.* (1997) examined the magnetic structures underlying the cores of active regions and found that persistent bright coronal features are rooted in strongly sheared magnetic fields near the polarity inversion line. This suggests that the heating may be due to low-lying reconnection accompanying flux cancellation at the inversion line.

The basic goals of a soft X-ray telescope (XRT) for the Solar-B mission are to facilitate the study of the dynamics of fine scale coronal phenomena, such as magnetic reconnection and coronal heating mechanisms, while at the same time recording the large scale global phenomena, such as coronal mass ejections. In order to meet these objectives, the XRT will work closely with the focal plane instruments of the optical telescope (OT) and with the EUV imaging spectrometer (EIS). The XRT on Solar-B is expected to observe and quantify the coronal response to changes in the photospheric magnetic flux. These range from splitting and rearrangement of the intergranular flux elements leading to tangential discontinuities and energy dissipation in the corona, to large-scale magnetic shear leading to global magnetic field rearrangements. These objectives imply that the instrument used must be capable of observing the fairly low-T

(<3 MK) pre-event plasma, as well as the higher-T (>5 MK) heated or activated plasma and of coordinating those observations with data from the Solar-B OT and EIS.

The U.S. and Japanese Solar-B science teams have identified key problem areas to be addressed by this mission. Among those in which the XRT plays a major role are:

1. *Flares & Coronal mass ejections.* How are they triggered, and what is their relation to the numerous small eruptions of active region loops? What is the relationship between large-scale instabilities and the dynamics of the small-scale magnetic field?

2. *Coronal heating mechanisms.* How do coronal loops brighten? *TRACE* has observed loop oscillations associated with flares (Nakariakov *et al.* 1999). Are other wave motions visible? Are they correlated with heating? Do loops heat from their footpoints upward, or from a thin heating thread outward? Do loop-loop interactions contribute to the heating?

3. *Reconnection & coronal dynamics. Yohkoh* observations of giant arches, jets, kinked and twisted flux tubes, and microflares imply that reconnection plays a significant role in coronal dynamics. With higher spatial resolution and with improved temperature response, the XRT will help clarify the role of reconnection in the corona.

4. *Solar flare energetics.* Although Solar-B will fly after the next solar maximum, there will still be many flare events seen. The XRT is designed so that it can test the reconnection hypothesis that has emerged from the *Yohkoh* data analysis.

5. *Photosphere/corona coupling.* Can a direct connection be established between events in the photosphere and a coronal response? To what extent is coronal fine structure determined at the photosphere?

The *Yohkoh* analysis and new results from *SOHO* and *TRACE* have clarified the directions in which solutions to the dual problems of structure and stability of the corona may be found, and indicate the types of observations which need to be made in order to address these problems. The corona is found to be highly non-uniform in spatial structure, in temperature structure and also as a function of time (Tsuneta, 1998). There are a number of conclusions arising out of this work which have implications for the type and design of XRT to be flown on Solar-B:

1. The corona is structured on small scales perpendicular to B, and on large scales along the field. This means that observations must be made with both high spatial resolution and a large field of view.

2. The corona is highly variable on very short timescales. Observations must therefore be made with short exposure times and with a high cadence rate.

3. The corona is multi-thermal, meaning that different structures are seen at only slightly different temperatures, i.e., a small change in temperature sensitivity can lead to a large change in what is observed. Observations must be made over a wide range of

temperatures (1-10 MK) with good temperature discrimination, and especially with the ability to detect coronal plasma at about 4-6 MK, where the peak of the differential emission measure distribution is located (e.g. Brosius *et al.* 1994).

4. CMEs have an identifiable on-disk soft X-ray signature (Hudson & Webb 1997), and events seen in the outer corona can now be traced to an origin on the disk (Thompson *et al.* 1997). It is therefore possible that, with higher spatial resolution, large field of view and higher data cadence, the initiation of these events can finally be studied.

In response to these requirements, we are building a full-Sun grazing-incidence X-ray telescope (XRT) designed to address the questions raised by the *Yohkoh*, *SOHO* and *TRACE* observations. In this section we discuss the scientific objectives of the Solar-B XRT, the ways in which the scientific requirements lead to the need for specific observations, and the manner in which the XRT will address these objectives.

1.1 Coronal Heating

Few problems in astrophysics have proved as resistant to solution as the coronal heating problem. Observational constraints on wave fluxes (based on line broadening measurements) have for all practical purposes completely eliminated the classical acoustic wave heating models. Theoretical models have focussed in recent years instead on the various ways in which energy may be transported to the corona, and there dissipated, through the mediation of magnetic fields. Virtually without exception, these models have in common the feature that the actual dissipation of energy transported to the corona occurs in spatially highly localized regions, although there may be either a few or many such regions distributed throughout a typical coronal loop.

The interaction between the magnetic fields and the fluid at the photospheric level causes two classes of disturbance, depending on whether the driving timescale is longer than the Alfvén transit time across a coronal structure (the DC models) or shorter (AC models):

1. Periodic motions of flux tubes generate MHD waves which propagate upward and may dissipate their energy in the corona. The dissipation is likely to involve phase-mixing: the development of fine-scale structure in the wave's velocity field due to density and/or magnetic-field inhomogeneities (Heyvaerts & Priest, 1983; Davila, 1987; Hollweg, 1987; Similon & Sudan, 1989).

2. The random walk of flux tubes produces DC field-aligned electric currents, which may dissipate resistively; this applies only to "closed" structures in which magnetic stresses are able to build up over time Parker (1972, 1983) proposed that the random footpoint motions lead naturally to the formation of "tangential discontinuities," which correspond to thin current sheets; van Ballegooijen (1985, 1986) described this process in terms of a cascade of magnetic energy to small spatial scales. The current sheets may be distributed more or less randomly within the corona, or may be preferentially located at the interfaces between the flux tubes (Démoulin & Priest 1997).

The new data from the *TRACE* satellite (Tarbell *et al.* 1994) show directly that there is structure present in the corona at 1 arcsec resolution (Fig1.1). In particular, we see fine "threads" of hot plasma in the cooler lines, such as Fe IX/X and Fe XII, but not in Fe XV. Although the explanation for this is not clear, it is apparent that the proposed emphasis on cooler material in Solar-B is appropriate at this resolution.

Priest *et al.* (1997) used *Yohkoh* SXT observations to determine the temperature profile along a large loop. Comparison with models shows that a heating function localized either near the footpoints or near the apex does not fit the observations well, whereas a uniform heating function provides a better fit (Fig.1.2). The model has been extended to analysis of a loop arcade (Priest 1997), showing that a constant heat flux for all loops does not provide a good fit, whereas a heat flux varying with B^2 does. In order to extend the range of applicability of such models, we require observations that can better isolate coronal structures, and that can also observe them with lower errors over a broader range of temperatures.

1.2 The Nanoflare Model

Observations of rapid hard X-ray fluctuations (Lin *et al.* 1984) and variable emissions from the chromosphere-corona transition region (Porter, Toomre & Gebbie 1984) have led to the suggestion that the corona is heated by nanoflares: small-scale reconnection events which release part of the magnetic free energy stored in a coronal loop (Parker 1988; Sturrock *et al.* 1990; Zirker & Cleveland 1993a; Cargill 1994; Cargill & Klimchuk 1997). The energy release likely occurs as an avalanche of such reconnection events (Lu & Hamilton 1991; Zirker & Cleveland 1993b). For the nanoflares to be energetically important they must be more frequent than predicted by extrapolation of the observed flare energy distribution (Hudson 1991; Shimizu & Tsuneta 1997).

The dynamical response of a coronal flux tube to impulsive nonoflare heating has been studied by a number of authors (e.g., Doschek *et al.* 1982; Mariska 1988; Serio *et al.* 1991; Kopp & Polleto 1993; Cargill, Mariska & Antiochos 1994). After the initial heating phase, the plasma is extremely hot ($T > 10^7$ K) but not very dense. Electron thermal conduction causes "evaporation" of chromospheric plasma, leading to a gradual increase of coronal n_e and decrease of T at the loop top. The n_e increase continues until T drops to a few MK, at which point radiative losses become important and the coronal n_e reaches a maximum. Further cooling causes mass to drain out of the tube and return to the chromosphere. Each such heating and cooling cycle requires some tens of minutes (Cargill 1994).

Cargill & Klimchuk (1997) have used nanoflare models to interpret observations of active region loops obtained with the *Yohkoh* SXT. They have found that for hot loops (T> 4 MK) small filling factors can fit the data (f < 0.1), although for cooler loops T ~2 MK) the nanoflare model cannot reproduce the observed temperature and emission measure for any value of the filling factor (also see Porter & Klimchuk 1995). Judge et al (1997) have studied the correlation between density sensitive line ratios and Doppler shifts of O^{+4} emission lines seen with SUMER on *SOHO*. If it is assumed that the observed correlations are due to wave motions, then they are consistent with downward

propagating compressive waves. Detailed models by Wikstol et al (1997) show that such waves are a natural result of nanoflare heating.

1.3 Specific Objectives

We will combine XRT, FPP and EIS data to study how coronal loops are heated. Specifically, we will determine the emission measure EM(T) as a function of time and position, determine the small-scale structure within the loops, and correlate the observations with magnetic structures seen in the photosphere. Some of the key questions are:

1. What is the emission measure EM(T) of coronal loops in the temperature range 1--10 MK on a spatial scale of a few arcsec?

2. How does the EM distribution vary with position along the loop? What is the nature of the pressure gradients found by Kano & Tsuneta (1996), and what do they imply about the heating mechanism?

3. How do coronal loops evolve in time? How does EM(T,s,t) evolve as a function of temperature, position and time? Can we confirm that mass is injected by chromospheric evaporation?

4. Can we obtain better observations of the fine structures and temporal variations associated with nanoflare heating? The variations in coronal T and in coronal n_e should have observable effects on the T and EM distributions at 1" resolution, which should be detectable by XRT.

5. Is there a relationship between coronal heating events and spicules seen in the chromosphere (e.g. Suematsu *et al.* 1995)? Spicules may be a chromospheric response to nanoflares in the corona (e.g. Porter *et al.* 1987; Sterling *et al.* 1991); coordinated observations of the XRT, EIS and optical instruments will determine whether such a relationship exists.

6. Can we detect MHD waves in coronal loops? At high cadence we will search for intensity fluctuations associated with compressional waves, and for undulation of fine threads associated with transverse waves.

1.3.1 Flares & CMEs

Traditionally, there are three different types of large-scale eruptive phenomena occurring in the solar atmosphere, namely coronal mass ejections (CMEs), prominence eruptions, and large two-ribbon flares. It has become increasingly clear with time that these phenomena are closely related and may, in fact, be different manifestations of a single physical process. The opening of the field lines in the active region by the CME leads to the formation of flare ribbons and loops, appear to move through the chromosphere and corona, and these motions provide some of the best evidence for magnetic reconnection in the solar atmosphere. Doppler-shift measurements show that the motions of the flare

loops and ribbons are not due to mass motions but rather to the upward propagation of an energy source in the corona, as required by the reclosing of open field lines by reconnection (e.g., Schmieder *et al.* 1987).

Figure~1.3 is a diagram showing one proposal for how reconnection occurs during the gradual phase of large flares and CMEs. It is based on Carmichael (1964), Sturrock (1968), Hirayama (1974), and Kopp & Pneuman (1976); on simulations of magnetic reconnection (e.g. Forbes & Malherbe 1991); evaporation (Nagai 1980, Cheng 1983, Doschek *et al.*. 1983, Fisher *et al.*1985, Yokoyama & Shibata 1998); and condensation (Antiochos & Sturrock 1982).

According to this scenario, flare loops are created by chromospheric evaporation on field lines mapping to slow-mode shocks in the vicinity of a neutral line. Conduction of heat along the field lines causes them to dissociate into isothermal shocks and conduction fronts as shown in the figure. The shocks annihilate the magnetic field in the plasma flowing through them, and the thermal energy which is thus liberated is conducted along the field to the chromosphere. This in turn drives an upward flow of dense, heated plasma back towards the shocks, and compresses the lower regions of the chromosphere downward. Figure 1.4 is a 4-panel view of a flare observed by *TRACE*, which exhibits the type of behavior predicted by such models.

Until the advent of *Yohkoh*, virtually all of the evidence for reconnection on the Sun was indirect. However, the high resolution and sensitivity of the *Yohkoh* SXT made it possible to see the reconnection region directly for the first time. The detection of a cusp-type geometry at the top of flare loops along with the detection of a nonthermal X-ray source in the same region now provides some of the best evidence that a reconnection site does actually occur in the corona.

To determine whether the reconnection process occurs in the manner proposed in Fig.1.3, one must observe the changes in shape of reconnected field lines with time. Because flare plasma on reconnected field lines undergoes an enormous temperature variation from 10^7 K to 10^4 K, no single instrument has been able to track continuously the plasma as it cools. For example, Figure 1.4 shows only the plasma at 1MK and at 10 MK but not in between. The XRT will make a major advance by observing at arcsecond resolution the cooling of the X-ray loops down to a temperature of 10^5 K, an order of magnitude better than achieved by the *Yohkoh* SXT.

Using Coronal Dimming to Measure the Magnetic Reconnection Rate: both the EIT on *SOHO* and the SXT on *Yohkoh* (Hudson & Webb 1997; Hiei & Hundhausen 1997; see also Rust 1983) have observed coronal dimming events at disk center which are caused by CMEs. The dimming is produced directly by the removal of hot coronal plasma by the CME, forming a transient coronal hole. The hole appears in about ten minutes, but it typically takes at least a day to disappear.

The size of the transient hole is a direct indicator of opening of the magnetic field by the CME. As the CME moves outwards into space, it drags the field with it. However, the photospheric footpoints of individual field lines remain attached to the Sun, so that field

lines which connect the photosphere to interplanetary space are created. Almost as soon as they are formed, these "open" field lines start to reclose by means of magnetic reconnection, and as they do so, the area of the hole diminishes. By using combined X-ray and magnetogram observations one can quantitatively determine the rate at which the open magnetic flux is converted into closed flux. With the resolution that will be available from Solar-B, it should be possible to make the most accurate measurements of the rate of reconnection ever achieved outside of a laboratory plasma, thereby providing a stringent test of the various theories of reconnection that have been proposed.

Careful tracking of the boundaries of transient coronal holes will also provide new information about the eventual fate of CMEs in the interplanetary medium. Observations of streaming electrons by the Ulysses spacecraft at 5 AU imply that even 10 days after leaving the Sun, a sizable fraction of the field lines within a CME (or magnetic cloud as it is normally referred to when observed by a spacecraft) are still connected to the photosphere (Gosling 1997). Comparing the amount of flux observed by spacecraft with estimates of the amount of flux opened by an erupting CME, Lepping (1997) infers that about 10--15 % of the area of a transient hole remains open for at least 10 days. Whether in fact this is the case is unknown because the error in existing measurements of coronal hole areas is ~20% (Webb & Cliver 1995). With the high resolution images from the Solar-B XRT it will be possible to reduce the error in the measurement of the area by more than an order of magnitude, and thus determine whether or not a small portion of a transient coronal hole remains open for a relatively long time.

1.3.2 Coronal Shock Waves.

There is still considerable debate about the number, origin, and structure of shock waves produced by coronal mass ejections (CMEs). In interplanetary space, only a single, fast-mode shock wave is seen in front of the ejecta (magnetic cloud) thrown out by the CME, but when and where this shock originates is not yet known with any precision. Indirect evidence for the existence of shock waves in the lower corona is provided by ground and space observations of Moreton waves and radio observations of metric type-II bursts, but it is far from clear whether these shocks are the same as those seen in interplanetary space (Cane 1984, Cliver & Kahler 1991).

The improved resolution and sensitivity of the XRT will allow better detection of coronal shock waves. In fact, the XRT should be able to observe directly the 3-D structure of shock waves as they propagate through the corona. A Mach 2 fast-mode shock propagating across the magnetic field increases the plasma density by a factor of ~2 and the temperature by a factor of ~80 (for a plasma $\beta = 0.01$), but immediately behind this heated region lies a rarefaction wave which progressively reduces both n_e and T with increasing distance from the shock. Thus, the combined shock-rarefaction wave has a unique density-temperature signature which the XRT will be able to detect with a sensitivity and resolution that has not heretofore been possible.

These observations will help resolve three long-standing scientific issues. First, determining the precise region in the corona where the shock originates will tell us the location, and extent of the driving force of a CME. For example, if the shock originates

from a volume which is larger than any active region or prominence, then we will know that the $\mathbf{j}\times\mathbf{B}$ forces which drives an eruption is not created by a local magnetic instability within the active region or the prominence. Second, knowing the shock strength as a function of its location in the corona can help determine whether the proposed relation between CME shocks and prompt (< 30 min) energetic particles (> 1 Mev) by (Reames 1990) is correct. Finally, if interplanetary shocks are distinct from the shock waves generated near the surface, then the XRT should be able to detect signs that such multiple shocks actually exist and determine when and where they are created and dissipated relative to one another.

1.3.3 Flare and CME Energetics.

Most models for eruptive flares and coronal mass ejections are based on the principle that the energy which drives them comes from magnetic energy stored in coronal currents (Svestka and Cliver 1992). The currents may form when a flux-tube emerges from the convection zone or when the footpoints of a pre-existing arcade are sheared. Since magnetic helicity is a well preserved quantity in the corona (see Berger and Field 1984 or Taylor 1986), only part of the stored magnetic energy can be released during a confined flare. Large eruptive events can remove helicity from the corona by ejecting flux ropes (see e.g. Low 1996), but this mechanism of helicity shedding is severely constrained by the fact that in a magnetically dominated medium the fully open field has maximum energy. Consequently, the field cannot be opened by an MHD instability, ideal or otherwise.

However, it has been shown recently that a partially open state can be reached by imposing photospheric stressing motions on a bipolar field (e.g. Amari *et al.* 1996). Therefore, to understand the energetics of flares and CMEs, it is necessary to observationally determine the fraction of the field which is opened during the event. Combining this information with measurements of the vector magnetic will establish the relation between the partially opened field and the region where currents are stored. The XRT is ideally suited to perform such studies, not only because of its sensitivity to high-temperature plasmas, full disk coverage, and capability to perform high-cadence observations, but also because Solar-B will also have an extremely accurate vector magnetograph. Thus, we expect the XRT to provide new observational constraints on theoretical models of the eruptive mechanism for CMEs.

1.3.4 Global-Scale Reconnection and the Solar Dynamo

Observations of active regions with *Yohkoh* SXT often show S or inverse-S shaped structures (Acton *et al.* 1992) which are due to large scale twist or shear of the active-region magnetic field. These structures exhibit a clear hemispheric pattern: active regions in the southern hemisphere predominantly have S-shaped structures, while those in the North have inverse-S shapes (Rust & Kumar 1996). This hemispheric pattern has also been found in the latitude distribution of α, the force-free field parameter $\nabla\times\mathbf{B} = \alpha\mathbf{B}$ as derived from photospheric vector magnetograms (Pevtsov, Canfield & Metcalf 1995; Pevtsov, Canfield & McClymont 1997). Similar patterns in chirality (handedness) of magnetic structures have been found for filament channels, quiescent filaments, sunspots

whorls, coronal arcades, and interplanetary clouds associated with CMEs (see review by Zirker *et al.* 1997). Recently, Canfield & Pevtsov (1998) found a correlation between α and the tilt angle τ of the active region axis with respect to the solar equator. While the origin of these global patterns is not well understood, it is clear that the electric currents responsible for sinuous active-region structures originate deep below the photosphere.

The proposed full-disk XRT will be ideally suited to perform synoptic studies of S and inverse-S shaped structures in a large number of active regions. The key question is: What is the origin of these twisted structures? Are these toroidal flux tubes themselves twisted, or do the twists arise during the ascent of the Ω loops through the convection zone? We hope to answer this question by studying the relationships between location, tilt and twist of active-regions loops. Detailed studies of changes in the large scale connectivity of coronal loops will show how the helicity concentrated in the active regions is dissipated in the corona. Is the loss of helicity always associated with eruptive events? Is reconnection across the equator important late in the solar cycle?

1.3.5 Coordination with the OT& EIS.

The photosphere and corona have generally been regarded very much as being independent entities that have been studied separately from one another. However it is now realized that they are closely coupled and that most of the subtle and nonlinear structure and dynamic behavior of the corona is a direct response to what is happening in the solar surface. The coronal magnetic field is anchored in the (as yet unresolved) intense magnetic flux tubes at the edges of granule and supergranule cells in the photosphere. Moreover, the interaction of coronal magnetic fields is directly driven by motions of the photospheric footpoints.

Observations of the corona with the NIXT and *TRACE* telescopes have revealed the fine structure and interactions of coronal magnetic fields in unprecedented detail. But corresponding simultaneous observations at the required resolution in the photosphere have been lacking, either due to inadequate spatial resolution or because the data were taken many hours before or after the coronal events. Solar-B will remedy this deficiency in spectacular fashion. Its unique feature is to be able to combine high resolution in space and time in both the photosphere and corona. In addition, the X-ray observations will provide the crucial information that is missing from the photospheric data alone: the connectivity (or lack thereof) between magnetic elements seen at the surface.

To design an XRT for joint studies between the X-ray and the optical, we must determine what resolution is needed in the corona given the 0.2 arcsec resolution in the optical. It is not necessary for the X-ray resolution to match that of the optical, since the photospheric magnetic field expands as it extends upward into the corona. Coronal heating may occur predominantly at the interfaces between the flux tubes (''tangential discontinuities"), in which case the expected separation of coronal structures is determined by the spacing of the flux tubes, not their size in the photosphere (Fig.~1.5). In plage regions this spacing is of order the diameter of granules (1--2 arcsec), and in quiet regions it is larger. Thus a pixel size of ~1 arcsec will generally be adequate to isolate and identify the coronal

structures which connect to photospheric magnetic structures. Recent studies from *TRACE* and LaPalma (Berger *et al.* 1999) support this view.

1.3.6 Magnetic Field Models & Coronal Structure.

Despite its fundamental importance for coronal physics, the magnetic field is difficult to measure in the corona and we must rely on numerical computations of the field using the observed photospheric field as a boundary condition. These extrapolations require a knowledge of the physical laws governing the coronal magnetic field. There have recently been several advances in this domain and applications to photospheric vector magnetograms have begun (see e.g. Amari *et al.* 1997 and McClymont *et al.* 1997). Complementary, but indirect, information on the magnetic field comes from loops seen in soft X-rays. The confrontation of the deduced magnetic field with the plasma observations permits progress to be made in understanding the physical processes involved.

A first step in this direction has been realized by using magnetograms obtained at various terrestrial observatories (Hawaii, Marshall, Potsdam, Kitt Peak). The topology of the magnetic configuration has been compared to observable manifestations of flares. In particular, Hα (or UV) flare brightenings have been found located at the intersections of quasi-separatrix layers (QSLs) and the brightenings are connected by magnetic field lines (Démoulin *et al.* 1997 and references therein). The notion of QSLs comes from recent developments of 3-D reconnection theory. QSLs are the generalization of separatrices to magnetic configurations with a non-zero magnetic field strength everywhere in a region (Priest & Démoulin 1995). Some flares observed by *Yohkoh* have also been studied in the same spirit (e.g. Mandrini *et al.* 1996, Schmieder *et al.* 1997). Two sets of soft X-ray loops have been identified as the reconnected loops, the flares being induced by the emergence of a magnetic bipole (identified in the magnetograms, and in Hα as an arch filament system). These results confirm that flares are coronal events where the release of free magnetic energy is due to reconnection localized in the regions where the magnetic field-line linkage changes drastically.

One difficulty encountered in previous studies is the precise co-alignment between the observations from different instruments. This limits our ability to cross-correlate the computed magnetic configurations with observed X-ray loops and determine where the energy is stored: in current sheets or in volume currents? Thus, a visible-light capability is needed as part of the XRT.

Another difficulty in interpreting existing flare observations is limited spatial resolution, which can lead to incorrect results even for large events. For example, in the flare studied by Schmieder *et al.* (1997), the *Yohkoh* soft X-rays are globally loop-shaped above the photospheric inversion line (of the magnetic field). This may lead to an interpretation as a one-loop flare process. In fact, with the help of the magnetic computations, it has been shown that the loop-shaped X-ray emission region was formed by several smaller loops in a nearly orthogonal direction, together with another set of long loops filled by X-ray emitting plasma only at their bottom. This completely changed our understanding of the

physical processes. We clearly need higher spatial resolution than that achievable with *Yohkoh* SXT while keeping the information on the large scales.

1.3.7 ***Specific Program.***

We propose to construct three-dimensional models of the coronal magnetic field by combining extrapolation of photospheric vector magnetograms obtained with the optical instruments on Solar-B, and comparison with observed coronal X-ray structures. The goal of this modeling is to understand how much free magnetic energy and helicity are stored in the corona. Strong magnetic shear is usually localized, so that high spatial resolution is needed to perform such studies (both in the optical and in X-rays). However, coronal magnetic structures are often connected over large distances, hence it is important to use observations with as large a field of view as possible. Using the full-disk images from XRT, we will be able to *TRACE* connections between distant regions and determine their contributions to the global helicity and energy budgets. Such coordinated studies using optical and X-ray data could drastically change our view of the processes that produce solar flares, filaments eruptions and coronal mass ejections.

1.4 Coalignment of X-ray to Optical.

Both grazing-incidence (GI) and normal-incidence (NI) X-ray telescopes will reflect visible light and may therefore be used to form a white light (WL) image, if light-blocking filters are not used to prevent this. The quality of the WL image is generally limited by diffraction. For a NI telescope such as the EIT or *TRACE*, this limit is of order 1-3" in the blue, and can thus be used to image sunspots and is almost adequate for observing granulation. For a GI telescope the situation is more complicated, since the entrance aperture is a narrow annulus; the diffraction limit is typically ½' in the narrow direction and ~1" along the opening. In this case, it is necessary to evaluate the accutance (sharpness) of the image as well as the resolution to determine how well it may be used for coalignment.

1.5 Flow-Down Science Requirements

Table 1.5.1 lists the scientific requirements derived from the above discussion, as it applies to Solar-B, and to the XRT in particular. All of the science objectives have instrumental requirements, as shown; each requirement has a scientific objective that produces the tightest requirement, as indicated by bold type in the last column. The specific flow down from this analysis are shown in Table 1.5.3.

1.5.1 Level 1 Science Requirements

Topic	Definition/Questions	General Instrument Impact (System drivers are boldfaced)
Coronal Mass Ejections	1. How are they triggered? 2. What is their relation to the magnetic structures? 3. What is the relation between large scale instabilities and the dynamics of small structures?	High time resolution High spatial resolution **Large FOV** Broad temperature coverage
Coronal Heating	1.How do coronal structures brighten? 2.What are the wave contributions? 3. Do loop-loop interactions cause heating?	High time resolution **High spatial resolution** Large FOV Broad temperature coverage
Reconnection And Jets	1. Where and how does reconnection occur? 2. What are the relations to the local magnetic field?	High time resolution High spatial resolution **Broad temperature coverage** Co-ordinated observing EIS/SOT
Flare Energetics	1. Where and how do flares occur? 2. What are the relations to the local magnetic field?	High time resolution High spatial resolution Large FOV Broad temperature coverage **High temperature response, Large dynamic range**

1.5.1 Level 1 Science Requirements Continued		
Photospheric-Coronal Coupling	1. Can a direct connection between coronal and photospheric events be established? 2. How is energy transferred to the corona 3. Does the photosphere determine coronal fine structure?	High time resolution High spatial resolution Large FOV Broad temperature coverage **Co-ordinated observing with SOT/EIS**

1.5.2 Other Level 1 Requirements

Item	Description	Value
Instrument Lifetime	Perform throughout the nominal Solar-B mission life	3 years
Instrument Weight		30 kg
Instrument Power		20 W (TBR)
Support SOT/EIS	Coordinated Observing capability	S/W timing and coordination

1.5.3 XRT Requirements Flowdown					
Requirement	**Definition**	**Value**	**Primary Hardware**	**Determining Factor**	**Resp.**
Exposure time	shutter open time (min)	4ms	Shutter	Flare brightness	SAO
	(max)	10sec		Quiescent corona	
Cadence	time between exposures	2 sec (reduced FOV)	Shutter/ MDP	Flare variability	SAO/ISAS
T-range	limits of temperature coverage	$6.1 < \log T < 7.5$	Coatings	coronal DEM	SAO
T-resolution	Temperature discrimination	$\log T = 0.2$	F.P. Filters	transverse gradients	SAO
X-ray image resolution	50% encircled energy	2 arcsec	G.I. Mirror	moss size scales	SAO
Field of View	angular coverage of telescope	> 30 arcmin	G.I. Mirror	global variations	SAO
White Light Rejection	reduction of solar visible light at focal plane	$>10^{11}$	Filters	Lx/Lopt ratio	SAO
Data Rate	Maximum bit rate out of XRT	2.4 MB/sec	MDP	Flare mode observations	ISAS
Data Volume	Maximum daily data volume	60 MB/orbit	MDP	CME mode observations	ISAS
Spatial Co-alignment (X-ray to WL)	Align Xray to white light images	1 XRT pixel	Mirror Assy	CCD	SAO
Spatial Co-alignment (X-ray to SOT or EIS)	Align Xray to white light images	1 XRT pixel	Structures	CCD	ISAS/SAO
Coordinated Observing	Image start time coordination	0.1 second	MDP	Solar Variations	ISAS/SAO

Figure 1.1

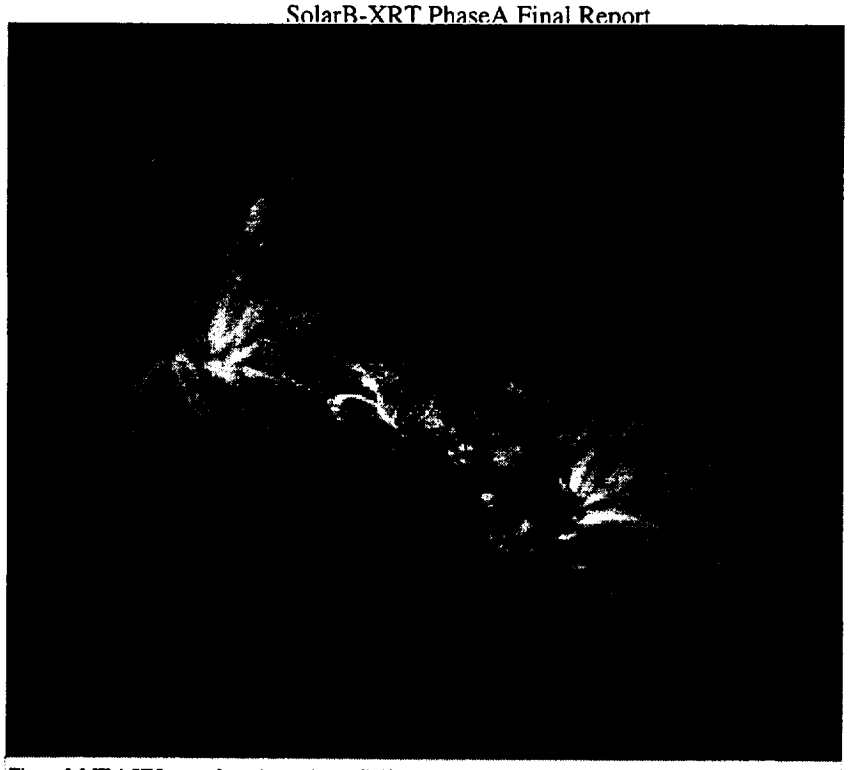

Figure 1.1 TRACE Image of an active region in Fe IX/X, 19May1998

Figure 1.2

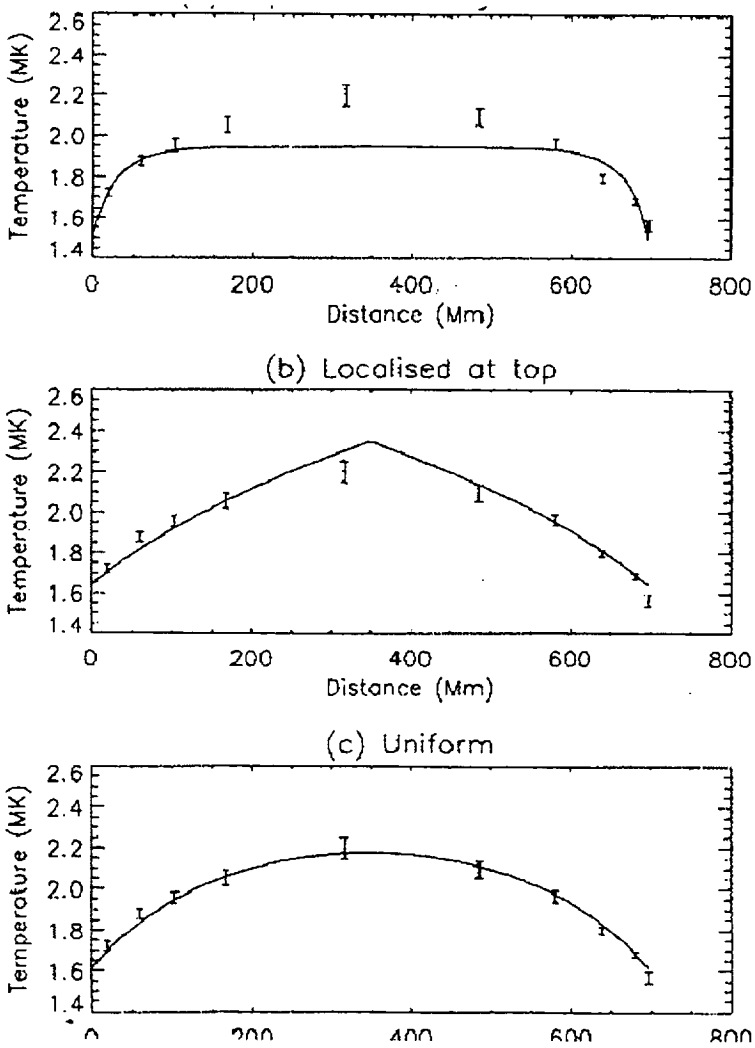

Figure 1.3

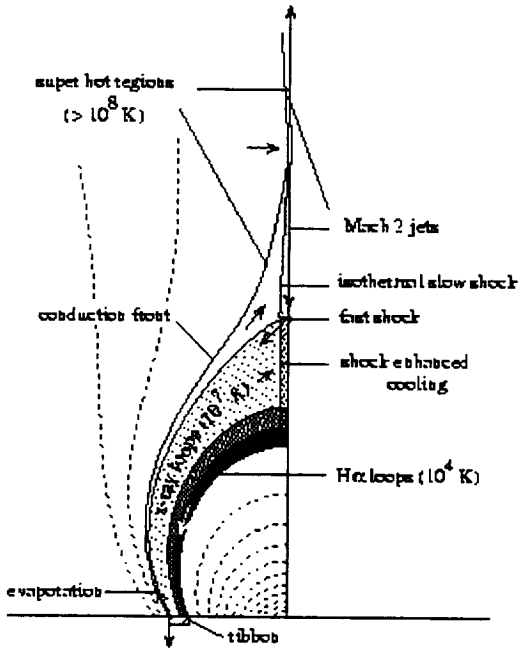

Figure 1.4

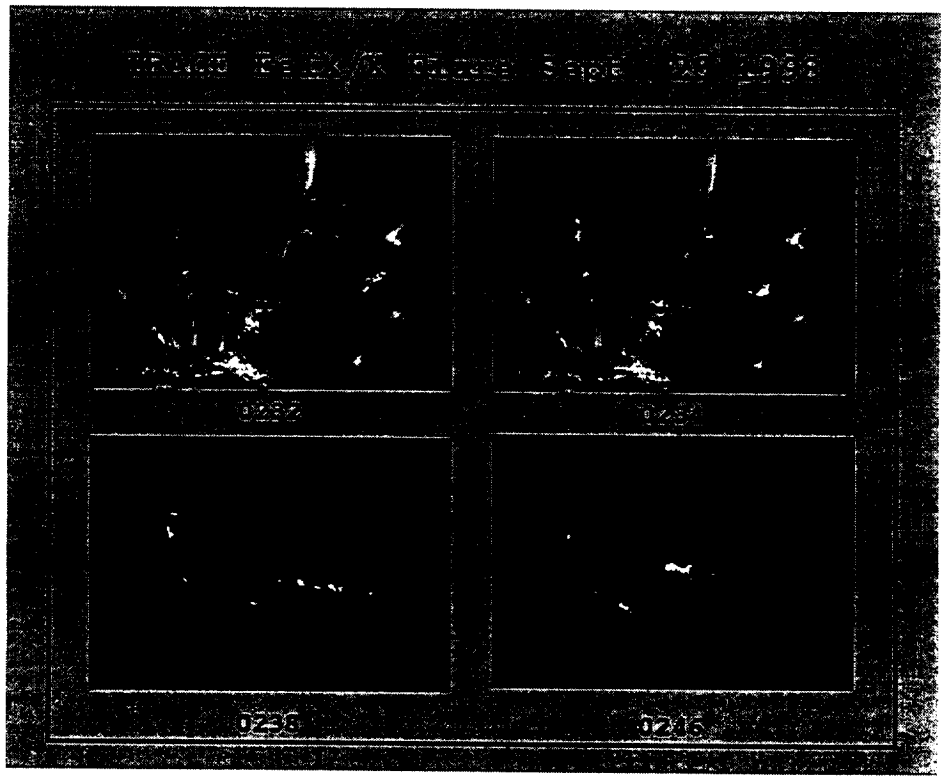

Figure 1.5

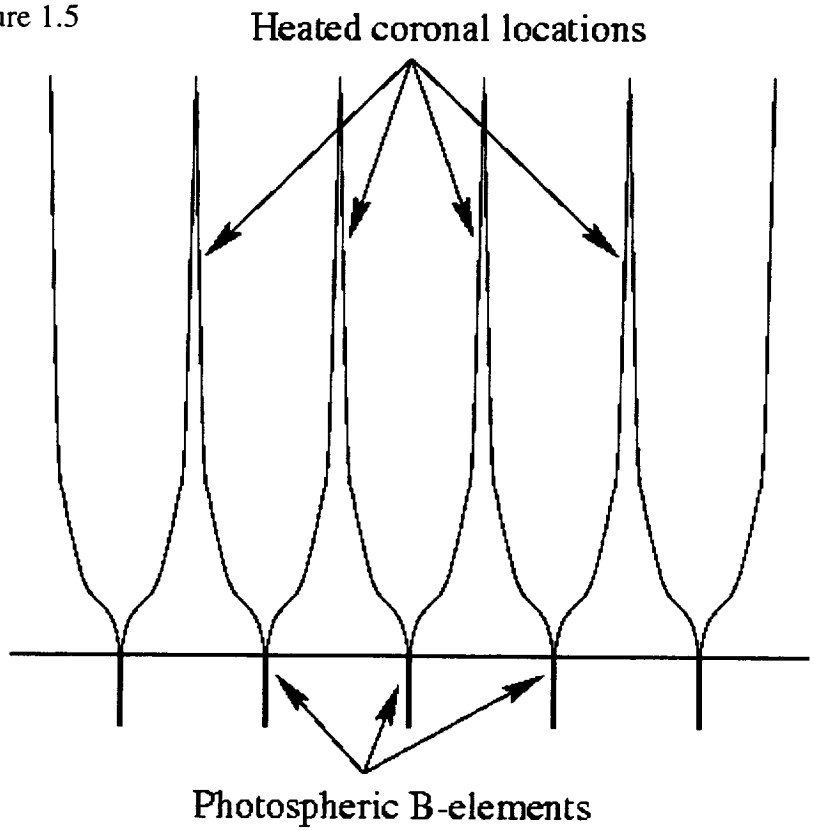

TABLE OF CONTENTS: EPO-SDB

1 EDUCATION, OUTREACH, TECHNOLOGY AND SMALL DISADVANTAGED BUSINESS PLAN 20

1.1 EO PLAN 20
1.2 SMALL & DISADVANTAGED BUSINESS PLAN 23

1 EDUCATION, OUTREACH, TECHNOLOGY AND SMALL DISADVANTAGED BUSINESS PLAN

1.1 EO PLAN

The current EO plan is to tie in the XRT project with educational activities that are currently on-going at SAO. This includes activities from other solar-related missions such as *SOHO* and *TRACE*, as well as astrophysics missions (*Chandra*). Dr. Golub will take the lead responsibility for ensuring that the EO plan is implemented; he will be supported in this effort by Drs. DeLuca, Warren, and Bookbinder.

The EO program will seek to engage education experts and scientists to translate the images of the solar corona into classroom modules, undergraduate level tutorials, and informal educational presentations. The spectacular images of the corona that we retrieve will be fully accessible via the internet in near real-time, and will be the starting point for inspiring interest in the methodology of scientific inquiry. We have repeatedly found that the highly dynamic images of the solar corona are able to inspire inquiry from all levels of scientific abilities. It is our intention to utilize this easily available and powerful outreach too. The process of developing, refining, and releasing educational materials will be fully tracked on the XRT EO website, which will be open to the public. SAO has a strong alliance with the Historically Black Colleges and Universities (HBCUs) and we will seek to increase the number of African-Americans (students and faculty) involved in space science. Dr. Golub is also in the process of discussing several video productions with National Geographic and PBS.

This plan is significantly more limited than the plan we originally conceived for the program, and has been tailored to accommodate the NASA-imposed cost cap and request to find an additional 5% of savings in our costs. Our original plan, as described below, is considered to be of high priority, and will be implemented if funding caps are sufficiently eased.

We originally proposed an innovative educational component for the Solar-B mission that we believed would have a larger impact beyond simply disseminating the data from this mission. By collaborating with a major educational materials developer and by leveraging the efforts of Solar-B with other NASA solar research missions, and by aligning ourselves with the broader national movement of science education reform, we hoped to create and distribute learning materials that have the potential to be used in thousands of classrooms and make a significant contribution to improving our nation's schools.

Our goal was to develop an inquiry-based science module called "Exploring the Sun". The module included a set of curriculum materials designed to be easily incorporated into

middle and high school science classes. It would have been developed by the SAO in collaboration with TERC, a highly-regarded, non-profit educational research and development company, through its Center for Earth and Space Science Education. TERC has a thirty year track record of successful innovative educational materials, and is centrally involved in several large NASA and NSF-funded projects, including Earth KAM, Mars Education, GLOBE, Visualizing Earth and Hands-On Universe. TERC had agreed to work in close collaboration with Solar-B scientists and educators to design and develop the materials.

In selecting this approach, we considered the experiences of other missions which disseminate their data to schools and the general public. We found that the least successful projects were those which simply posted data and images on the web. In contrast, the most successful projects transcended the data and details of their particular mission within a larger context directly aligned with school priorities.

Based on this analysis, we decided not to limit ourselves to the specific data and focus of Solar-B (advanced analysis of the solar corona and magnetic fields), although these data will be a central element. Rather, based on this analysis and on advice from TERC, we decided to take a larger view and develop an interactive, inquiry-based set of activities dealing more broadly with the Sun. The Sun is prominent in the Earth and Space Science component of the National Science Education Standards and is a major section in every Earth science textbooks in common use in schools.

Hence, our goal was to create a module that can be readily and easily incorporated into existing Earth science courses. More importantly, our module would be a major contribution to the transformation of how students learn about the Sun, and would provide them with an exciting new window into NASA's missions of space exploration and discovery.

In current textbooks, students read basic information about the sun, including its structure, its role as gravitational center and energy source for our solar system, and in some cases, more details about specific aspects such as the chromosphere, photosphere, corona and solar wind. However, students rarely use an inquiry-based approach, rarely work with authentic learning materials, and rarely take advantage of the burgeoning new understandings about the sun derived through the solar exploration missions of the past decade. In short, the way students learn about the sun is far removed the real, dynamic and inquiry-based approach used by solar scientists.

Our proposed module, "Exploring the Sun," would create a set of resources and learning activities that would enable teachers and students to take a new approach to learning about the Sun. The learning activities will focus on a series of questions, relating to such topics as sunspots, solar flares and other coronal structures, elemental composition, and solar thermodynamics. Students would try to find answers to these questions using authentic data from Solar-B and from other solar missions. We would provide the data through a combination of printed materials (graphs and images), CD-ROM and web-based data. We would provide a viewer, developed by TERC, which enables students

easily to interact with images, animated sequences, data overlays, and three-dimensional virtual environments. Through a direct linkage to the web, students will also link their investigations with live data from Solar-B, SoHO, Yohkoh, and other current and pending solar missions. With such highly visual data and tools, the Sun becomes a very engaging, interactive, dynamic and exciting topic -- much different from the static Sun depicted in textbooks.

The module would emphasize core concepts in Earth and Space Science, and would support development core skills of inquiry-based learning, technology and telecommunications, visualizations, and what the Standards call "unifying" concepts and processes such as systems, models, evidence and explanation. All of these concepts and skills will be developed in the framework of an integrated science education module, which features inquiry-based curricula, data and innovative visualization technologies. It would be published and distributed by a major educational textbook publisher with a strong track record of marketing innovative educational materials. We estimate that these materials could be used in over 1,000 *classrooms* in the first year, and over 10,000 classrooms within three years. We believe that these are conservative but achievable goals.

Based on TERC's experience with other educational innovations (such as the Kids Network program developed by TERC, marketed by National Geographic, and currently in use in over 30,000 schools), we believe that schools would find this integrated module on Exploring the Sun to be effectively designed and implemented and easily adopted and incorporated into existing Earth science and other classes. These two aspects -- solid educational design and ease of integration into existing materials -- are key to the successful distribution of innovative educational programs.

The development team will be codirected at the Smithsonian Astrophysical Observatory in coordination with Dr. Harold McWilliams at TERC. Dr. McWilliams heads the team that developed TERC's Global Explorer series, which integrate technology and curricula in modules for Earth science and biology classes. The Global Explorer is the same tool which we would use for the module on Exploring the Sun. Dr.\ McWilliams is also an experienced senior curriculum developer, with experience in leadership roles in several others of TERC's educational innovations.

TERC's involvement in this program is fully supported by Daniel Barstow, the Director of TERC's Center for Earth and Space Science Education (CESSE). Mr. Barstow will help assure that this program is well integrated with other educational innovations of CESSE.

As originally conceived, the materials would be developed and distributed in two phases. The first phase will take place early in the project, and well before the Solar-B launch date of February 2004. During the first phase, the initial materials are developed, field tested and distributed. This first phase will incorporate all of the core design concepts and existing image and data resources, such as SOHO, Yohkoh and TRACE. During the second phase, which will take place from the launch of Solar-B in February 2004, to the

end of the planned operational phase, we will add the Solar-B data and images, through a second-version release, supplemental CD-ROM and web-based data distribution.

Although the module on Exploring the Sun would be our major educational effort, we would also support two related efforts. It is still our plan to create a web site for large scale distribution of the images and data from Solar-B to the general public. We expect that public interest in the web will continue to grow dramatically, and that the web's role as a primary means for large scale public education and data delivery will similarly grow. This web site will be highly interactive, and include tutorials, animations, and news updates relating to solar exploration. It also will be directly linked to NASA's educational web sites and to NASA Spacelink.

It is also currently our plan to work with museums that express interest in enhancing their exhibits relating to the sun. There is a growing movement in museum to enhance exhibits by providing direct access to live data and images from spacecraft. We will work initially with the Boston Museum of Science and the Science Museum of Virginia, and then with other museums, with a special focus on providing data and images for their enhanced exhibits relating to the Sun.

A key component of our efforts will include formative and summative evaluation. We will build on the evaluation methodologies used by TERC for similar programs and through the expertise of faculty at the Harvard Graduate School of Education. We will compile lessons learned, assess the impact of our programs on our target audience, and identify the best means for engaging scientists in education and public outreach programs.

Again, we are committed to developing an effective education and public outreach program guided by the goals described in NASA's Office of Space Science Partners in Education: A Strategy for Integrating Education and Public Outreach into NASA's Space Science Programs and Implementing the Office of Space Science Education/Public Outreach Strategy.

1.2 Small & Disadvantaged Business Plan

It is the policy of SAO that Small, HUBZone Small, Small Disadvantaged, and Women-Owned Small Business concerns shall have the maximum practicable opportunity to participate in the performance of any subcontracts or teaming agreements necessary to fulfill contractual commitments with the Federal Government.

SAO recognizes its obligation to seek out these Small, HUBZone Small, Small Disadvantaged, and Women-Owned Small Business concerns to ensure opportunity for subcontracts or teaming agreements to the fullest extent possible consistent with efficient performance of a government contract.

SAO policies on the use of Small, HUBZone Small, Small Disadvantaged, and Women-Owned Small Business concerns in subcontracting are:

Consistent with the work to be performed, seek to determine work areas, which can be subcontracted to Small, HUBZone Small, Small Disadvantaged, and Women-Owned Small Business concerns.

Maintain information on Small, HUBZone Small, Small Disadvantaged, and Women-Owned Small Business concerns including capabilities, size of firm, and location.

Comply with the Federal Acquisition Regulations (FAR) and other appropriate regulations and executive orders pertaining to use of Small, HUBZone Small, Small Disadvantaged, and Women-Owned Small Business concerns.

The PM is responsible for identifying areas of work that can be subcontracted. The PM is responsible for preparing a written scope of work, technical specifications, and estimate of requisite effort for these areas. The PM will present this material to the Program Liaison Officer. The Program Liaison Officer, in conjunction with the Program Manager, will prepare a solicitation package, notify selected qualified candidates and actively seek their proposals, and send the solicitation package to those candidates who express a desire to respond. The Program Liaison Officer will forward proposals received in response to the solicitation to the Program Manager. Each proposal will be evaluated and awards will be made to that responsible offeror whose offer conforming to the solicitation will be most advantageous to SAO and the Government, price and other factors considered.

SAO will include FAR clause 52.219-8 entitled "Utilization of Small Business Concerns" in all subcontracts that offer further subcontracting opportunities. SAO will require all such subcontractors (except Small Business concerns) who receive subcontracts in excess of $500,000 to adopt a plan in consonance with FAR 52.219-9 and notify the Contracting Officer of the names of such subcontractors.

TABLE OF CONTENTS: TECHNICAL APPROACH

1. INTRODUCTION TO THE TECHNICAL SECTION.....28

1.1 OVERVIEW 28
1.2 CHANGES FROM THE INITIAL PROPOSED INSTRUMENT 28

2. SYSTEM BUDGETS 29

2.1 OVERALL SYSTEM REQUIREMENTS 29
2.2 IMAGING ERROR BUDGET 29
2.2.1 Overview 29
2.2.2 Focus 30
2.2.3 Optical Alignments 31
2.3 POWER BUDGET 32
2.4 WEIGHT BUDGET 32
2.5 DATA REQUIREMENTS 33
2.5.1 Primary Science Observations 33
2.5.2 Synoptic Observations 33
2.5.3 Supporting Science Observations 34
2.5.4 Summary 34
2.6 ENVIRONMENTAL INFLUENCES 34
2.6.1 Mechanical Loads 34
2.6.2 Thermal 40
2.6.3 Electronic 41

3. OPTO-MECHANICAL SYSTEM DESCRIPTION 41

3.1 X-RAY MIRROR ASSEMBLY 41
3.1.1 Requirements 41
3.1.2 X-ray Mirror 41
3.1.3 X-ray Mirror Mount 46
3.1.4 X-ray Baffle System 56
3.2 VISIBLE LIGHT TELESCOPE 57
3.2.1 Requirements 57
3.2.2 Design 57
3.2.3 Mounting 57
3.3 VISIBLE LIGHT SHUTTER 58
3.3.1 Requirements 58
3.3.2 Design 58
3.3.3 Operation 59
3.3.4 Testing 59
3.3.5 Trade off, buy versus build 59
3.4 X-RAY FILTERS, FRONT APERTURE AND FOCAL PLANE 60
3.4.1 Requirements 60
3.4.2 Design 60
3.4.3 Heritage 62
3.4.4 Acoustics Issues 62
3.4.5 Testing 64
3.4.6 Handling Fixtures for XUV Filters: 65
3.5 VISIBLE LIGHT PREFILTER 65
3.5.1 Requirements 65
3.5.2 Design 66
3.6 TELESCOPE TUBE 66
3.6.1 Requirements 66
3.6.2 Design 66

3.6.3 *Performance* 67
3.6.4 *Trade off Aluminum vs. CFRP, Titanium vs. CFRP* 71
3.6.5 *Issues* 72
3.7 MAIN SHUTTER 72
3.7.1 *Requirements* 72
3.7.2 *Design* 73
3.7.3 *Heritage* 74
3.7.4 *Predicted Performance* 74
3.7.5 *Testing* 74
3.8 FILTER WHEELS 74
3.8.1 *Requirements* 74
3.8.2 *Design* 75
3.8.3 *Heritage* 75
3.8.4 *Predicted Performance* 76
3.8.5 *Testing* 76
3.9 FOCUS MECHANISM 76
3.9.1 *Requirements* 76
3.9.2 *Design* 77
3.9.3 *Predicted Performance* 78
3.9.4 *Testing* 79

4. ELECTRONICS DESIGN 79

4.1 OVERVIEW 79
4.2 MECHANISM CONTROLLER 80
4.2.1 *Requirements* 80
4.2.2 *Design* 81
4.3 FILTER WHEEL/MAIN SHUTTER CONTROLLER 82
4.3.1 *Requirements* 82
4.3.2 *Design* 82
4.3.3 *Heritage* 83
4.4 VISIBLE LIGHT SHUTTER 83
4.4.1 *Requirements* 83
4.4.2 *Design* 83
4.5 FOCUS MECHANISM 84
4.5.1 *Requirements* 84
4.5.2 *Design* 84
4.6 DOOR MECHANISM CONTROLLER 84
4.6.1 *Requirements* 84
4.6.2 *Design* 84
4.7 ANALOG HOUSEKEEPING 84
4.7.1 *Requirements* 84
4.7.2 *Design* 85
4.8 THERMAL CONTROL 85
4.9 POWER SUPPLIES 85
4.9.1 *Requirements* 85
4.9.2 *Design* 85
4.10 SYSTEM CABLING 85
4.10.1 *Connectors* 85
4.10.2 *Wire* 85

5. SOFTWARE DESIGN 86

5.1 REQUIREMENTS 86
5.1.1 *Science Requirements* 86
5.1.2 *Control of Mechanisms & Electronics* 86
5.1.3 *Interface* 87

5.1.4 Reporting on Status *87*
5.1.5 Instrument Safety *87*
5.2 DESIGN 87
5.2.1 Heritage *87*
5.2.2 Software Modes *88*
5.2.3 Real-time Tasks *89*
5.2.4 Commands *90*
5.2.5 Tables *91*
5.2.6 Software Environment *91*
5.3 SOFTWARE MANAGEMENT 91
5.3.1 Revision Control *92*
5.3.2 Interface Control *92*
5.4 HARDWARE AND SOFTWARE EGSE 92
5.4.1 Hardware *92*
5.4.2 Software *93*

6. THERMAL DESIGN 93

6.1 OVERVIEW 93
6.2 REQUIREMENTS 94
6.3 DESIGN 95
6.3.1 Passive Thermal Design *95*
6.3.2 Operational Active Thermal Control *96*
6.3.3 Thermal Modeling *96*
6.3.4 Survival Heaters *97*
6.4 IMPACT OF MECHANICAL DESIGN OPTIONS 97
6.5 TESTING 98

7. SYSTEM INTERFACES 98

7.1 SPACECRAFT 98
7.1.1 Mechanical *98*
7.1.2 Electronic *99*
7.2 CAMERA 100
7.2.1 Mechanical *100*
7.2.2 Electronic *100*
7.3 INTERNAL INTERFACES 101
7.3.1 X-ray Mirror *102*
7.3.2 Visible Light Optics *102*
7.3.3 Main Shutter *102*
7.3.4 Filter Wheels *102*

8. CONTAMINATION REQUIREMENTS 102

8.1 REQUIREMENTS 102
8.1.1 Particulates *102*
8.1.2 Condensibles *103*
8.2 SAO RELEVANT EXPERIENCE 103
8.3 MATERIAL SELECTION 103
8.4 MATERIAL PREPARATION, AND HANDLING 103
8.5 ASSEMBLY PROCEDURES 103
8.5.1 Facilities *104*

1. Introduction to the Technical Section

1.1 Overview

All aspects of the Solar B X-ray Telescope (XRT) design were reviewed during Phase A. The study focused on design aspects that had the greatest affect on the final instrument imaging performance, and the interfaces. The error budget affecting the quality of the image was examined, and analyzed in great detail. The spacecraft, and camera mounting interfaces were reviewed with our collaborators in Japan at two visits to Tokyo, and numerous emails and telecons.

The technical section outlines the conceptual design, and the analysis that lead to its selection. In many cases the design trade-offs that were examined (and in some cases are still being reviewed) are discussed.

1.2 Changes from the initial proposed instrument

The instrument that SAO began to design at the inception of Phase A was somewhat different from what we had initially proposed. The instrument that SAO proposed met the requirements of the announcement of opportunity (AO), and included an x-ray mirror that could image the entire sun at a resolution commensurate with 1 arcsec pixels, a visible light telescope that met similar optical requirements, a CCD camera, instrument controller, and associated mechanisms (shutters, filters wheels, cover deployment system). Selection of the XRT for Phase A Study was contingent upon removal of the camera and its associated electronics, and acceptance of a stringent cost cap. During the course of the Phase A study, it was determined that two additional items needed to be included in the XRT design to ensure a successful instrument – a modified mechanism controller and a focus mechanism.

The original instrument controller was primarily intended to control the camera, while collecting and compressing the images. However, once removed, the XRT was left without control electronics for the instrument mechanisms. The Phase A XRT design effort began without clear guidance on how to proceed in the direction of instrument control. Early thoughts of having the mechanisms controlled directly from the spacecraft were abandoned for a number of reasons, though two were key:

- The large thermal conduction through the interface cables,
- The difficulty in performing comprehensive testing before delivery.

To solve these problems, a mechanism controller was added.

Early Phase A work to establish an image quality error budget produced the understanding that an additional mechanism was required in the system, one that would be able to adjust the system focus on orbit. It was clear, once all the influences affecting the focal stability of the system were enumerated, that there was a high risk of launching the telescope at an undesired focal position. This problem was magnified by the fact that SAO no

longer controlled the details of the camera design; additional discussions with ISAS revealed that the flight camera would not be ready for integration until very late in the program, adding additional error terms to the overall focus budget. Ensuring that the correct focal position would be achieved at launch and maintained throughout the mission lifetime would have required spending a lot of time and money (hence exceeding our cost cap). Two other factors were also at play here:

- determining the focal plane is difficult due to the nature of the Wolter I optic, and the spectral regime that we are working in, and
- selecting a focal position is a compromise at best because of the functional dependence of point spread on both the position in the field, and the back focal distance.

For these reasons a focus mechanism was added. The added mechanism was conceived to be a joint responsibility between ISAS, Meisei (the Japanese company designing the camera) and SAO. While an unusual arrangement, this was the result of two separate arguments,

- the addition of the focus mechanism is a cost burden to be shared by both sides of the interface,
- the most effective mechanism would be one that carried a minimum amount of weight, in this case only the CCD and its header.

These arguments led to a design with an actuator that would be made by SAO, while the moving stage would be made by Meisei. The interfaces are conceived to be simple to minimize risks associated with a shared mechanism. Various configurations were examined during Phase A.

The remainder of the XRT design baseline matches the proposed configuration.

2. System Budgets

2.1 Overall System Requirements

The XRT top level requirement is to produce an x-ray image of the full sun that is limited only by the 1 arcsec pixel size of the CCD in the focal plane. This fact, combined with a physical pixel size of 13.5μm, sets the instrument focal length, the allowable focus error, and the allowable distortion-induced image blur.

In addition the mirrors must have an energy response that covers the spectrum from 2Å-60Å, while being capable of capturing ¼ of the full frame image every 2 seconds.

2.2 Imaging Error Budget

2.2.1 Overview

The Imaging Error Budget for the XRT allocates the various error sources that will ultimately contribute to, and define the on-orbit performance of the XRT. This is presented at this time primarily as a framework. Thus many entries are shown as TBD, or in some cases as 0.01 arcsec if they are considered at this time to be too small to matter. We have

included all known large sources to ensure that the baseline design meets the overall imaging error budget; other sources will be included as they are identified and estimated.

A significant portion of the top-level error is the as-delivered mirror from Raytheon. Lumped in this box are all errors that result from the mirror element fabrication, including nominal figure, figure errors, polishing and coating surface errors, etc. It should be noted that these errors are estimates for a free-standing mirror that is ideally supported (i.e. zero-g).

The optic will be ground, polished and coated by Raytheon based on an SAO design specification. A key component of this design is a deliberate alteration from a pure Wolter I optic to provide better overall focus over the entire design field-of-view. This results in a "built-in" best focus error of 0.6 arcsec which, although part of the total optical performance requirement levied on ROSI, is shown separately in this budget as "Mirror Design Figure" to distinguish it from the actual fabrication errors.

The rest of the errors are induced in the mirror based on SAO assembly of the mirror into a structure and the on-orbit effects on the optical performance. These can be divided into two main categories: bias errors, whose directions are known but cannot be compensated for (e.g. epoxy shrinkage), and those that vary randomly or are uncertainties in bias errors. Bias errors must be summed, since a one-sided error cannot be RSS'd with random errors.

2.2.2 Focus

The distance between the mirror and the CCD can vary from a theoretically perfect value by 53μm before the focal error will begin to dominate the system imaging resolution. Thus 53μm was initially budgeted as the maximum allowable error for this source.

The system focus is the most obvious and largest contributor to the image resolution budget. The XRT is a difficult telescope to focus on the ground. The small annulus of the x-ray aperture, coupled with the fact that the actual observations are to be made in x-rays make focusing the system with visible light a difficult process, at best. Thus the ability to identify the actual focal plane is quite difficult without placing the telescope in a vacuum chamber. Once it is placed in a vacuum chamber and trained on an x-ray source, two other complications come into play: first, the finite source distance between the x-ray source and the telescope places the best test focus about 25mm away from where it would be for an x-ray source at infinity; and second, the range of spot sizes that this mirror produces throughout the image field, combined with how those spot sizes change as the distance between the mirror and the CCD are changed, make the selection of the optimal focal plane location very difficult to determine, and non-unique. These uncertainties combine to produce a large error source in the error budget governing the ability to find and maintain focus, in the absence of the ability to re-focus the telescope once it has been launched.

Another large contributor to the focus error budget is the telescope tube. The tube is very long, 2.7m, and therefore small changes in its temperature, or moisture content, result in large changes in focus. In the case where the telescope is focused once on the ground for

all time, the possible changes in lifetime temperature and moisture levels are quite high. Even with the ability to focus the telescope on orbit, the changes in the tube temperature induced by orbital variations dominate the focal error budget.

Other large contributors to the focus error budget are the temperature uncertainties of the camera, the flatness of the CCD, and the ability to move the focus stage to exactly where we want it to go.

2.2.2.1 On Orbit Focus

The XRT instrument, as initially proposed, did not include the ability to adjust the system focus on orbit. The top level error budgets, one of which is included in Foldout 4, indicated that the system would be unable to maintain the necessary focus throughout the mission lifetime. *It was decided that the system would be less expensive, and the risk of unacceptable performance lower, if we included a focus mechanism.*

2.2.3 Optical Alignments

There are several alignment budgets that affect the design, assembly and integration of the XRT:

- X-ray mirror optical axis to the telescope axis.
- Visible light optics to the telescope axis.
- Visible light telescope to the x-ray telescope.
- XRT to the other telescopes on the Solar-B spacecraft.

For the most part these have large error budgets. The visible light optics and the x-ray mirror both behave as thin lenses. Thus tilting them with respect to the telescope axis has a small affect on the resulting imaging performance.

The co-alignment of the x-ray and visible telescopes, within the XRT instrument, is set by the need to have the entire image of the sun from both telescopes on the CCD at the same time. The images from each telescope will be aligned to well within a single pixel after the data has been relayed to the ground. The effort to align the data from the images is independent of the degree of starting misalignment. Thus the two images need only be aligned well enough to ensure that all the information required to align the images on the ground is available in the data from both instruments. This means that, with the Solar B spacecraft pointed at the center of the sun, both telescopes produce images of the full solar disk including the entire solar limb. Since the sun under fills the CCD in both cases, the required alignment necessary to ensure that the full sun will be available in the image of both telescopes is ±1 arcmin. This easily met in practice.

The XRT must be aligned to other instruments on the Solar B telescope well enough to overlap their fields of view. The Solar Optical Telescope (SOT) and the Extreme Ultraviolet Imaging Spectrometer (EIS) have small fields of view, and are aligned with the observatory optical axis. Since the XRT field of view is so large, ensuring that the XRT is aligned with the spacecraft pointing axis to within ±1 arcmin will guarantee sufficient alignment.

2.3 Power Budget

The power allocation is 5.3 W for the instrument, excluding the heaters. The table below shows the power budget for the XRT instrument. As can be seen in the subtotal row under "Operational Power" the budget is exceeded by 0.8 W, once adjusted for power supply efficiency. This is based on the unlikely scenario that all the mechanisms operate at once. In operation the mechanisms will be run separately, thus not exceeding the power budget.

Table 2-1 Power Budget

Mechanism	Individual Mechanism Power		Operational Power	
	Peak	Continuous	Peak	Continuous
Mechanism controller	1.5	0.5	1.5	0.5
Focal plane shutter	1	0.1	0.1	0.1
Filter wheel #1	2.7	0.1	2.7	0.1
Filter wheel #2	2.7	0.1	0.1	0.1
Visible light shutter	2.7	0.1	0.1	0.1
Focus mechanism	1	0.1	1	1
Controller	2	2	2	2
Housekeeping board	1	1	1	1
Subtotal	NA	NA	8.5	4.9
Adjust for Power Supply Efficiency (80%)			10.6	6.1
Instrument heaters	30	12	30	12
Adjust for Power Supply Efficiency (85%)			37.5	15.0

2.4 Weight Budget

The present weight budget for the XRT, less the camera, is 30 kg. Presently we are predicting a weight of 32.3 kg (See Foldout 1). This is a problem this early in a program where experience indicates that the weight estimates will grow with time. The extra weight comes from an increase in weight in the tube assembly required to deal with the high testing loads, the new electronics that were not accounted for after the camera was removed, and the inclusion of the focus assembly. A detailed examination will be required to determine exactly how much weight can be removed from the system, but a

preliminary effort suggests that the weight would not drop below 30kg. We have initiated discussions with ISAS on the contingency and margins available for this instrument.

2.5 Data Requirements

The data requirements for the XRT are driven by the science plans. The physical processes in the solar coronal result in significant and important changes on timescales from micro-seconds to years. The highest cadence XRT observations are limited by the read time of the CCD and the size of the FOV (we assume 512kpixel/s serial read rates and 10krow/s parallel shifts). We have looked at data requirements from three types of science observations: primary, synoptic and supporting.

2.5.1 Primary Science Observations

During discussions with the J-Side at the "Physics of the Solar Corona and Transition Region Workshop" an outline of flare observations was developed. Notes from that meeting were distributed by Dr. DeLuca on 1999-09-01 to the solarb-usxrt mailing list. To observe flares XRT will enter a flare mode; pre-flare data will be saved in a rotating buffer. To achieve significant progress over present knowledge of flares, at least 15 minutes of high-cadence pre-flare data must be retained. Higher cadence (and perhaps smaller FOV) data during the rise and maximum phases of a flare are needed as well. Lower cadence, but larger FOV data during the decay phase are also seen to be needed. To store 1000s of pre-flare XRT data 640Mbits of storage are required. During a flare the XRT will take data at the 512kpixel/s rate for the first 1000s and may continue to take data at 128kpixel/s for a second 1000s. This data will be stored in the main buffer and will require 2Gbits of storage. At the nominal XRT downlink rate of 0.8Mbits/s (20% of 4Mbits/s), the flare data can be downloaded in four 10-minute or six 7-minute downlinks.

As part of a joint science planning exercise with the US EIS and FPP teams we have generated, as a sample program, an XRT primary science sequence to study the physical processes associated with the emergence of magnetic flux into the corona. The data requirement for this program (and the supporting and synoptic programs described below) is based on an XRT simulator written in IDL. The simulator includes our best estimates of: mechanism move and settle times, CCD read times, and spacecraft move and settle times. The emerging flux program has a data rate of 53 Kbits/s (compressed) and will generate 4.6Gbits of data per day requiring 9.5 10-minute downlinks at the nominal XRT rate of 20% of 4Mbits/s. If XRT had 80% of the downlink during this program, only 2.4 10-minute downlinks would be needed.

2.5.2 Synoptic Observations

An important and unique contribution of the XRT to the SolarB mission is its synoptic science plan. Synoptic observations taken every 90 minutes for the duration of the mission will generate a key data set to study the long time scale and global evolution of multi-thermal coronal structures with high spatial resolution, unavailable from any other instrument. In the synoptic program we take long and short exposures in three x-ray bandpasses that span our temperature range and a white light image for context. This

program produces about 1.4 Gbits (175 Mbytes) of data per day, and requires 3 10-minute downlinks at the nominal XRT rate of 20% of 4Mbit/s.

2.5.3 Supporting Science Observations

An XRT science program to support FPP observations of magnetic flux in the quiet sun (the Flux Tube Physics program), generates 41 Kbits/s or 3.5 Gbits/day. This program requires 7.4 10-minute downlinks.

2.5.4 Summary

The above discussion clearly shows that the XRT needs substantial on-board storage (~2Gbits), one or more rotating buffers (~640Mbits) and around 12 10-minute (or 17 at the more likely 7-minute duration) downlinks per day to carry out its science program.

2.6 Environmental Influences

2.6.1 Mechanical Loads

2.6.1.1 Summary

Solar-B XRT loads are a significant contributor to the design requirements of the XRT. Applied loads, factors of safety, test load factors, dynamic response factors, and documentation revision all contribute to the total load requirements placed on the XRT design. This section consolidates all documented applied XRT and spacecraft loads without additional load factors.

From the complete list of applied loads in Table 2-2, the highest load vector is 44 G's (31 G's X, 31 G's Y, 6.25 G's Z) from load case 1, quasi static 1st stage burnout. The highest loads in the individual X and Y directions are 31 G's from load case 1, the quasi static 1st stage burnout. The highest loads in the Z direction is 25 G's from load case 7, the mechanical shock test.

Many potentially significant loads have not yet been determined. The determination of many of the most critical XRT loads depend on the dynamic response of the Solar-B spacecraft and are subject to the final design of the spacecraft. Improved estimates of the spacecraft dynamic behavior will not be available until the spacecraft contractor, MELCO, completes the preliminary structure modeling effort and releases the results. This is scheduled for early in Phase B.

2.6.1.2 Discussion

Load conditions for the XRT have been generated exclusively by ISAS and MELCO. All documented loads are listed in this section for completeness and visibility: However, not all the documented loads are design critical. Design critical test loads are documented in section 2.6.1.2.

Loads are applied to the XRT by two methods. First, loads are applied to the base of the XRT directly. Second, loads are applied to the base of the spacecraft with the XRT mounted to the spacecraft. Loads are defined as four basic types: Quasi static, shock, random vibration, and acoustic. Quasi static loads are derived from dynamic loads that occur when any one of the three stages of the rocket burns out. These loads are generated in test by static mechanical loading of major portions of the structure. Shock loads occur due to sudden temporal events during handling and flight. Three specific shock loads documented include mechanical shock, pyrotechnic shock, and rocket separation shock. Mechanical shock is a general shock load. Pyrotechnic shock is load that occurs due to explosive bolt events that occur in flight. Rocket separation shock occurs from rapid changes in the dynamic characteristics of the launch vehicle. Defined shock loads have been quantified are idealized as 10 ms half sine shock loads with a specific peak amplitude given in terms of G level. Shock loads are generated in test by a controlled drop or by a shaker table. Random vibration loads quantify the random vibration spectrum that is mechanically applied to the base of the XRT or spacecraft as a result of rocket firing and aerodynamic vibration. Random vibration loads are generated in test by a shaker table. Acoustic loads are caused by an Overall Sound Pressure Level (OASPL) that acts on the exposed surfaces of the structure. Like random vibration, acoustic load occurs in the frequency domain. Acoustic loads are generated by high power tuned horns acting in an enclosed test area.

- Load cases 1-3 of Table 2-2 summarize the quasi static axial and lateral loads at 1st, 2nd, and 3rd stage burnout, respectively. These loads are applied to the XRT directly. For the 1st stage burnout lateral direction, the load value varied from 31 to 40 G's along the axial direction of the spacecraft. The shape of the load variation showed that most of the XRT was subject to the 31 G level with only the forward end slightly in the linear ramp up to 40 G's. This small length of XRT subjected to slightly more than 31 G's was neglected: thus, 31 G's was used.
- Load cases 4-6 of Table 2-2 summarize the static axial and lateral loads at 1st, 2nd, and 3rd stage burnout, respectively. These loads are applied to the spacecraft base.
- Load case 7 summarizes the component mechanical shock test loads applied to the base of the XRT.
- Load case 8 summarizes the pyrotechnic shock. Pyrotechnic shock values have not been determined at this time.
- Load case 9 summarizes the rocket separation shock test loads applied to the base of the spacecraft.
- Load case 10 summarizes the system random vibration test loads. Random vibration loads are applied to the base of the spacecraft. Load case 10 consists of applying 5.5 G's RMS axially and 6.8 G's RMS laterally to the spacecraft.
- Load case 11 summarizes the acoustic vibration test loads.

Note that many of the loads in table 2.2 are "to be revised". Many of these loads are a function of the combined dynamic response of the spacecraft and XRT. The dynamic response, in turn, is a function of the mass, stiffness, supports, and damping of the flight hardware. As the project goes forward, these loads will be revised analytically and experimentally. It is expected that the load revisions will have a tendency to lower, not raise, the overall requirements for the XRT design. Until this information becomes available, however, the highest documented loads presented here constitute the design drivers.

Table 2-2 Summary of XRT Applied Loads

Description (where load is applied)	Direction	Value	Ref. Doc
Load case 1 (to be revised) max vector and max X, Y quasi static 1st stage burnout (XRT base)	**Axial (Z)**	6.25 G	**SolarB, 1999b**
	Lateral (X,Y)	31 to 40 G	**SolarB, 1999b**
Load case 2 (to be revised) quasi static 2nd stage burnout (XRT base)	axial (Z)	7.5 G	**SolarB, 1999b**
	Lateral (X,Y)	TBD	**SolarB, 1999b**
Load case 3 (to be revised) quasi static 3rd stage burnout (XRT base)	axial (Z)	12.5	**SolarB, 1999b**
	Lateral (X,Y)	TBD	**SolarB, 1999b**
Load case 4 quasi static 1st stage burnout (spacecraft base)	axial (Z)	5.0 G	**SolarB, 1999b**
	Lateral (X,Y)	12.0 G	**SolarB, 1999b**
Load case 5 quasi static 2nd stage burnout (spacecraft base)	axial (Z)	6.0 G	**SolarB, 1999b**
	Lateral (X,Y)	2.0 G	**SolarB, 1999b**
Load case 6 quasi static 3rd stage burnout (spacecraft base)	axial (Z)	10.0 G	**SolarB, 1999b**
	Lateral (X,Y)	TBD	**SolarB, 1999b**
load case 7–max Z (to be revised) mechanical shock test (XRT base)	**axial (Z)**	25 G, 10 ms half sine	**SolarB, 1999a**
	Lateral (X,Y)	8 G, 10 ms half sine	**SolarB, 1999a**
Load case 8 (to be revised) pyrotechnic shock (XRT base)	axial (Z)	TBD	**SolarB, 1999a**
	Lateral (X,Y)	TBD	**SolarB, 1999a**
Load case 9 rocket separation shock test (spacecraft base)	axial (Z)	15 G, 10 ms half sine	**SolarB, 1999b**
	Lateral (X,Y)	NA	**SolarB, 1999b**
Load case 10 system random vibration test (spacecraft base)	axial (Z)	5.5 G's RMS	**SolarB, 1999c**
	lateral (X)	6.8 G's RMS	**SolarB, 1999b**
	lateral (Y)	6.8 G's RMS	**SolarB, 1999b**
Load case 11 acoustic vibration (XRT tube profile)	axial (Z)	148.8 dB OASPL	**SolarB, 1999a**
	lateral (X)		
	lateral (Y)		

2.6.1.3 Transportation Loads

The XRT engineering and flight models will be exposed to transportation loads at many times during calibration, checkout, test, and flight preparation. Transportation loads occur for the following configurations: ground transportation with XRT in its shipping container; air transportation with XRT in its shipping container; ground transportation with XRT mounted to the spacecraft; and while being moved at testing and assembly facilities.

The XRT shipping container provides shock and vibration isolation for the instrument during ground and air transport. The shipping container provides XRT protection for maximum external shock of 5 G's. The shipping container will provide 2, 5, and 10 G trip indicators to verify maximum external load conditions during shipping. The shipping container provides tip indicators.

Several transportation environments for the spacecraft and components have been specified in SolarB, 1999b. These conditions are listed in Table 2-3.

Table 2-3 Container Environment for Spacecraft and Components

Environment outside shipping container	Expected value
temperature	-5 to +30°C
relative humidity	100% maximum
Ambient pressure	730 to 790 mm Hg

2.6.1.4 Mechanical and Acoustical Test Program

The test program consists of testing at different levels of integration to minimize program risk. The primary purposes of subcomponent level tests (see Table 2-4). is to test filters in the acoustic environment and to test the X-ray optic mount subject to mechanical loads. The Component Level Engineering Model (EM) Qualification Tests (see Table 2-5) test the Engineering Model (MTM) of the XRT by imposing all component level test levels. It is expected that the component test levels will be modified during Phase B to reflect the coupled loads analysis result on the spacecraft structural model. To date, no coupled loads documentation has been received. Flight Model (FM) Acceptance Tests (in Table 2-6) are designed to test flight hardware at levels generally lower than qualification levels for all major load conditions. The flight X-ray optic is a subcomponent test, with all other acceptance tests performed on the XRT flight hardware. System Level Engineering Model Qualification Tests (in Table 2-7) are designed to test the full spacecraft EM for all qualification level tests. System Level Flight Model Proto Flight Tests are listed in Table 2-6. These tests expose the flight model to qualification test levels for a reduced amount of time where applicable. Please note, what ISAS refers to as "Proto flight testing" is generally considered flight testing in a NASA program. These are tests performed on the final flight hardware build before launch.

Table 2-4 Assembly Level Testing

Test #	Supervisor/ location	Test ref	test hard-ware/ setup	SAO hard-ware tested	test type and level (Table 2-2 load case #)
1	SAO/US	----	rigidly mounted fil-ter wheel	Filters	acoustic proto flight test levels (load case 11)
2	SAO/US	----	rigid tube	X-ray optic mass model	low level sine sweep (NA)
3	SAO/US	----	rigid tube	X-ray optic mass model	quasi static coupled loads from proto flight test levels (load case 1)
4	SAO/US	----	rigid tube	X-ray optic mass model	random coupled loads from proto flight test levels (load case 10)
5	SAO/US	----	rigid tube	X-ray optic mass model	shock coupled loads from proto flight test levels (load case 7)

Table 2-5 Component Level Engineering Model Qualification Testing

Test #	Supervisor/ location	Test ref *	test hardware/ setup	SAO hard-ware tested	test type and level (Table 2-2 load case #)
6	SAO/US	2p7	XRT MTM	XRT MTM	quasi static coupled loads analysis from qualification test levels (load case 1)
7	SAO/US	2p7	XRT MTM	XRT MTM	acoustic from qualification test levels (load case 11)
8	SAO/US	2p7	XRT MTM	XRT MTM	random coupled loads analysis from qualification test levels (load case 10)
9	SAO/US	2p7	XRT MTM	XRT MTM	shock coupled loads analysis from qualification test levels (load case 7)
10	SAO/US	2p7	XRT MTM	XRT MTM	thermal / vacuum ref 2, fig 3-1 (NA)

*SolarB, 1999b

Table 2-6 Flight Model Acceptance Testing

Test #	Supervisor/ location	Test ref	test hard-ware/ setup	SAO hardware tested	test type and level (Table 2-2 load case #)
11	SAO/US	----	rigid tube	flight X-ray optic	low level sine sweep (NA)
12	SAO/US	----	rigid tube	flight X-ray optic	random coupled loads analysis -6 dB from acceptance test lev-els (load case 10, -6 dB)
13	SAO/US	2p7	XRT FM	XRT FM	acoustic from acceptance test levels (load case 11, -3 dB)
14	SAO/US	2p7	XRT FM	XRT FM	random coupled loads analysis from acceptance test levels (load case 10)
15	SAO/US	2p7	XRT FM	XRT FM	shock coupled loads analysis from acceptance test levels (load case 9)
16	SAO/US	2p7	XRT FM	XRT FM	thermal / vacuum (Solarb, 1999b, fig 3-1)

Table 2-7 System Level Engineering Model Qualification Testing

Test #	Supervisor/ location	Test ref	test hard-ware/ setup	SAO hardware tested	test type and level (Table 2-2 load case #)
17	MELCO Japan	2p6	S/C MTM	XRT MTM	quasi static from qualification test levels (load case 1)
18	MELCO Japan	2p6	S/C MTM	XRT MTM	acoustic from qualification test levels (load case 11)
19	MELCO Japan	2p6	S/C MTM	XRT MTM	random from qualification test levels (load case 10)
20	MELCO Japan	2p6	S/C MTM	XRT MTM	shock from qualification test levels (load case 9)
21	MELCO Japan	2p6	S/C TTM	XRT MTM	thermal / vacuum (Solarb, 1999b, fig 3-1)

Table 2-8 System Level Flight Model Proto Flight Testing

Test #	Supervisor/ location	Test ref	test hard-ware/ setup	SAO hardware tested	test type and level (Table 2-2 load case #)
22	MELCO Japan	2p6	S/C FM	XRT FM	random from proto flight test levels
23	MELCO Japan	2p6	S/C FM	XRT FM	shock from proto flight test levels
24	MELCO Japan	2p6	S/C FM	XRT FM	thermal / vacuum (Solarb, 1999b, fig 3-1)

2.6.2 Thermal

The XRT will be exposed to an environment that mimics space. In thermal testing, we will impose environments that produce temperatures or total power loads equivalent to 10K beyond worst hot and cold case model predictions. All thermal loads imposed on the XRT during manufacturing and transportation will be maintained within these limits.

2.6.3 Electronic

EMI/EMC testing will be performed at the instrument level. The document entitled "Electronic Design Standards", which has been provided by ISAS, contains test levels for EMI/EMC testing. These levels are not fully in agreement with NASA test specifications. The test levels are under discussion.

The instrument will be exposed to the ambient radiation environment of low Earth orbit. An analysis of this environment, in which it was assumed that the electronics are protected by a 10 mil aluminum shield, showed that the electronics will be exposed to a 5000 rad cumulative dose over a two year operational period. Radiation tolerant electronics parts are available that can survive in this environment for a much longer period of time. Procurement of suitable parts will reduce the risk of radiation induced errors.

3. Opto-Mechanical System Description

3.1 X-ray Mirror Assembly

3.1.1 Requirements

The central goal of the XRT instrument is to image the full solar disk in x-ray, at a resolution consistent with putting 55% of the incoming energy from a spot within 1.5 arcsec. The Wolter-I grazing incidence optic must focus the incoming light to a spot size compatible with this goal.

3.1.2 X-ray Mirror

3.1.2.1 Mirror Design

A standard Wolter-I optic designed for the Solar B focal length and spectral range would not yield the required resolution across the entire field of view. In order to improve the resolution at the edges of the field, several mirror optimizations were attempted and compared. It was found that, with small mirror surface deviations from a true conic section, the image resolution across the field of view can be brought into sharper focus. The cost of doing this is lower resolution in the center of the field. This is a minor drawback as the resolution in the central portion of the field of a standard Wolter-I optic would have higher resolution than can be registered with this camera.

An added effect is the axial position of the CCD. As the separation of the changes, the image resolution across the entire field changes. The point of the best image moves. The performance of the optimal optic, at various focal positions, is shown in Figure 3-1.

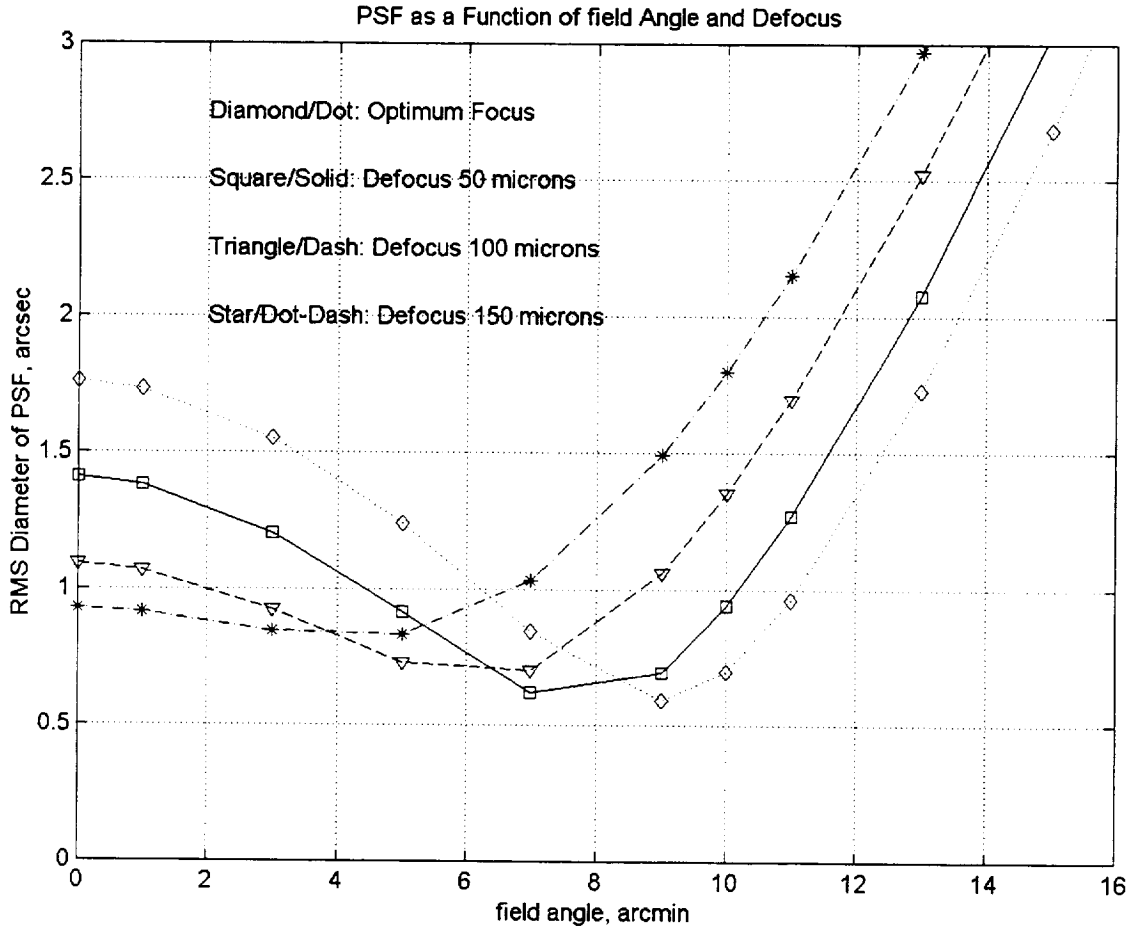

Figure 3-1 XRT Image Spot Size with Focus Position and Field Angle

3.1.2.2 Fabrication

Fabrication of the XRT grazing incidence optics will utilize the processes and technology developed for the GOES SXI program. This approach will minimize cost to Solar-B and maximize the benefits of the SXI learning curve. This fabrication approach employs the use of a monolithic blank which will include both the primary and secondary mirrors. This eliminates the program constraint of holding the two elements in alignment to one another. Fabrication of the optics will start with CNC generation of the best fit cones to each optical element, and a relieved gap between the two elements. A full, controlled grind schedule will be used to eliminate sub-surface damage ensuring maximum material strength and figure stability. Grinding will be accomplished using both "small" tools under computer control and large tools for bridging/smoothing and end figure control. In grinding, Raytheon will remove the ~60μm of material necessary to take off the machining damage from generation, bring the two elements into coarse alignment, and impart the best fit quadratic shape to the two elements. Following grinding Raytheon will remove the grinding subsurface damage by polishing the optic with large compliant laps. After polish-out is complete, all subsurface damage is removed. Raytheon will then polish the final figure, again using computer control for low and mid-spatial frequency errors and large, full length laps for bridging, removing errors of higher spatial frequency than

can be addressed under computer control, and smoothing micro-roughness. These techniques were employed in fabrication the Chandra optics. Particular attention will be placed upon maintaining figure close to the gap between the two optics.

The optical elements will be made longer than the desired final length. This eases the fabrication constraints by making maintenance of figure at the "open" ends of the optics easier. At or near the completion of figuring the excess material will be cut off using a CNC generating machine, and the edges of the blanks will be beveled, control ground, and polished. It is possible that the optics may distort after end-cutting due to the relieving of built in stresses that survived blank annealing. (At present, no information is available regarding this for SXI. The Chandra elements, which were both much larger and flimsier did distort, although all elements did not distort equally).

The AXAF Automated Cylindrical Grinder/Polisher (ACG/P) computer controlled polishing machine, modified for SXI, will be used for the XRT as well. A minor modification to the ACG/P will need to be made to adjust for the larger diameter of the XRT relative to SXI. During grinding and polishing we will hold the XRT optic on the ACG/P using a similar approach to the SXI glass support fixture (GSF). This is essentially a large "can" with three radial supports that preload the optic so that it will not "walk" out of the polishing machine as it is being fabricated, but with a light enough and controlled preload so that the optic does not distort significantly. Again, due to size differences between XRT and SXI, a new GSF will be required. New laps will also be necessary, but only minimal changes, if any, are required of the lap assemblies.

3.1.2.3 Metrology

3.1.2.3.1 Figure and Surface Finish Measurement

XRT metrology will follow the SXI (and Chandra) approach: precision axial profiles will be obtained interferometrically and combined with azimuthal data to produce surface error maps.

Two types of data are require: coarse metrology for grinding, and precision metrology for polishing (figuring/smoothing). Coarse metrology, like SXI, will employ the WEGU coordinate measuring machine (CMM). The WEGU is a three axis CMM that uses a contact profilometer and has an absolute accuracy of about 0.5 microns, rms. In grinding axial profiles will be taken at a variety of azimuthal positions and two azimuthal profiles, one at each end of an optical element (i.e., 4 per blank) will be acquired. Since the WEGU is an absolute CMM, absolute mirror inner diameter data is also provided by the WEGU. The azimuthal profiles (or circularity rings) are combined with the axial profiles (or meridians) to produce the surface error map used for analysis and determination of the following grinding run parameters. No modifications to the WEGU are required for XRT other than an optic support plate and minor software modifications (i.e., new parameter files for the XRT optics).

Precision metrology is acquired with three instruments: the PMI (a Zygo phase measuring interferometer with associated folding optics), the Circularity Test Stand (CTS), and the WYKO micro-phase measuring interferometer. The PMI will measure the axial pro-

files. This instrument will be the same as that used on SXI with the minor modification of some folding optics (to bring the interferometer beam inside the XRT and nearly normal to the optic surface). Spatial sampling is about 0.1 mm. Circularity profiles are provided by the CTS which contains four contacting probes (LVDTs), one for each of the circularity measurement axial locations (the same locations as were used in grinding metrology on the WEGU). CTS modifications for XRT (from the SXI configuration) consist solely of new mounting brackets to support the four probes at the appropriate locations. Diameter data is still provided by the WEGU. The combination of PMI meridians, CTS roundness profiles, and WEGU diameter data is all that is required to piece together the surface error map. Fine alignment betwen the primary and secondary mirrors is determined by fitting Legendre-Fourier polynomials to the surface of each element, where the "one-theta" Fourier terms and the zero and first order Legendre terms are used to determine decenter and tilt of the secondary to the primary. The WYKO is used for measurement of surface roughness. Overlap in instrument bandwidth exists between the WYKO and the PMI, although Raytheon will increase that amount of bandwidth overlap by also measuring optic subapertures with the PMI (at higher axial sampling). All metrology will be calibrated and fully tested.

Finally, a new metrology mount will be designed and built. Again, the approach is to build upon the SXI and Chandra heritage. The optics will be supported on the metrology mount with the optical axis vertical. A three or six point kinematic support system is envisioned. Detailed finite element models will be developed allowing Raytheon to determine the sensitivity of the metrology mount and optic system to gravity, random "setup" loads, temperature variations, etc. A self-weight deflection calibration file (for metrology) will be employed if the self-weight deflection is large enough to be considered significant, as was done for the flimsier Chandra optics.

3.1.2.3.2 Focal Length Testing

The focal length of the XRT will be determined in at least two ways. First, based upon the metrology, the focal length will be computed by raytracing. Based upon estimated metrology the raytracing should be accurate to ~ ±4mm. This is not sufficient to position the detector precisely enough without x-ray testing. Alternative approaches that will be further investigated are two different visible light tests. In the first, simpler test, the telescope aperture is illuminated with a plane wave from an interferometer (e.g. a 12 inch or 24 inch Zygo), simulating a point source at infinity. A CCD detector is used to capture the image. The detector is mounted to an axial positioning stage. One can either measure the size of the ring image formed on either side of best focus and compute the best on-axis focus, or alternatively adjust the axial position of the detector relative to the mirror to find the position of minimum spot size. This approach is being employed on SXI. Preliminary testing with a spherical lens and an annular aperture matching the SXI annulus indicate accuracies of the two different approaches of about ±0.1 mm. Digital processing of the CCD image (not planned for SXI) may improve upon this number. Note that this method of test takes into account the effects of the "large" amount of diffraction due to a highly obscured aperture viewed in visible light.

The second possible visible light focal length determination method utilizes the Hartmann test. This approach was developed at Raytheon in Danbury and used to align the elements of the AXAF Technology Mirror Assembly (TMA), and then used by Kodak to align the elements for Chandra. A laser pencil beam is made to, discretely, scan the annular aperture of the telescope and the focused beam position is measured in the "focal" plane as a function of aperture position by a quad cell detector or CCD. Mirror element alignment errors - tilt and decenter - produce coma which causes the beam at the detector move about a circle as the angular position of the beam at the aperture is varied. The detected beam, though, makes two revolutions of the circle to one revolution at the aperture: alignment errors cause the beam at the detector to move twice as fast in theta as the beam at the aperture ("two theta"). The radius of the motion is proportional to the magnitude of coma. Defocus also causes the beam position to move in a circular path, with a circle radius proportional to the defocus of the detector. Defocus, though, causes the beam at the detector to move with the same rate of angular variation as at the aperture - one theta motion. The sign of the motion (plus or minus one theta) determines whether the detector is forward or aft of focus. Therefore by measuring the beam position at the detector as a function of aperture position and fitting a cosine and sine of one-theta to that position, the axial position of the detector relative to best focus may be determined. The accuracy of this process needs to be estimated and budgeted to compare with the full aperture illumination method to determine which approach offers better performance.

3.1.2.4 Coating

At soft X-ray wavelengths the refractive index of all materials approaches unity. The complex index of refraction $\mathbf{n} \equiv n+ik$ is given by

$$\mathbf{n} \equiv n+ik = 1-\delta+i\beta = 1- ((r_0\lambda^2)/(2\pi))\, n_a\, (f_1-if_2) \qquad (1)$$

where r_0 is the classical electron radius $r_0=e^2/mc^2$, n_a is the number density of atoms in the material, and $f = f_1 - if_2$ is the (complex) atomic scattering factor, which is approximately equal to the number of free electrons per atoms. The number density of electrons is then given by $n_a f$.

Because of the λ^2 dependence, the values of both δ and k are quite small at wavelengths shorter than 1000Å. Thus the refractive index is close to unity. Note also that the index is less than one, implying that there is a critical angle for near-grazing incidences, below which total *external* reflection will occur. This limit forms the basis for one of the two main techniques of x-ray imaging, *grazing-incidence optics*.

By applying Snell's law, we find that the critical angle for total external reflection is given by

$$\cos \theta_c = n. \quad (2)$$

If the imaginary part of n is small, then the critical angle is given approximately by $1-{}^1/_2\theta_c^2 = 1-\delta$ so that

$$\theta_c = (2\delta)^{1/2} \quad (3)$$

From Eq. 1 we find that

$$\delta \cong (r_0/2\pi)\,\lambda^2\, n_e = (r_0/2\pi)\lambda^2\, n_a\, f. \quad (4)$$

Note that θ_c turns out to be linearly proportional to the wavelength of the incoming x-rays. This means that at shorter wavelengths, or higher energies, the angle of reflection becomes smaller. For example, a grazing-incidence mirror made of, or coated with, beryllium will reflect 0.5 keV x-rays at angles up to 3°. The same mirror will reflect 3 keV x-rays only at angles less than about 30 arcmin, or 0.5°.

The form factor f is dependent on the choice of material making up the mirror surface, so that the reflectance as a function of wavelength, and the value of the critical angle, varies with the choice of coating material. For the mirror design parameters being used in the XRT, we have calculated the curves of R vs.λ for a wide range of coatings; four representative curves are shown on Foldout 3, for silicon, nickel, iridium and gold. These cover a large range of cut-off energies, from ~ 2 – 7A (6–2 keV).

Foldout 3 shows the mirror response for four different coatings: Si, Ni, Au and Ir. The location of important emission lines are indicated. Based on the scientific objectives of the Solar-B mission, a coating that gives a broad energy response and a high energy cut-off is preferred, while maintaining a high reflectivity in the vicinity of 1 keV. This indicates that iridium is a good choice for the XRT mirrors. However, silicon has a higher reflectivity between 8 and 20Å and might also be considered.

3.1.3 X-ray Mirror Mount

3.1.3.1 Mirror Flexures

The baseline XRT X-ray optic mount design consists of three flexures bonded to the mirror and attached to the front end of the telescope tube. Since the flexures are bonded to the mirror, a low coefficient of thermal expansion (CTE) material like Invar is desired. Preliminary calculations indicated that Invar flexures which have sufficient strength to withstand launch loads would be too stiff to provide the needed radial flexibility. Titanium was chosen for its high yield strength ($8.62\text{x}10^8$ Pa, 125,000 psi) and its relatively low elastic modulus ($1.1\text{x}10^{11}$ Pa, $16\text{x}10^6$ psi), and the flexures will be mechanically fastened to Invar pads bonded to the mirror. A number of factors influence the design proc-

ess: available space, launch loads, assembly tolerances, material strength, and optical performance during orbital conditions are the main considerations.

Analyses were performed both with and without flex-pivots at the mirror attachment ends of the flexure blades. The results show that a simple blade design meets the strength requirements of launch loads and is sufficiently compliant to meet optical performance requirements. This design eliminates the need to machine complex spokes. All structural modes have frequencies over 100 Hz.

A finite element model of the mirror was generated, and three flexure configurations were analyzed. Two of the flexure designs were simple blade flexures, and one had an integral flex-pivot at the mirror end. The flexure properties are given in Table 3-1. The material for all three cases is Titanium.

Table 3-1 Flexure Dimensions

	Blade Dimensions (mm)			Pivot Spokes (mm)		
	Length	Width	Thickness	Length	Width	Thickness
Flexure Design 1	38.1	17.78	1.524	-	-	-
Flexure Design 2	38.1	17.78	1.524	6.07	4.0	1.27
Flexure Design 3	50.8	25.4	1.143	-	-	-

The models were run for acceleration loads in all three axes (section 3.1.3.1.2.1), assembly tolerance displacements at each flexure attachment to the telescope tube (section 3.1.3.1.3), gravity induced errors (section 3.1.3.1.4), and structural modes (section 3.1.3.1.5). The acceleration loads are 32 g□s in the lateral directions and 45 g's in the axial direction.

The analyses performed to date show that flexure design 3 meets the strength and performance requirements without incorporating a flex-pivot in the flexure, although some benefit exists in doing so. Also, gravity induced deformations produce errors at the focal plane less than 2 pixels. All three flexure designs have structural modes greater than 100 Hz.

A detailed analysis of the attachment of the flexures to the glass is necessary and will be performed in Phase B

3.1.3.1.1 Sensitivity to External Loads

The Solar-B XRT X-Ray optic is supported on three flexures bonded to the outer surface of the mirror at its mid-length. The flexures are designed to provide support at each mounting point in the axial and tangential directions, while remaining flexible in the radial direction. In this way the support approximates a kinematic mount. A perfect kine-

matic mount does not induce any deformations of the mirror if the support points are displaced; only rigid motion of the mirror occurs. Such a mount would have three support points, infinitely stiff in the axial and tangential directions, and no stiffness in the radial directions, as well as no rotational stiffness. In practice, the flexures have some stiffness in the non-kinematic directions. The effects of non-kinematic loads on the focal plane image are presented here, to use in determining an acceptable flexure design.

The idea behind a kinematic mount is to fully support the mirror in the telescope tube, while completely isolating it from loads which would distort it. By definition, a perfect kinematic mount cannot impart any forces or moments in non-kinematic directions, since no stiffness exists in those directions. Three support points which only restrain the mirror in the axial and tangential directions accomplishes this. For example, if one of the support points is displaced axially, the mirror pivots about an axis running between the two other supports, and results in a rigid body tip of the mirror, without any reaction forces or distortions. Similarly, a tangential displacement at one point causes the mirror to translate and rotate, moving radially inward at one of the other supports, and radially outward at the other remaining support, again without any reaction forces or distortions

Since a perfect kinematic mount does not exist, flexures are used, which are stiff in the axial and tangential directions, and sufficiently flexible in the other directions, based on the operational conditions, assembly tolerances and performance requirements of the telescope. The first step in accomplishing this is to determine the effects of loads in the non-kinematic directions on optical performance. The resulting sensitivities can then be used to apportion the allowable loads that can be imparted to the mirror. An acceptable flexure design can then be sought based on these loads, assembly tolerances, and operational conditions of the telescope. A typical flexure design is shown in Foldout 4. It is stiff in the axial and tangential directions. Flexibility in the radial direction and for tangential moments is provided by weak axis bending of the flexure blades. Axial moments are relieved by torsion of the flexure blade. Radial moment relief, if required, is accomplished with the flex-pivot spokes at the mirror attachment.

A model was developed for the baseline mirror assembly design. Unit non-kinematic forces and moments were place in each of the support locations. The resulting predicted mirror surface deformations were used as input to a raytrace program developed for designing the AXAF optical system (see Figure 3-2). The predicted change in imaging performance is outlined in Table 3-2 below:

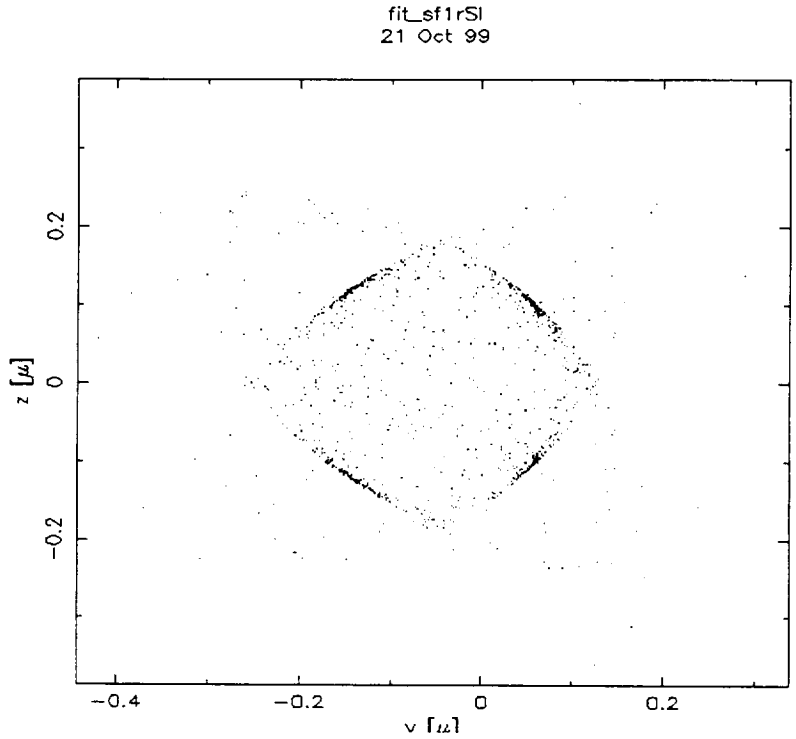

Figure 3-2 Typical Spot Diagram

Table 3-2 Image Distortion Due to Unit Non-kinematic Loads

		surface displacements			
		max rad disp	min rad disp	Pk-pk	RMS spot size
Loadcase	load value	(mm)	(mm)	(μ)	Diameter, μ
1 radial force	1 N	1.19E-04	-7.48E-05	0.194	0.478
3 radial forces	1 N	2.42E-05	-2.10E-05	0.045	0.290
1 radial moment	1 N-M	2.36E-04	-2.36E-04	0.472	1.374
3 radial moments	1 N-M	8.28E-05	-8.28E-05	0.166	0.776
1 tangential moment	1 N-M	2.68E-04	-2.13E-04	0.481	1.267
3 tangential moments	1 N-M	2.65E-04	-2.24E-04	0.489	1.864
1 axial moment	1 N-M	5.13E-04	-5.13E-04	1.026	4.167
3 axial moments	1 N-M	3.67E-04	-3.67E-04	0.733	6.470

A preliminary error budget for non-kinematic loads is 0.25 arc-sec RMS diameter (~3.4 μm) . At the focal plane, an arc-sec is ~13.5μm. The loads are assumed to combine in a "square root sum of squares (SRSS) fashion. For each load direction, the larger of √3 times a single load, or the three point load is used. A loads budget based on the mirror sensitivities is presented in Table 3-3. These loads are used in determining flexure dimensions and may be redistributed as the flexure design matures.

Table 3-3 Preliminary Mirror Loads Budget

Loadcase		Image RMS spot size(Unit Case)	√3 x single case	Allowable load	ImageRMS spot size
	load	Diameter, μ		(N or N-M)	Diameter, μ
1 radial force	1 N	0.478	0.828	2.578	2.578
3 radial forces	1 N	0.290			
1 radial moment	1 N-M	1.374	2.380	1.344	1.344
3 radial moments	1 N-M	0.776			
1 tangential mo-	1 N-M	1.267	2.195	0.744	0.744
3 tangential mo-	1 N-M	1.864			-
1 axial moment	1 N-M	4.167	7.218	1.223	1.223
3 axial moments	1 N-M	6.470			
RSS					3.240

3.1.3.1.2 Sensitivity to Temperature Changes

The Solar-B XRT X-Ray optic is evaluated for optical performance degradation due to temperature variations in the optic. The optic is modeled as Zerodur, with a coefficient of thermal expansion (CTE) of 0.1×10^{-6}/°C. Four cases of temperature variations were run on the ANSYS model of the mirror. A kinematic mount consisting of three axial and tangential restraints were used. The temperature cases are as follows:

- Linearly varying temperature from –1°C to +1°C across the diameter
- Linearly varying temperature from –1°C to +1°C along the length
- Radially varying T=1°C*R/Rmax
- Uniform +1°C temperature increase

The resulting mirror surface deformations were used to perform raytraced images. These results can then be scaled to on-orbit temperature predictions to evaluate on-orbit performance. RMS image diameters are presented in Table 3-4 at the nominal focal plane

and at the location of minimum RMS spot size. The focus change for minimum RMS is also given.

Table 3-4 Raytrace Results for Unit Thermal Cases

Load Case	RMS Image Diameter at Nominal Focus, μ	RMS Image Diameter at Best Focus, μ	Focus Change μ
+/- 1°C Diametral Gradient	0.1687	0.1687	0.0086
+/- 1°C Axial Gradient	0.2027	0.1405	-1.1607
1°C Radial Gradient	0.3786	0.1648	2.7074
+1°C Uniform Temperature	0.0682	0.0012	0.5414

These image diameters can be used to derive allowable temperature gradients in the mirror. For example, using a total error budget for thermal deformations of 0.25 arc-sec (3.4μ), the budget for all thermal variations combined might look like that presented in Table 3-5. The actual budget is dependent on the thermal analysis results. The nominal focus values are used for conservatism. Thermal control is expected to be better than the variations budgeted in Table 3-5 (see section 6).

Table 3-5 Typical Error Budget for Temperature Variations of the X-Ray Mirror

Load Case	**Multiplier for Temperature Variation Case**	**RMS Image Diameter at Nominal Focus, μ**
+/- 1°C Diametral Gradient	3	0.5060
+/- 1°C Axial Gradient	3	0.6082
1°C Radial Gradient	5	1.8932
+1°C Uniform Temperature	4	0.2727
Absolute Sum		**3.2802**
RSS		**2.0699**

3.1.3.1.2.1 Launch Loads

Stresses due to launch loads were calculated by applying accelerations of 32 g's in the lateral directions and 45 g's in the axial direction. Results of the analyses are presented in Table 3-6.

The allowable stress for the titanium flexures is based on both the yield and the ultimate strengths. A safety factor of 2.0 on yield strength and 1.25 on ultimate strength are used.

The yield stress of titanium is 862 MPa (125000 psi), and the ultimate strength is 931 MPa (135,000 psi), making the limiting allowable stress 465 MPa (67500 psi) based on ultimate strength. All configurations meet this allowable.

Table 3-6 Launch Load Stress Results

		Mirror Max Stress		Flexure Max Stress	
Flexure Case	Load	MPa	psi	MPa	psi
Flexure Design 1	32 g's X	15.89	2305	293.53	42571
	32 g's Y	17.75	2574	311.70	45206
	45 g's Z	4.25	617	39.41	5716
Flexure Design 2	32 g's X	9.58	1390	410.01	59465
	32 g's Y	10.54	1529	424.73	61600
	45 g's Z	4.25	617	97.27	14107
Flexure Design 3	32 g's X	18.66	2706	282.38	40954
	32 g's Y	20.85	3024	325.02	47139
	45 g's Z	4.26	618	36.57	5304

The analysis was performed with a coarse mesh, which is not conducive to modeling bond zones. Detailed analysis of the bonded attachment of the flexures to the mirror will be performed in Phase B. Hand calculations based on the loads at the flexure attachments are presented below in, Table 3-7 for a range of attachment diameters.

Table 3-7 Estimated Glass/Bond Stresses at Flexure Attachments

		Pad Diameter					
		20 mm, 0.787 in 0.787 in		25 mm, 0.984 in 0.984 in		30 mm, 1.181 in	
		Stresses					
		MPa	psi	MPa	psi	MPa	psi
Flexure Design 1	max shear stress	14.692	2131	7.879	1143	4.766	691
	max normal stress	5.686	825	2.911	422	1.685	244
Flexure Design 2	max shear stress	8.701	1262	4.805	697	2.984	433
	max normal stress	5.592	811	2.863	415	1.657	240
Flexure Design 3	max shear stress	17.206	2495	9.172	1330	5.518	800
	max normal stress	5.783	839	2.961	429	1.713	248

The above results show that there is a reduction of stress levels with the flex pivots, but reasonable stress levels can be obtained by increasing pad diameter. The final pad size and design configuration, with or without flex pivots will be determined in Phase B.

3.1.3.1.3 Assembly Tolerance Errors

Optical Performance for assembly induced deformations are calculated for the three flexure designs. Displacements of 0.076mm (0.003") and rotations of 1 arc-min are applied to the base of each flexure in a number of combinations, but separately in each degree of freedom. The maximum values for each degree of freedom are then combined by taking the square root of the sum of the squared values (SRSS). A budgeted value for combined assembly tolerances is 4 microns at 68% encircled energy. The results are presented in Table 3-8. Only flexure design 3 meets this budget with the applied displacement tolerances. Also, comparisons between design 1 and design 2 results indicate that the addition of pivot spokes to design 3 might reduce the errors induced by axial displacements.

Table 3-8 Raytraced Spot Sizes for Assembly Tolerance Cases

	68% Encircled Energy Diameter, microns		
Description	Flexure Design 1	Flexure Design 2	Flexure Design 3
Maximum of radial displacement cases	7.092	6.799	1.954
Maximum of tangential displacement cases	7.398	7.083	2.000
Maximum of axial displacement cases	1.207	0.450	2.338
Maximum of radial rotation cases	0.694	0.967	1.425
Maximum of tangential rotation cases	0.344	0.326	0.092
Maximum of axial rotation cases	0.658	0.664	0.203
SRSS SUM	10.369	9.903	3.920

3.1.3.1.4 Gravity Induced Errors

The performance of the XRT mirror in gravity oriented in X, Y, and Z directions is summarized in Table 3-9. Although these errors are not present on orbit, it may be necessary to test the telescope prior to launch. The flexure designs have little effect on the 1-g performance, as it is very close to the performance on perfect kinematic mount points (tangential and axial restraints only). The highest of these is less than 1 pixel (13.5 μm).

Table 3-9 Gravity Induced Errors of Flexure Mounted Mirror

	68% Encircled Energy Diameter, microns		
Description	1-g X	1-g Y	1-g Z
Flexure Design 1	6.38	6.54	0.959
Flexure Design 2	5.65	5.85	0.959
Flexure Design 3	6.95	7.13	0.963
Ideal Kinematic Mount	6.19	6.13	0.842

3.1.3.1.5 Structural Modes

The mirror was analyzed for structural modes with the three flexure designs. All three designs have modes with frequencies above 100 Hz, as shown in Table 3-10 below.

Table 3-10 Structural Modeshapes and Frequencies

		Flexure Design 1	Flexure Design 2	Flexure Design 3
Mode	Description	Frequency - Hz		
1	Lateral Translation	216.3	159.5	202.7
2	Lateral Translation	216.3	159.7	202.7
3	Axial Rotation	342.6	242.8	323.6
4	Mirror Ovalization	443.8	432.2	440.2
5	Mirror Ovalization	444.0	432.4	440.4
6	Out-of-plane Ring Bending	561.6	523.0	554.2
7	Out-of-plane Ring Bending	561.7	523.3	554.3
8	Axial Translation	853.3	703.5	798.8
9	Mirror Trefoil	1192.0	1188.3	1189.7
10	Mirror Trefoil	1202.2	1201.3	1202.0

3.1.3.2 Mounting Procedure

The following procedure describes in detail the philosophy and mounting scheme for the optical elements in the SolarB XRT instrument. The visible light optics and the x-ray optic have to be mounted such that their respective images fall within 1 arcmin of one another. The focal length for the optics is 2.7 M, which translates to an axial concentricity of one optic relative to the other of 0.810mm.

Both optical assemblies will be mounted off the mirror support. The mirror support will have a single reference plane that all measurements and final machining is based on. This reference plane shall hold the x-ray optic, and control the focal length of the XRT telescope. The mirror support will have a second parallel surface, which supports the visible light optical bezel assembly. (See Figure 3-3) The visible light optical interface consists of a parallel surface with a lead in pilot diameter to control the bezels radial position. The visible light optics shall be mounted in a single bezel machined and assembled by ROSI. Prior to the installation of the optics into the bezel, ROSI will supply the final machined bezel to SAO so that a mechanical fit and tolerance check can be performed prior to match drilling and pinning the bezel to the mirror support. The bezel will be shipped back to ROSI for the installation of the two optical elements. Once ROSI returns the visible light bezel assembly with optical elements installed , the bezel assembly

will be mounted to the mirror support. Next the x-ray optic will be prepared for mounting to the mirror support. At this point the titanium flexures are mechanically attached and pinned to the mirror support. The x-ray optic will be placed in mounting fixture. The mounting fixture will be used to adjust and align the optic to the designed orientation for bonding of the three (3) invar pads. The fixture uses a three point adjustable mounting scheme to support the x-ray mirror relative to the mirror support reference plane. The fixture has three (3) radial adjustable screw supports, which align the x-ray optic to the pilot diameter of the visible light bezel controlling the concentricity of the two optical assemblies. Prior to bonding of the invar pad flexure assembly to the x-ray optics, precision measurements of the orientation and alignment between the two optical elements will be performed to verify the required alignments. Once it is oriented correctly, the titanium invar flexure assembly will be bonded to the x-ray optical body. The whole system will stay in the fixture until the epoxy has set.

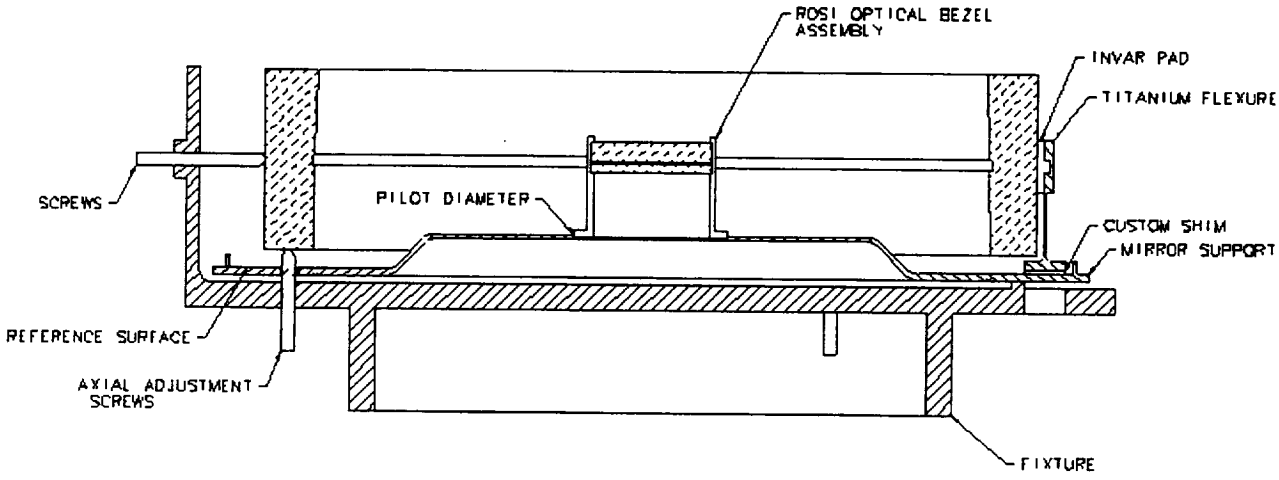

Figure 3-3 X-ray Mirror Alignment and Bonding Concept

3.1.4 X-ray Baffle System

The XRT x-ray optical system consists of a modified Wolter-I mirror system. The mirror system is made up of 2 surfaces of revolution, the forward one is very close to a paraboloid, while the second one is close to an hyperboloid. The shallow angle of both mirror sections permit the glass to reflect the incoming x-ray without absorbing the energy. A consequence of the design is a path for stray light to enter the telescope either by reflecting off only one of the surfaces or simply passing straight into the aperture unimpeded. This added light raises the optical background, producing lower contrast images and ghosts. A preliminary optical ray trace, combined with SAO experience with the AXAF (Chandra) mission suggest that two baffles, one placed at the mirror node, and the other at the rear mirror surface, will be enough to ensure that the most of the stray light is

eliminated. Selection of the exact location, number and size of the baffles will be determined in phase B.

The usable x-ray aperture annulus, is very narrow, less than 1mm wide at the mirrors, where the baffles will be placed. This presents a design, fabrication, and alignment challenge. The baseline baffle system assembly is mounted on the anti-sun surface of the mirror. Options for careful mounting and adjustment of this system will be examined in phase B.

3.2 Visible Light Telescope

3.2.1 Requirements

It is essential that the XRT be capable of coalignment with the optical telescope. We will use two methods to accomplish this. First, a blue neutral-density filter near the focal plane will produce a sharp, low contrast image formed by the grazing-incidence telescope. Second, we have baselined an optical system similar to that flown on *Yohkoh*. The main optical requirement is to provide a visible light image with spatial resolution compatible with the 1" pixel size of the focal plane CCD detector. To minimize the size of the optic it is best to work at short wavelengths, such as ~ 430nm. Our baseline is an achromat lens the same focal length as the GI telescope.

3.2.2 Design

The lenses are simple achromats designed to correct axial color between the wavelengths 405 and 490 nm. It is also corrected for spherical aberration at 431 nm as well as coma over the half-degree field. The diameter is 50 mm and the focal length 2700 mm; the system is therefore f/54. The bandpass of the white light telescope is restricted to 10nm, as described in section 3.5.

The choice of glasses is based on minimizing sensitivity to radiation darkening. To this end, fused silica is the best known material. For the other material, SF16 is often used in such applications. The performance of this system is shown in Foldout 3.

3.2.3 Mounting

The lenses of the visible light telescope will be pre-aligned by Raytheon and placed in a bezel to simplify the mounting and alignment. The mounting flange on the bezel will be a precision turning, aligned and concentric to the telescope line of sight. The bezel will be mounted into the mirror support and used as a reference surface for the co-alignment of the x-ray optic.

3.3 Visible Light Shutter

3.3.1 Requirements

The visible light shutter assembly permits light in the small visible spectrum band to enter the main shutter. The main shutter can then control the exposure timing. When closed, the visible light shutter must provide adequate light blocking.

Table 3-11 Visible Light Shutter Requirements

Characteristic	Requirements	Expected Performance
Open/Close Time	<1.5 sec	0.2 sec
Light Blockage	99.9%	>99.9%
Induced Torque Noise	<0.2Nm	~0.1 Nm
Lifetime Electrical/Mechanical	360,000 cycles	1,000,000 cycles

3.3.2 Design

The visible light shutter assembly mounts on the sun side of the x-ray mirror support. It is completely accessible, and removable, from the front of the telescope, without having to affect the optics assembly. In addition to controlling the visible light, it provides the structural support for the visible light pre-filter.

The assembly consists of an oval aluminum shutter blade blocking the light from entering the instrument, two limit switches, a stepper motor, and shutter housing. The shutter blade uses multiple light bounces to guarantee that the visible light blockage requirement is met. To open, the shutter blade rotates through a 60° angle at a rotational speed of 2.0 rad/sec. The direct drive double-wound stepper motor rotates the shutter blade through a single mounting flange, which is attached to the shutter blade. The limit switches verify that the shutter blade is in the open or closed position. The fail-safe mode for the shutter assembly is in the closed position. If the first winding of the stepper motor fails, the second winding will be used place the shutter in the fail-safe position. If there is a failure in the primary winding, the visible light shutter will be left in the fail-safe mode for the rest of the mission. (See Foldout 2)

The complete visible light shutter assembly is a self-contained unit, which can be installed and removed from the SolarB XRT instrument without effecting any other sub system. The shutter assembly is mounted to the mirror support with five captive screws. All of the electrical control circuits will be supplied through a miniature electrical connector allowing for easy removal and installation of the visible light shutter assembly.

3.3.3 Operation

The operational scheme for the visible light shutter is as follows. Starting with the shutter in the closed position and the closed limit switch is engaged: The motor is powered off, the detent torque of the stepper motor holds the shutter in the correct orientation. Opening the shutter simply requires the stepper motor to step through two 30° steps. When the shutter blade completes the second the open limit switch signals that the blade is in the correct open position. The motor power is then turned off for as long as the exposure requires, again relaying on the detent torque to hold the shutter blade in this orientation. When the exposure is finished the stepper motor is rotated back to the closed position, re-triggering the closed limit switch. If at any time these functions do not occur and it is found to be a fault in the stepper motor, the second stepper motor windings will be used to position the shutter blade back to the closed position and the shutter will not be re-used again during the mission.

3.3.4 Testing

1) Life cycle testing of the shutter's operational mechanical and electrical components. This includes the testing of the double wound stepper motor and dual limit switches.

2) Prototype: Shake testing of the shutter system for survivability during launch, shipping and handling. Included in the test is the mechanical and electrical function testing after each shake test.

3) Prototype: Light leak testing of the shutter will be done in the light leak chamber, which is used to test the XUV filters. The shutter will be mounted on an adapter plate, a known amount of light will be supplied to the input of the shutter and the amount of light entering the chamber will be measured.

4) Prototype and Flight: Torque margin tests.

5) Flight Models: In addition to workmanship and performance testing, the flight models shall be subject to the same acceptance and environmental testing as the rest of the instrument.

3.3.5 Trade off, buy versus build

The decision of whether to buy an existing component, modify it for our needs, and fly it, or design a system from scratch was examined during Phase A. The proposed instrument had a modified commercial shutter. When the suitability of that system was examined in detail, it was found that significant modification was required in order to make the unit fit our needs and achieve qualification. Instead we examined a simple shutter that we would design and fabricate. What the commercial unit offered, that the simple system lacked, was a wide range of usable shutter speeds. Since this device does not control the exposure timing for the visible light images, this capability was not important.

3.4 X-ray Filters, Front Aperture and Focal Plane

3.4.1 Requirements

The XRT prefilter serves two purposes: a) to reduce the amount of visible light entering the telescope (10^{-4} visible light rejection needed), and b) to reduce the heat load on the optics and at the focal plane (10^{-3} visible light rejection needed). In general, because the corona is so faint relative to the solar visible light, accomplishing requirement (a) automatically fulfills requirement (b). We will therefore concentrate on examining this condition. However, the choice of prefilter materials has an effect on the response of the telescope as a function of soft X-ray wavelength. This in turn affects the response of the telescope to source plasma temperature, and must therefore be taken into account when choosing the prefilter design.

The focal plane filters also serve two purposes: a) to further reduce the amount of visible light reaching the focal plane (10^{-8} visible light rejection needed), and b) to limit the X-ray wavelength passband, in a manner that will provide useful plasma diagnostics for solar observations. It is also useful in some situations to have a focal plane filter that greatly reduces the overall throughput, to avoid saturation of the detector.

Competing with the requirement to reject as much visible light as possible, is the desire to transmit as large a fraction of the X-rays as possible at a given X-ray wavelength. In addition, the filters must be physically strong enough to survive launch, and they must be able to survive for many years in the space environment. This often means that filters are thicker than desired, and that the mounting hardware must be specially designed for filter survival.

3.4.2 Design

Table 3-12 shows the filters presently under consideration for the front aperture and focal plane. The thin Al front filter has a polyimide backing to strengthen it. This reduces the long wavelength transmission, but does not significantly affect the performance. For the focal plane filters we use polyimide where the strength is needed and mesh otherwise. The focal plane filter mechanism has 6 filter positions in each of two wheels. One position in each wheel will be open leaving 10 available filter positions.

Table 3-12 XRT Filter Properties

Name	Material Thickness(A)	Backing,Thick (Å)	Heritage
Entrance	Al2O3 (50), Al (1.0 x10^3)	Polyimide (1.2x10^3)	SXI
Thin Al	Al2O3 (50), Al (1.5 x10^3)	Polyimide (2.0 x10^3)	SXI, TXI
Thick Al	Al2O3 (50), Al (1.16 x10^5) Al203 (50)	Mesh, 82%	SXT
Thin Be	BeO (50), Be (6.0 x10^4) BeO (50)	Mesh, 82%	SXT
Thick Be	BeO (50), Be (2.4 x10^6) BeO (50)	Mesh, 82%	SXT
WL	SiO2 (2.5 mm), ML coating		TRACE
Carbon	C (6.0 x10^3)	Polyimide (2.0 x10^3)	NIXT
DAG Filter	Al2O3 (50), Al (2.93 x10^3) Si (29.3), Mg (2.07 x10^3) Mn (5.62 x10^2), C (1.9 x10^2)	Mesh, 82%	SXT
Thin Mg	MgO (50), Mg (1.5 x10^3) MgO (50)	Mesh, 82%	
Titanium	TiO2 (50), Ti (2.0 x10^3)	Polyimide (2.0 x10^3)	
Neutral Density		Mesh, 8%	SXT
Open			

Table note: 50 Å oxide layer included on all exposed metal surfaces. Indices of refraction for filter materials obtained from Lawrence Berkeley National Labs web page at: http://www-cxro.lbl.gov/optical_constants/

Foldout 3 shows the transmissions of the filters in Table 3-12. combined with the mirror reflectivities shown on Foldout 3 to give the telescope throughput (effective area vs. wavelength). We will choose a mirror-filter set that provides for diagnostic capabilities over a wide range of temperatures and a large dynamic range in intensity.

3.4.3 Heritage

All the filters under consideration are available from Luxel Corp. Table 3-12 lists the missions that have flown particular filters. We plan on have duplicates of the most commonly used filters in the filter wheel; 6-8 different filters will be flown.

3.4.4 Acoustics Issues

One of the critical issues that faces any telescope operating in the x-ray is protecting the thin system filters from the loads induced by launch. The launch of a rocket produces acoustic forces that are transmitted to the surface of the filters in several ways.

- the acoustic pressure can directly impinge on the fiber membrane,
- the acoustics can set up a standing wave in the tube, resulting in effective amplification at the membrane,
- the vibration of the filter support can force the membrane to move quickly against the surrounding air,
- standing waves in the filter membrane, interacting with the interface between the filter membrane and its support, can tear the membrane.

The standard solution for large pre-filters is to launch them in a vacuum; this was how TRACE operated. In XRT, the x-ray pre-filters are small, covering a thin annular section. Each filter covers less than $1/8^{th}$ of the 1mm wide 0.4m diameter x-ray input aperture. Experience with filters of this size and aspect indicate that they can survive launch.

However, a second set of filters mounted inside the instrument near the focal plane, provide another concern. These are large (50mm in diameter), and are located near the camera end of the tube. Past missions, including TRACE, have launched filters similar to these without taking any precautions. However the Solar B acoustic test levels, and presumably the launch levels, are many times larger than those experienced in previous missions (e.g. 148dB vs. 132dB for TRACE).

3.4.4.1 Mitigation:

The design of the XRT includes several design measures that will reduce the risk of destroying a filter during launch.

- The front of the telescope has a door,
- The front aperture filters are mounted at the base of small slit structures that reduce the amount of acoustic energy that can get to them,
- The focal plane filters will be placed inside a housing to protect them.

Finally a mock-up of the system will be tested in Phase B to determine if the instrument enclosure can reduce the intensity of the acoustical input to safe levels. If we find that the filters are unable to survive this acoustic test, then evacuation of the entire instrument will have to be examined. It is extremely important to know the time history of the acoustic loads expected during the launch, so that a meaningful test can be performed.

A preliminary acoustical analysis of the system has been performed on the system to determine how much attenuation can be expected from the instrument enclosure, the tube, endplates and front door. Examining one of the standard texts on the subject, "Noise Reduction" by Beranek 1960, we found that sound attenuation, in the spectrum of interest, is proportional to the areal density of the enclosure. Our calculations resulted in the prediction of attenuation shown in Figure 3-4. The baseline tube wall, and front door design will attenuate less than 2dB at 20 Hz, attenuation will rise from there to nearly 34dB at 2000 Hz.

The slit structures in front of and behind the front aperture filter membranes will protect the membrane to some degree. Experience at Lockheed in testing the SXI instrument found that this structure was enough to protect the filters at 143dB, even without a front door.

The focal plane filters are further protected by their supporting enclosure, the XRT rear mounting flange, and the camera body. The present plan is to leave either an open filter, or a glass filter in the active filter positions during launch. This will place the fragile filters inside the filter housing. They will be protected from direct acoustical forces, and dead weight loads due to the accelerating column of air.

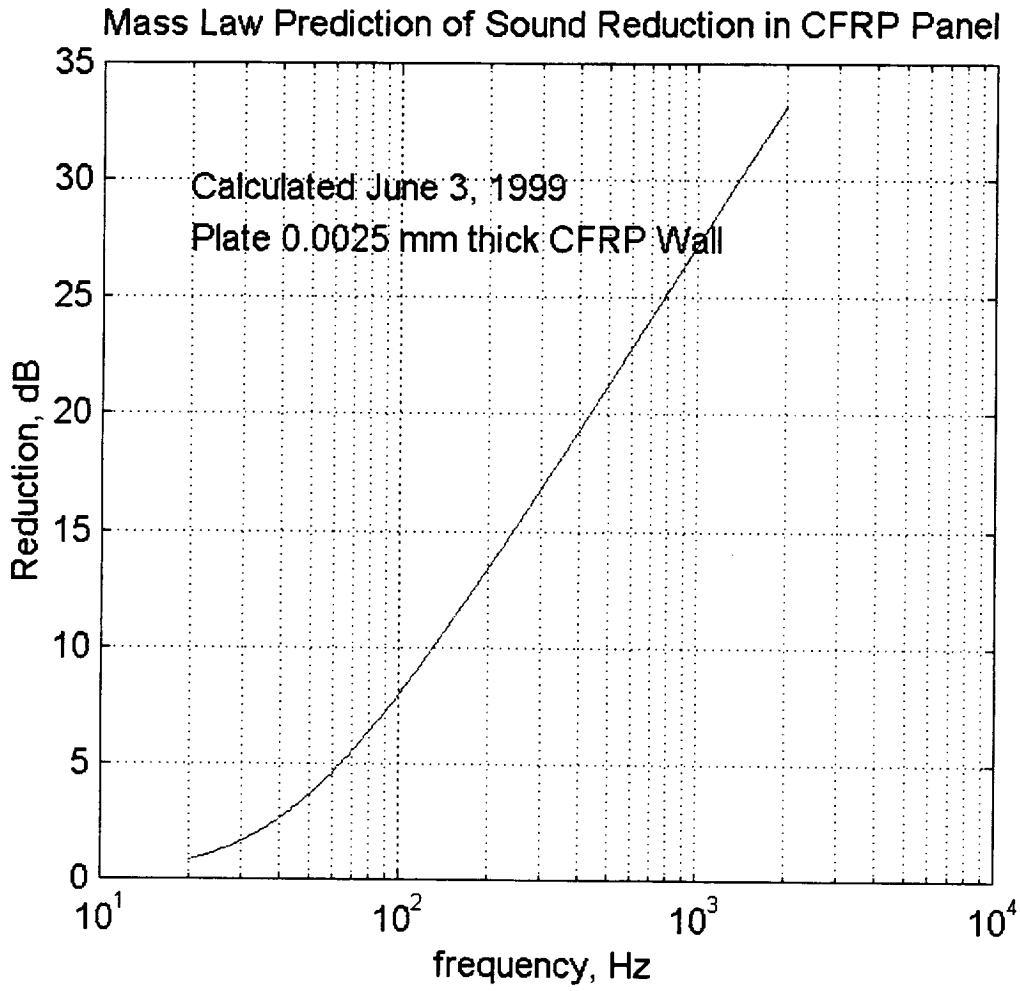

Figure 3-4 Mass Law Prediction of Telescope Structure Attenuation

3.4.5 Testing

Once the set of filters is chosen, a set of engineering filters will be purchased. The filters and one of each witness sample will be placed in vacuum containers. The other witness samples are stored under vacuum in separate containers. These containers will be used for transport storage, and both mechanical and vibration testing. The filters will be photographed in a light leak chamber to estimate the visible light transmission and to record the pin-holes. The engineering filters will be subjected to a full spectrum mechanical, and vibration tests (and acoustic tests as described above). Our baseline design does not call for the filters to be launched under vacuum, so all testing will be held in air. The visible light transmission will be measured after each test to ensure that no significant damage was done.

If the tested filters are shown to be able to survive launch flight filters will be purchased. The flight filters will be photographed in a light leak chamber to estimate the visible light transmission and to record the pin-holes. As a result of these tests the filters will either be qualified for flight or rejected. The visible light transmission must not exceed: 1×10^{-4}

(front filters) or 1 x10^{-8} (focal plan filters). Filters of the same composition will be ranked by their visible light rejection. All the filters be held under vacuum. We will have two (TBR) full sets of flight qualified filters ready for installation 1 week (TBR) before launch.

Table 3-13 Summary of Tests

Test	FILTER	
	Engineering	**Flight**
Acoustic	Qual.	Accept
Thermal Cycle	Qual.	Accept
Light Leak	Qual.	Accept
Mechanical	Qual.	Accept
Vibration	Qual.	Accept
Spatial Unif.		
x-ray	----	Accept
visible	----	Accept
X-ray Trans.	Sample	Accept

3.4.6 Handling Fixtures for XUV Filters:

The XUV filters are very susceptible to damage during installation into test fixtures ,and flight systems. To avoid this problem protective/installation covers will be used during all installation procedures where damage can happen to the XUV filters. The protective/installation covers shall be similar in design to the units used on the TRACE program with very high success. The cover attaches to the frame of the filter, and has a handle that is used to transport the filters from their respective storage containers to the desired location. These covers are left in place until the last possible minute before the system is closed for operation.

3.5 Visible light prefilter

3.5.1 Requirements

The visible light telescope will operate in a narrow wavelength region in the blue, ~430nm. Restricting the passband to ~10nm will maintain achromaticity and provide high resolution performance. The overall throughput will also be adjusted to provide exposure times of order 0.1 sec.

3.5.2 Design

The visible light filter will consist of a 3 mm thick, optical quality fused silica window, with an optical multilayer coating for transmission of the passband shown in Foldout 2.

3.6 Telescope Tube

3.6.1 Requirements

The Telescope Tube provides the main structure that mounts the camera, optics, focus mechanism, mount brackets, thermal control, and electronics box. The tube must be lightweight and provide accessability for assembly and optical alignment / checkout tests. The tube must provide the required cleanliness standards. The structure must withstand test loads, launch loads, and provide a thermally stable platform during on orbit operation. The mounting feet of the tube must provide for ease of alignment to test fixtures and to the SOT for all phases of the Solar-B program. The mounting feet must also provide for convenient attachment and removal from the transportation container, test fixtures, and spacecraft hardware.

3.6.2 Design

The XRT telescope tube assembly consists of the tube, front mount brackets, rear mount bracket, end fittings, accent vents, and access covers. The structure is bonded together except for the access covers, which are bolted into place.

The XRT telescope tube is a tapered tube 2719 mm (107 inch) long. The outside diameters of the front and back ends are 418 mm (16.5 inch) and 330 mm (13 inch), respectively. The tube material is an isotropic laminate of CFRP with a uniform 1.5 mm (0.06 inch) wall thickness.

The telescope tube is attached to the spacecraft at three locations at a single forward point and two rear points. The three mount points are in a plane 244 mm (9.5 inch) from the tube centerline. The forward mount point is 409 mm (16 inch) from the plane of the front OD. The rear mount points are 1514 mm (60 inch) from the plane of the front OD. The side to side spacing of the two rear mount points is 390 mm (15.4 inch). The front and rear mount brackets are quasi isotropic CFRP of various thicknesses. Inserts are provided at the three mount points (see Foldout 1).

The front end of the telescope tube provides a bond area for a titanium flange that supports the entrance aperture covers and optics. The rear end provides bond area for a titanium flange that will support the camera and associated hardware. The tube has four cutouts for electrical and internal hand access. Electrical access is provided at the middle of the tube by 38 mm (1.5 inch) diameter hole. The first hand access hole is located 240 mm (9.5 inches) from the front edge of the tube. Two diametrically located hand access holes are located 2489 mm (98.0 inches) from the front edge of the tube. The diameter of the three hand access holes is 127 mm (5.0 inches).

The Solar-B project requires two telescope tube / bracket assemblies. The first structure is the engineering model for engineering testing and the second structure is the flight model for flight tests and flight.

3.6.3 Performance

3.6.3.1 Weight

The total flight weight of the XRT tube assembly is 11.89 kg (26.2 pounds). This total is comprised of the tube, the forward flange, the rear flange, the front bracket, and the rear bracket. The weights for the parts are listed in Table 3-14, excluding some margin that is carried in the overall weight budget.

Table 3-14 Part Weights for the XRT Tube Assembly

part name	material	weight, kg	weight, pound
tube	CFRP	8.02	17.7
forward flange	titanium	0.38	0.8
rear flange	titanium	2.00	4.4
front bracket	CFRP	0.37	0.8
rear bracket	CFRP	1.12	2.5
ASSEMBLY TOTAL		11.89	26.2

3.6.3.2 Stiffness

The tube assembly stiffness is driven by the requirement that the XRT first mode resonant frequency be above a minimum value when attached to a "rigid" spacecraft. Because of design constraints and weight considerations, SAO has imposed the minimum value of 50 Hz on the XRT. The J-side documentation specifies a minimum value of 100Hz for components attached to the spacecraft. SAO and the J-side are currently negotiating the final requirement for the XRT first mode resonant frequency.

The current stiffness for the XRT is listed in Table 3-15. The table represents the stiffness in the form of the XRT's natural mode frequencies. The table shows two sets of natural frequencies: those as installed on a rigid spacecraft and those without any supports in a free-free condition.

The first three major modes on a rigid spacecraft range from 57 to 83 Hz. These values meet SAO's minimum requirement of 50 Hz. These resonant frequencies are subsequently used to compute the dynamic load response factors of the XRT.

The first three non trivial free-free mode frequencies for the XRT range from 117 to 163Hz. Note that the trivial first 6 rigid body modes of 0 Hz are present, but not listed.

The free-free modes indicate that no significant stiffness is added or required from the spacecraft mount points. The differences between the rigid spacecraft mount and the free-free conditions check with the more simplified, manual beam calculations. The free-free modes are also used as a check of the stand alone XRT structure, even though the free-free configuration is not considered a test or flight configuration. Note that no free-free modal testing is planned for the XRT.

Table 3-15 XRT Mode Frequencies

mode number	XRT mode frequency, Hertz	
	installed on rigid spacecraft	free-free
1	57	117
2	60	134
3	83	163

3.6.3.3 Stress

Studies have been conducted on the structural response of the XRT subject to test and launch loads. The preliminary studies included configurations involving various tube/bracket combinations of aluminum, Invar, titanium, and CFRP. These studies indicated that two issues played a key role in selecting materials for the XRT tube assembly: weight and thermal stability. Stress fundamentally became a secondary consideration because any of the materials listed above could be made to survive launch loads. Overall the XRT tube assembly constructed of CFRP gave us the best performance. When this was determined, we were able to concentrate on the stress analysis of critical areas on a CFRP tube assembly.

The study included finite element analysis of the CFRP tube assembly that included all identified flight weights. The analysis impacted the design by minimizing the bracket weights. The analysis surveyed the stress in the tube, bracket-tube bond lines, brackets, and loads at the structural interface to the spacecraft. All tube assembly stress was found to be within acceptable limits. The stresses are listed in Table 3-16. Note that this analysis is preliminary and is subject to revision as the specific CFRP material selection is made and the design moves forward. Some high joint stresses were predicted in the CFRP. These are reflected in the table. These values will be examined in detail during Phase B.

Table 3-16 Results Summary from Preliminary Stress Analysis of the XRT

Material	allowable stress, MPa (PSI)	maximum stress from all load conditions, MPa (PSI)	factor of safety
CFRP	89.9 (13,000)	83.0 (12,000)	1.08
Adhesive	29.7 (4,300)	13.8 (2,000)	2.15
Titanium	553.0 (80,000)	138.0 (20,000)	4.01

3.6.3.4 Buckling

Studies have been conducted on the buckling response of the XRT. Buckling is a structural issue for the XRT because the telescope tube is an inherently thin walled tube supported primarily at the center with significant camera and optic mass cantilevered from either end. Because buckling stability is driven by the specific stiffness of the structure, CFRP offered the best overall buckling stability characteristics of the candidate XRT tube materials surveyed.

Buckling analysis was conducted by subjecting the finite element model to 1 G loads in the X, Y, and Z directions. The buckling load factors obtained from the analysis were then compared to the G factors associated with launch and test loads to obtain the factor of safety in buckling for each load condition. All buckling load factors were found to be within acceptable limits and are listed in Table 3-17. The analysis also determined that mount design plays a key role in the buckling characteristics of the XRT.

Table 3-17 Results Summary from Buckling Analysis of the XRT

direction	allowable buck-	maximum load fac-	factor of safety
X	74.9	31.0	2.4
Y	159.7	31.0	5.2
Z	302.7	43.0	7.0

3.6.3.5 Thermal Stability

The focal stability of the XRT is dominated by the thermal properties of the tube. Secondary effects include the mounting hardware for the optical elements and the telescope mount brackets to the spacecraft. The critical load case that effects performance is a temperature change across the diameter of the tube. The temperature change produces tube deformation that is directly related to the coefficient of thermal expansion (CTE) of the tube material. This deformation effects performance by essentially tilting the optical elements relative to the focal plane.

Studies were conducted to determine the best way to reduce the effects of the tube deformation resulting from a thermal gradient. Two obvious methods are to: first, reduce the deformation by reducing the temperature change across the tube and second, select a tube that has a low CTE. The first method presents a fixed number of design constraints. While the thermal control design is detailed in another section, is it sufficient to say here that heater power and sensor limitations provide a practical minimum temperature change over the tube. Given that, the only remaining design option is one of material selection.

Table 3-18 presents the CTE for the candidate materials surveyed. The table shows that CFRP has a CTE advantage factor of about 14 on the next best material, Invar LR36, and has an advantage factor of about 270 over aluminum.

Table 3-18 Representative CTE Properties of Candidate Tube Materials

Material	CTE, ppm/°C
quasi isotropic CFRP	-0.1
Invar LR36	1.3
Titanium	9.5
stainless steel	18
Aluminum	24

Our preliminary performance assessments indicated maximum tilts of the order 0.035 arc seconds per °C variation over the diameter of a CFRP tube. This compares to a significant tilt of 0.25 arc seconds per pixel at the focal plane. As part of our material selection study, an aluminum tube with Invar rods was analyzed. The result produced an unacceptably heavy tube (3.4 times heavier than CFRP). Furthermore, this tube would produce a comparable tilt of 0.49 arc seconds per °C variation over the tube diameter. As a practical matter, this means for the tube with Invar rods, the tube would have to be thermally controlled to better than 0.5 °C. Such a thermal requirement is considered difficult to obtain. Note that titanium, stainless steel, and aluminum have much higher CTE's. However, calculations show that XRT will have precise enough thermal control that a invar or titanium tube can maintain the required focus.

3.6.3.6 Moisture Stability

Moisture stability is not an issue for metallic tube assembly materials. However, for a CFRP tube and mount brackets, the material will change dimension as it dries out on orbit. This is a one time moisture diffusion process that shrinks the tube dimensions. These changes will require focus adjustments during the dry out period only. Because the system requires a focus mechanism for other reasons, moisture stability impacts the design in that it is only a factor in determining the maximum travel for the focus mechanism. Moisture stability is not an issue for long-term on-orbit observing.

The dimensional changes that occur in a CFRP tube are a function of the following parameters: The length of the tube (2.719 m); The maximum moisture content (%M) of the material during ground calibration, and the coefficient of moisture expansion (CME) of the material. Knowing these parameters, the impact of moisture stability on the focus mechanism design can be determined. Table 3-19 summarizes these requirements for two exposure conditions of two representative resin systems.

Table 3-19 Summary of Focus Requirements of a Quasi Isotropic Laminate with a 60% Fiber Volume (data courtesy Hexcel Satellite Products)

Exposure condition	Resin system	moisture content, %M	CME, m/m/%M	Focus range requirement μm
room temp, RH 50%, 184 days	Hexel 996	0.091	65×10^{-6} [1]	16.0
room temp, RH 50%, 184 days	Hexel 954	0.122	65×10^{-6}	21.4
70° C , RH 95%, 260 days	Hexel 996	0.360	65×10^{-6} [1]	63.2
70° C, RH 95%, 264 days	Hexel 954	0.630	65×10^{-6}	110.7

Notes: 1. CME from 954 assumed.

Table 3-19 provides a range of focus requirements. Our error budget includes the 21.4 micron value of the room temp, RH 50% exposure condition as a baseline.

3.6.4 Trade off Aluminum vs. CFRP, Titanium vs. CFRP

Although many candidate materials are available for the XRT application, the XRT requires both high specific stiffness and low CTE. To determine the best material, several candidate materials were compared for both specific stiffness and relative thermal stability. The summary is shown below in Table 3-20. Candidate materials reviewed included CFRP, stainless steel, titanium, and aluminum.

The relative specific stiffness listed in the table is from the modulus of elasticity and the density of the material normalized from 0 to 1, with 1 being the best. Stiffness of the XRT design is largely determined by the specific stiffness of the tube. As pointed out in previous sections, stiffness is a critical parameter that contributes to the modal response of the XRT during exposure to launch loads. As the relative specific stiffness of Table 3-20 shows, CFRP is more than twice as effective as the next best material.

The relative thermal stability listed in the table is computed from the inverse of the CTE of the material normalized from 0 to 1, again with 1 being the best. As shown in the table, the relative thermal stability of CFRP is over 100 times better than the closest ranked

material, titanium. The issue to thermal stability, as described in section 3.6.3.5, underscores the role this property plays in the material selection process for the XRT.

CFRP is relatively favorable in both specific stiffness and thermal stability. Regardless of how stiffness and thermal stability are weighted (they are weighted equally in the table), the combination of the two factors produced CFRP as the best overall candidate material. This analysis will be revisited during Phase B to examine the cost issues.

Table 3-20 Material Trade Off Considerations

	relative specific stiffness	relative thermal stability	combined relative stiffness - stability
CFRP	1.00	1.00	1.00
Aluminum	0.43	0.00370	0.00160
Titanium	0.40	0.00943	0.00377
Stainless Steel	0.38	0.00505	0.00194

3.6.5 Issues

Several material options have been examined for the tube structure. The proposed design, and the present baseline use a carbon fiber reinforced plastic (CRFP). At the start of Phase A we examined using either an aluminum tube, or an aluminum tube with invar metering rods. Both options were rejected, either for weight or thermal stability. With the low weight budget, and tight focal requirements, there is little leeway. Later, as part of a cost cutting exercise, we examined a titanium tube. This proved a possible choice, though relaxation of the weight budget would be required, in order to meet similar structural performance as the CFRP. The thermal stability performance is much worse, and better thermal control would be required. This option will be examined during Phase B.

3.7 Main Shutter

3.7.1 Requirements

The XRT focal plane shutter has the following requirements:

- minimum exposure: 2 msec
- minimum shutter blade thickness 0.005".
- shutters a minimum aperture covering the 28 by 28 mm CCD chip
- minimum lifetime is 2 years with a design goal of 5 years at 1,000,000 exposures per year.
- Operating temperature 0 to 40 C with a survival temperature of –20 to +50 C.

Note: The 0.005" thickness is the minimum requirement and is adequate for active region observations. In hot flares the EPIC shutter blade has a residual X-ray transmission. For flare observations, the 0.005" the EPIC shutter transmits $2x10^{-4}$ of 20 MK emission in

XRT (assuming a 100 micron Be analysis filter). For the shortest exposure, the readout time is 2000 times the minimum exposure, implying an additional 40 percent of the hottest flare emission spread over the flare column during readout.

3.7.2 Design

The shutter design is shown on Foldout 2. The shutter uses a brushless DC motor with an integral optical shaft encoder that provides position feedback for commutating the motor and for measurement of the actual exposure.

The brushless DC motor drives a thin aluminum blade with 3 pie shaped openings; a wide, medium, and a narrow opening. Exposures using the narrow or medium openings expose the CCD by moving the opening across the beam in a single motion. Exposures using the wide opening expose the CCD with a separate motion to start and end the exposure.

Table 3-21 Main shutter operating temperatures

Modes	Temperatures
Operating:	0 to +40 C
Survival:	-20 to +50 C

Design Life: 2 years, 5 year goal. 2 exposures per minute is about 1,000,000 exposures per year. Based on our experience with other instruments this should not be a problem. The TRACE instrument takes about 1,300,000 exposures per year and the shutter is very similar. The MDI shutter has taken over 30,000,000 exposures and was life tested to 67 million exposures.

Table 3-22 Shutter Assembly Characteristics

Characteristic	Performance
Blade diameter	0.15M (6.0")
Peak current	200 mA @ 15V.
Peak disturbance torque	113mNm (16 oz-in.)*
Mass	360 grams

*calculated

3.7.3 Heritage

The shutter is an exact copy of the shutter provided by LMSAL for the Triana/EPIC project. The shutter design is based on the very successful shutters flown on SXT, TRACE, and MDI. The MDI shutter has taken over 30,000,000 exposures without difficulty.

3.7.4 Predicted Performance

Exposure Capability:

- Wide Opening (80 degrees)

Exposure(ms)	44	50	60	70	80+
Uniformity(p-p ms)	2.3	1.5	0.7	0.3	0.05

- Medium Opening (17.5 degrees): exposure 10.0 ms, uniformity 1.2 ms p-p.
- Narrow Opening (3.5 degrees): exposure 2.0 ms, uniformity 0.3 p-p.

Exposure Repeatability: +/- 80 us.

Exposure Accuracy

- Wide: ±1 ms for exposure > 70 ms (can be calibrated for shorter exposures)
- Medium: 5%
- Narrow: 10%

Multiple narrow or medium exposures will be possible on a 100 ms cadence.

3.7.5 Testing

The shutter will undergo acceptance testing at LMSAL. LMSAL has designed a control board for testing the shutter and filter wheel. The board uses the parallel port of a PC to interface to the mechanism and provides a functional testbed. After delivery to SAO, the shutter will receive the same battery of tests that the rest of the flight hardware is subjected to.

3.8 Filter Wheels

3.8.1 Requirements

The plan is to build filterwheels for XRT which are exact copies of the filterwheels that LMSAL is providing for Triana (EPIC).

- The filter wheels will have holes for 6 filters.
- The holes are large enough to ensure that the CCD is unvignetted.
- Minimum lifetime is 2 years with a design goal of 5 years at 1,000,000 exposures per year.

3.8.2 Design

The filter wheel design is shown on Foldout 2. The filter wheels use brushless DC hollow core motors with an integral, optical encoder that provides position feedback for commutating the motor and for measurement of the filter position The filter wheel holes are 50 mm diameter to avoid CCD vignetting.

Table 3-23 Filter Wheels Operating Temperatures

Temperatures	
Operating	0 to +40 C
Survival	-20 to +50 C
Flight Acceptance	-10 to +50 C

3.8.3 Heritage

The filter wheel is an exact copy of the wheels provided by LMSAL for the Triana/EPIC project. The EPIC wheels are very similar to the SXT, TRACE and MDI filter wheels produced and successfully flown by LMSAL. The MDI wheel underwent a successful 67 million cycle life test.

3.8.4 Predicted Performance

S/N 01 Measurements:

Table 3-24 Filter Wheels Measured Performance Characteristics

Characteristic	Perfromance
Mass (with encoder)	725 g
Snapover (commutated)	7.4 V
BEMF (commutated average)	6.12 V / rad/sec
Viscous Damping	22mNm/rad/sec (3.1 oz-in/rad/sec)
Hysteresis Drag	53mNm (7.5 oz-in)

3.8.5 Testing

The EPIC filter wheel design has been completed and the first filter wheel has been built, tested, and shaken, proving that the design is robust. The XRT filter wheels will undergo a functional test at LMSAL. LMSAL has designed a control board for testing the shutter and filter wheel. The board uses the parallel port of a PC to interface to the mechanism and provides a functional testbed. After delivery to SAO, the shutter will receive the same battery of tests that the rest of the flight hardware is subjected to.

3.9 Focus Mechanism

3.9.1 Requirements

An examination of the error budget affecting the XRT instrument focus and the mirror mounting procedure quickly suggested that performance risk could be reduced if the system had the capability to focus on orbit. Experience with other instruments, including the x-ray imager on Yohkoh, support this conclusion.

Table 3-25 Focus Mechanism Requirements

Characteristic	Requirement	Performance
Induced CCD Tilt/Mechanism Travel	<1 arcmin over 150 μm of travel	2.3 arcsec over 150 micron
Spring Constant of the flexure plates	N/A	0.8N/μm
Range/Limits of Travel	±150 μm	>150 μm
Force Capacity of drive	N/A	700N (for baseline lead screw)
Life Time (ball screw life)	300,000 cycles	~2,000,000 cycles Determined by test
Lubrication	Meet TBD contamination requirement	Space Grade Grease
Motor Requirements	>0.05Nm	~0.4Nm
Induced Torque Noise	<0.2 Nm	<0.1Nm

3.9.2 Design

The XRT telescope design is such that the only components that matter in setting the focus are the mirror and the CCD. Unlike normal 2-element telescopes, the separation between the two mirrors is fixed since they are fabricated on a single substrate. The visible light telescope will be operated the same way, fixing the separation between the elements and changing the back focal distance. Thus there are 3 options for achieving the desired focal adjustment:

- Move the mirror/lens with respect to the telescope tube,
- Change the telescope tube length.
- Move the CCD or camera with respect to the telescope tube,

Because of the complexity of the mirror mount and its weight SAO rejected the first option. Changing the length of the telescope tube was examined in detail. First we examined making a small portion of the telescope tube from aluminum, a material with a large coefficient of thermal expansion. The aluminum section would have a large heater on it that would drive the temperature to a point that was calculated to force the overall tube length to the desired value. There were several problems with this approach, but it was abandoned for three main reasons:

- Power was required at all times,
- Control was onesided and slow,
- Inducing a tilt was possible, and angular control was impossible.

An alternative approach, still under discussion, would use the baseline focus mechanism design (see below), and instead of moving the CCD would move the camera mounting flange. It must support more weight during testing and launch, but it avoids having an interface in the middle of a mechanism.

Moving the CCD offers one important advantage over other approaches, there is very little moving mass. The options that have been examined, both by Meisei (the Japanese company in charge or fabricating the camera), and SAO involve mounting the CCD on a small moving stage and forcing it back and forth with an actuator. After several design iterations, it was agreed that the focus stage, the moving portion of the mechanism, will be mounted to flexures. The actuation will be accomplished by stepper motor connected to the stage by a lead screw or eccentric cam.

The baseline design (shown on Foldout 2) supports the CCD support plate on 2 parallel, annular diaphragm flexures. These structures would be the responsibility of the camera contractor to construct. The actuator would consist of a standard vacuum compatible stepper motor, and ball bearing set rotating an eccentric spindle. A connecting arm is mounted around the eccentric spindle, moving like the wheel drivers on an old stream engine. A coupling in the connector allows forces only along the direction of desired focal motion to be transmitted to the stage. This coupling also isolates the actuator from any cocking that might result from motion of the stage. A previous design (also shown on Foldout 2) induced the stage to move on a ball screw that was integral to the motor shaft.

The relative advantages of the 2 systems were compared and the eccentric was selected as the baseline design. Though the ball screw provided near unlimited travel length, bound only by the flexures, it required a specialized motor and ball screw design. In addition, the limited motion of the ball screw in order to cover the entire focal range left the system open for friction and wear issues if the small bearing area in the ball screw were starved for lubricant. The range of travel of the baseline system is set by the eccentricity of the spindle. The larger the eccentricity, the longer the range, but the smaller the placement resolution. These factors have to be balanced.

Near the end of Phase A Meisei offered an alternative mechanism design, one that resides entirely within the camera housing. The connecting link pivots on a flexure, and is connected directly the CCD support stage. The motor is mounted right behind the CCD. The CCD header is mounted on a set of 4 small flexure blades. This design option will be reviewed in the early part of phase B.

3.9.3 Predicted Performance

Once the design concept was envisioned, several issues were examined by analysis to help set the mechanism design parameters, and select components. The main concerns were that:

- With the offset drive connection between the actuator and the movable stage, the CCD would be forced to tip, possibly by an unacceptable amount,
- The flexure plates would have an unacceptably high spring force, making the selection of a drive actuator impossible.

To address these concerns an FEA model was made of the system. The model was run for a range of forces sufficient to cover the desired focus adjustment range. Non-linear effects were included in the analysis, however the results are reasonably linear over the range of interest. The results show a tip of less than 0.04 arc-min for a 150μm focus adjustment. This represents an axial displacement of ±0.15 microns across the CCD at the extreme ranges of focus, much smaller than the allowable range of 2-5μm. A force of 185N is required to obtain a focus motion of 150μM. Though the flexures are sufficiently limber to permit the selection of a standard motor, they are stiff enough to produce a mechanism that can withstand the launch and testing loads. The first axial mechanism mode is at 70Hz, and the first lateral membrane mode is over 700Hz.

3.9.4 Testing

Several levels of testing are envisioned. The mechanism has been re-designed to make prototyping it with standard, commercial components possible. We intend to build a brass board version for testing early in phase B. The electronic operation of the brassboard will prototype the flight design exactly, permitting the drive electronics and software to be designed, develop and de-bugged.

Next a full mechanical prototype will be built, either based on modified brassboard components or build with new, possibly customized components. The prototype will be used for life tests, then mounted and put through a battery of environmental tests along with the mechanical test model.

The flight model system will receive the full set of workmanship, acceptance, performance and environment tests that the rest of the system is subject to.

4. Electronics Design

4.1 Overview

The responsibilities of the electronics system are to operate mechanisms as part of taking images with the CCD camera, to accept and execute commands uplinked from the ground, to gather and transmit status information to the ground and to monitor instrument health. Note that the CCD camera is not part of the system being discussed here.

Commanding and communication are done through the Mission Data Processor (MDP) which is part of the spacecraft. Commands are transmitted from the ground to the spacecraft, where they are stored in the MDP. The MDP then sends the commands to the appropriate instrument. As data and housekeeping are collecting, these are sent to the MDP for transmission to the ground.

The instrument contains six mechanisms: the Focal Plane Shutter, two filter wheels, the Visible Light shutter, the Aperture Door and the Focus Mechanism. The Focal Plane Shutter controls the path from both telescopes to the focal plane. The Filter Wheels are also in this optical path. These mechanisms will be used most frequently. The Visible Light Shutter can be opened in order to take visible light images, but this is of secondary

importance to the x-ray path. The Focus Mechanism provides the ability to adjust the focus if necessary. Finally, the door is closed only during launch. The door is opened at the beginning of the mission, and is never closed again.

System status consists of the positions of the six mechanisms, temperatures as reported by thermal sensors located on the instrument and the values of power supply voltages and currents. The evaluation of mechanism positions can indicate whether or not a command was executed correctly. Temperatures or voltages outside of expected limits can indicate possible problems. In some cases, the instrument may be able to take corrective action, such as repositioning a mechanism.

4.2 Mechanism Controller

4.2.1 Requirements

The Mechanism Control Unit (MCU) is involved in all aspects of instrument operation. Communications with the spacecraft are handled here, including receiving commands and transmitting housekeeping. Commands related to mechanism operations are decoded and instructions are issued to the appropriate mechanism. Housekeeping data is continuously gathered and transmitted to the ground via the spacecraft data channel.

The MCU was incorporated in the instrument design after the first concept was developed. Initially, the design had the Mission Data Processor (MDP) on the spacecraft directly controlling all the mechanisms. This scenario created numerous complications. Subsystem and instrument level testing could not easily be done without considerable GSE and high fidelity simulators of the MDP. Hardware I/O was complicated, with long cable runs containing a large number of wires required to connect the instrument to the MDP, thus increasing weight and the chances for signal degradation. Operation of the instrument then also required knowledge of the operation of the MDP, details of which are not available, since the MDP is currently under development.

Without the MCU, the mechanisms in the instrument are a group of subsystems of the MDP, each of which requires a separate integration plan. The MCU groups these into a single system, with a common controller and a common standard interface to the spacecraft. The electrical interface is simplified to being a power connection, a serial connection for commanding, and a serial connection for data reporting. Cable runs to the mechanisms are internal to the instrument, and can be made considerably shorter. The command interpreter in the MCU allows more flexibility in developing and testing commands, as well as in thoroughly testing all the mechanisms prior to integration with the spacecraft.

In particular, the MCU will control the six mechanisms. In the case of all these mechanisms, the MCU will have two functions: to send commands to and monitor the status of each mechanism. In some cases, the commanding is uncomplicated. In the case of the aperture door, it will consist of one command at the beginning of the mission, and will not be operated again. Other mechanisms are more complicated. The Focal Plane Shutter, for example, requires a sequence of commands for each exposure, and must be carefully coordinated with the operation of the Filter Wheels. This sequence of commands will be

repeated frequently.

The MCU is also tasked with collecting housekeeping data from several sources: Mechanism position indicators, mechanism limit switches, thermal sensors, voltage and current readouts and software status. The mechanisms that use position indicators are the Focal Plane Shutter, the Filter Wheels and the Focus Mechanism. These positions must be read out regularly and included in the housekeeping to be reported to the ground in order to verify that the correct position was reached and maintained. Limit switches provide the status information for the Aperture Door and for the Visible Light Shutter, since each of these is either open or closed. In addition to these position indications, there will be a number of analog values reported in housekeeping. These will consist of temperatures, system voltages and system currents. Housekeeping will be read out of the instrument approximately every 2 seconds, on receipt of a request from the spacecraft.

The MCU will maintain a real time clock, which can be synchronized with the spacecraft clock.

The MCU will handle all communication with the spacecraft. The line from the spacecraft to the instrument is a synchronous RS-422 serial line, as is the line from the instrument to the spacecraft. The line from the spacecraft to the instrument will be used for sending commands, for updating software limit tables, for updating flight software, for reading global flags containing spacecraft information. The line from the instrument to the spacecraft will be used to transmit housekeeping to the ground, to select observing tables which are kept by the spacecraft, to provide values for global flags and to notify other instruments of solar flare activity.

4.2.2 Design

The primary tasks of the MCU will be controlling mechanisms and command interpretation. A microcontroller with 64k memory can do this. A core operating system will be kept in one time programmable ROM, and EEPROM will be used for the rest of the flight software, allowing updates in flight if necessary.

Three microcontrollers are being considered:

1) The 80C31 microcontroller is available from several sources. It is a widely used device for control applications. Space qualified versions are available and have been used in flight programs. A controller board using the 80C31 has been developed for another flight program at SAO. This board is a possible candidate.

2) A variation on this board has been developed which uses the Motorola 68HC11A microcontroller.

3) The ESN (Essential Services Node) is based on the UT69R000 microcontroller from United Technologies. This device was developed for Goddard Space Flight Center for space flight applications. Space qualified versions are available and have been used in flight programs. Technical support and some driver software is available from Goddard Space Flight Center.

In all three cases, comparable development tools are available. A detailed evaluation of these three choices to select the one best suited to the requirements of the instrument is continuing. A selection will be made early in Phase B.

4.3 Filter Wheel/Main Shutter Controller

4.3.1 Requirements

This subsystem operates the filter wheels and focal plane shutter as part of taking an image. There are two filter wheels, each having five filters and one open position. The controller selects a filter position in response to a command from the MCU, and rotates the filter wheels to put that filter in the optical path. The positions of the wheels are read into housekeeping to allow verification of the filter selection.

The Focal Plane Shutter has three openings of different sizes, which are selected for different exposure lengths. On receiving a command for an exposure, the controller must position the opening of the appropriate size in a ready position, and then move it across the optical path at a speed which will give the correct exposure time. The selected shutter position and the actual exposure time are read into housekeeping.

Taking images with the CCD camera requires accurate timing and coordination between the CCD camera, the Focal Plane Shutter and the Filter Wheels. Signals indicating shutter and filter wheel status must be available to allow taking images at a high repetition rate. Details of this are discussed below under "Camera Interface".

4.3.2 Design

The Filter Wheel/Focal Plane Shutter controller will be purchased from Lockheed/Martin along with the mechanisms. These mechanisms are also used on the Focal Plane Package (FPP), another instrument on Solar-B. The controller is preprogrammed with the commands mentioned above, as well as several others related to filter and shutter operations. The mechanism positions are read out by the controller on receipt of a command from the MCU. The interface signals include a serial RS-422 command interface (from the MCU), a serial RS-422 data interface (to the MCU), a serial clock (from the MCU), a strobe to enable the controller (from the MCU) and a shutter open/closed status signal (to the MCU).

Table 4-1 Filterwheel/Shutter Control Board Characteristics

Characteristic	Performance
Power Dissipation:	Less than 1 Watt avg.
Voltage:	+5 V at 150 mA peak
	+15 V at 400 mA peak
Operating Temperature:	-40 C to +80 C
Size:	195mm (7.7") square
Mass:	.3kg (0.7 lbs)

4.3.3 Heritage

The electronics interface board is an exact copy of the board LMSAL is providing for Triana/EPIC. The EPIC board is derived from the board LMSAL is providing for GOES/SXI.

4.4 Visible Light Shutter

4.4.1 Requirements

The Visible Light Shutter is a stepping motor based mechanism. It has two valid positions: open and closed. The shutter position is indicated by limit switches. The shutter will be used to take images in visible light using the same CCD camera that takes x-ray images. Because the visible light image will overwhelm the x-ray image in brightness, it is not necessary to block the x-ray image during this exposure. However, for this same reason, it is necessary to ensure that the visible light shutter can be closed.

4.4.2 Design

A simple driver circuit for a stepping motor can be operated at a single fixed speed. Exposure times for visible light images is controlled by the focal plane shutter. The visible light shutter is opened, the CCD is exposed and then the visible light shutter is closed. To increase reliability, the stepping motor will have two windings. Each winding will have its own drivers. The primary winding will be used for normal operation. The secondary winding will be used if the shutter cannot be closed using the primary winding. In the event of a failure of the primary winding, the secondary winding will be used to close the visible light shutter permanently. In this situation, the visible light shutter will no longer be used.

4.5 Focus Mechanism

4.5.1 Requirements

The Focus mechanism is a stepping motor based mechanism. The position is measured by an encoder. Focus will be adjusted interactively from the ground. The position as indicated by the encoder is mainly for informational purposes. Limit switches will be installed at the allowable extremes of mechanism travel.

4.5.2 Design

A simple driver circuit for a stepping motor can be operated at a single fixed speed. As the control and driver circuitry are similar to those used by the Visible Light Shutter, a similar design may be used in both places. Designs developed for other in-house flight programs are being studied for possible use here. The limit switch status and the position indicated by the encoder are read out in instrument housekeeping.

4.6 Door Mechanism Controller

4.6.1 Requirements

As part of the commissioning of the instrument after the initial switch-on of power, the aperture door will be opened. The Aperture Door is operated only once during the mission. As this is a critical step, reliability is a major concern.

4.6.2 Design

The Aperture Door will be opened using a wax actuator. To increase reliability, the wax actuators have a redundant heater circuit. Position is indicated by limit switches. The actuator requires only that power be switched on. Thus, the control circuitry will be a relay to switch on power to the actuator. After switching power on, the MCU will monitor the temperature of the paraffin linear actuator body and the limit switches. When the switches indicate that the door is fully open or the temperature exceeds a predetermined threshold, power to the mechanism will be switched off. For safety concerns, if a predetermined time interval expires before the switches indicate that the door is open, power will be switched off. In this circumstance, the redundant heater circuit in the wax actuator will be switched on.

4.7 Analog Housekeeping

4.7.1 Requirements

There will be approximately 24 temperature sensors on the instrument. There will be at least four voltages and at least four currents to be monitored. These analog values will be converted to digital values for inclusion in the housekeeping. It is anticipated that all the housekeeping will be read out approximately every two seconds.

4.7.2 Design

The design concept is shown in the block diagram below. Analog inputs, consisting of the output of temperature sensors, power supply voltages and power supply currents, are connected to the input of a 32:1 multiplexer. The output of these will go into a 10 bit Sampling Analog to Digital Converter. The Channel Select Logic will step the multiplexer through 32 analog inputs, and will control the timing of the converter. The output of the analog to digital converter will be stored in system memory as part of the housekeeping frame. Designs developed for other in-house flight programs are being studied for possible use here.

4.8 Thermal Control

Heater settings will be controlled by electronic thermostat on each heater circuit. Heater power will be taken from the 28V main power bus. The issue of switching heater power is under discussion. The ability to switch heater power on and off will allow more control over the internal power configuration. In particular, it could be used to limit switch-on surge when instrument power is switched on. However, each additional switch may be considered an incremental compromise of reliability.

4.9 Power Supplies

4.9.1 Requirements

Derive low voltage power for operation of the instrument from the spacecraft power bus. The voltages that will be used by the electronics will be +/- 12 Volts at +/- 0.5A and +5 Volts at 0.5A. EMI filtering will be required between the power supply input and the spacecraft power bus. The ability to switch off power to mechanisms by command from the MCU will be included.

4.9.2 Design

Suitable modular power supplies are available from several vendors. A design used at SAO on the Chandra/HRC flight instrument may be adaptable for use here. An EMI filter design exists for this power supply.

4.10 System Cabling

4.10.1 Connectors

The document entitled "Electrical Design Standard" provided by ISAS specifies that connectors of the following types are acceptable: D-Sub connector of type D_MA, MDM connectors and SMA coaxial connectors. These types will be used when they conform to the appropriate military or NASA standard.

4.10.2 Wire

Wire will be used that conforms to the appropriate military or NASA standards for space

flight.

5. Software Design

5.1 Requirements

The flight software resides in the Mechanism Control Unit (MCU), or processor of the XRT. The design of the software for the XRT MCU is driven by the science requirements, the characteristics of the mechanisms to be controlled, the nature of the electrical interfaces between the MCU and external components and the necessity to protect the XRT from harm. The remainder of this section discusses the requirements and how the software supports them.

5.1.1 Science Requirements

The science requirements which drive the software design are the need to manage telescope configuration, control and report on the timing of CCD exposures, receive, store and execute observation plans and coordinate observations with the other instruments.

5.1.1.1 Telescope Configuration and Exposure Control

The taking of exposures requires selecting filters, selecting shutter slit, the allowing CCD to clear, waiting for the designated time for the exposure to begin, informing the camera to prepare for CCD exposure, operating the shutter, informing the camera that the exposure is finished so that it can start reading out the image, measuring the actual start and duration of exposure and reporting the exposure conditions to the MDP.

5.1.1.2 Observation Plans and Coordination with Other Instruments

The flight software will maintain a catalog of observing scripts. Some will be loaded prior to flight. Others will be uploaded during flight. Scripts no longer needed can be deleted by command. Commands received from the MDP will select the script to be run. If a script is running when a new one is received it will be terminated in favor of the new script.

The flight software will also receive flags and parameters from the MDP which originate in the MDP or in the other instruments. The command script currently being executed may make use of these parameters and flags to alter the course of the observations. The software will include its own flags and parameters in its status messages to the MDP. The MDP may make use of them to affect its operations and provide them to the other instruments.

5.1.2 Control of Mechanisms & Electronics

The flight software controls the door mechanism, the focus mechanism, the filter wheels the focal plane shutter and the visible light shutter. The focusing mechanisms and visible light shutter are operated by stepping motors. The door is operated by a wax actuator and is only operated once -- to open it. The focus mechanism will be operated as required

either by command via the MDP or, if it is necessary to provide intra-orbit focusing changes, the mechanism will be operated via table lookup in the MCU based on orbit phase information from the MDP. The filter/shutter assembly is controlled by the software via a single bidirectional serial interface.

The electronics controlled by the software are the digital and analog multiplexors and the analog-to-digital converter which are used to collect temperatures, voltages, currents, and mechanism positions.

5.1.3 Interface

The software will control interfaces with the MDP, the camera, and the XRT mechanisms. The software supports variable length messages to and from the MDP over a serial synchronous interface. It supports fixed length messages to and from the mechanisms over a serial synchronous interface to select filters and control exposures. The camera is controlled using a single command line and a single status line. The camera CCD has three modes, clearing, exposing, and dumping. The software controls the transitions form clearing to exposing mode and from exposing to dumping mode by raising and lowering the command line. The transition from dumping to clearing is determined by the camera electronics and is indicated by the camera status line.

5.1.4 Reporting on Status

The software maintains a status table which contains readings of mechanism positions, temperatures, voltages and currents as well as any other mechanism status. Upon request from the MDP, the software sends status information to the MDP for its use and for transmission to the ground. The frequency of the status reporting is presently set to every two seconds.

5.1.5 Instrument Safety

As well as recording and transmitting status, the software periodically compares recorded values to the values maintained in limit tables. Should limits be exceeded, the software will trigger an instrument safe mode, adjusting the mechanisms to safe positions and preventing any further mechanism operations until released by ground command.

5.2 Design

This section presents the top-level design of the XRT MCU flight software.

5.2.1 Heritage

The models for the XRT MCU software are primarily the flight software for the controller for the Spartan 201/UVCS instrument and secondarily the flight software for the controller for the UVCS/SOHO instrument. Both systems were designed and built by SAO.

5.2.1.1 Spartan 201/UVCS Flight Software

This software operated without failure on all four Spartan 201 missions between 1987 and 1998. It performed the following functions:

- Collected instrument health and status information at a fixed periodic rate and stored it in internal tables.
- Monitored various safety conditions and safed (protected) the instrument when conditions were exceeded.
- Received, interpreted and dispatched commands from the spacecraft.
- Operated several mechanisms and electronic devices, including stepper-motor mirror drive, solenoid-operated slit mechanism, vacuum pump, ion gauge, and high-voltage power supplies.
- Assembled health and status information into packets and sent them to the spacecraft for recording.
- Accepted control and diagnostic commands from the EGSE and sent data to the EGSE for display as required.
- Protected the detectors when safety limits were exceeded.
- Received and stored flags and parameters.

The software was operated as a real-time multitasking system with the following tasks:

- Status Collector
- Safety Checker
- Command Reader
- Command Interpreter
- Status Sender
- Stepping Motor Controller

The functions and organization of the Spartan 201/UVCS flight software are similar to those which are to be performed by the XRT MCU flight software.

5.2.1.2 UVCS/SOHO Flight Software

This software has been operating continuously for more than three years without the necessity of making software changes while in flight. Significant features of this software which are included in the XRT MCU flight-software design are

- Software modes.
- Multitasking structure.
- Receiving, queuing and interpreting commands.
- Receiving and managing stored observation scripts.
- Receiving and storing of flags and parameters.
- Modification of software during flight.

5.2.2 Software Modes

The XRT MCU flight software is always in a unique Software Modes. The Software Mode (or simply Mode) affects what subset of the commands will be executed and which

table of safety limits will be used in deciding to safe the instrument. There are also rules which govern the transition from one Mode to another. The modes are

- Initialization Mode - Initializes the software and hardware and switches to Standby Mode. No commands are accepted except status requests. This mode automatically switches to Standby Mode when initialization is complete.
- Standby Mode - Does not accept any commands affecting the hardware.
- Operations Mode - Allows all operational commands.
- Safehold Mode - Similar to Standby Mode, but first configures all mechanisms to the designated safe positions.
- Bakeout Mode - For baking out the camera. Accepts commands related to bakeout. Uses a separate table for limit checking.
- Diagnostic Mode - For checking out mechanism operation. Status information is transmitted at a much higher rate than normal, nominally 10Kbytes/second. This will allow transmitting mechanism position, voltages and currents at a rapid rate for characterization of the mechanisms during ground testing and early in the flight. Later it will be used to evaluate trends and to diagnose problems.
- Installation Mode - similar to Standby Mode except that software, tables, and observing scripts may be uploaded.

The software mode is usually selected by command received from the MDP. Exceptions are

- A transition into Safehold Mode will be triggered by the detection of out-of-limit conditions.
- Upon initial application of power or receiving a reset signal from the MDP or upon a watchdog timer interrupt, Initialization Mode will be entered.
- Upon completion of initialization, the Initialization Mode will automatically switch to Standby Mode.

The normal mode is Operations Mode.

5.2.3 Real-time Tasks

The flight software for the XRT MCU operates within the environment provided by a multi-tasking real-time operating system. This means that the software can perform several functions at the same time. In all software Modes, multitasking is in effect. Each function which is capable of simultaneous execution is called a "task". The tasks are described as follows:

- Command reader --This task reads commands from the MDP interface and places them in a queue awaiting execution. The task operates the command interface with the MDP. It waits until a command starts appearing on the MDP interface. It reads each command into a buffer and checks it for validity. It then checks to see if the command requires immediate action. If so, it executes it. If not, it places the command in the command queue for interpretation by the Command Interpreter. It then waits for the next command. Note that a status request from the MDP is an immediate command which sets a flag. This flag is interpreted by the Status Writer.

- Status writer -- This task transmits messages to the MDP. It waits until a status request is detected by the Command Reader task. It then operates the status interface to send the appropriate status message.
- Housekeeping Collector – The Housekeeping Collector will be driven by a timer interrupt at a TBD rate. It will operate the digital multiplexor and the analog multiplexor and converter to obtain instrument and electronic status and will record this information in the Status Table. It then waits for the next timer interrupt.
- Safety Checker -- This task compares values in the status table to values in the limit table for the current Software Mode and triggers Safehold Mode if a limit is exceeded. This task will be driven by a timer interrupt at a TBD rate.
- Command Interpreter -- The command interpreter removes the next command from the command queue. It looks it up in the Command Table. If found, it executes the command. If not found, it reports the error by making an entry in the status table. It continues removing commands from the queue and executing them. When the command queue is empty, it waits.
- EGSE Console Task -- This task reads and executes commands from the EGSE keyboard. It displays information on the EGSE screen as requested. This allows testing of individual software components, provides a debugging interface, and provides for display of diagnostic information. This task is used during development and testing. Its use during integration is limited, and it is not used in flight.

5.2.4 Commands

The XRT MCU responds to commands received from the MDP. These commands may be issued by the MDP directly or issued from the ground and passed to the MCU by the MDP. Commands may also be compiled into Command Scripts which are installed in the MCU. Entire scripts can be executed by a single command from the MDP.

The command types are

- Exposure Commands – These commands tell the software the parameters for configuring the telescope, the time to start the exposure, the length of the exposure and the exposure serial number. The software responds by configuring the telescope and taking the exposure.
- Time Synchronization -- The time synchronization command informs the MCU of the current value of the spacecraft clock. The enable signal on the command interface associated with the command transmission is used as a time synchronization pulse.
- Wait -- Wait commands tell the MCU to wait for a specific length of time or until an absolute time or until a flag is set or reset before executing the next command.
- Mode change – Mode Change commands tell the MCU software to switch from the present mode to the specified new mode.
- Execute – Tells the MCU software to execute a specific script held in the MCU Script Catalog.
- Micro commands -- Micro commands perform low-level operations which are not used for normal operations but are used during development and kept for diagnostic purposes.
- Status requests – These commands request that the MCU return a status message to the MDP. Status request types are

  - Normal Status
  - Image Header
  - High-rate housekeeping
  - Other
- Informational -- Informational commands include information from the MDP to the MCU. The information will be flags and status from the MDP or from other instruments.

5.2.5 Tables

The XRT MCU software maintains several tables. In turn, the behavior of the software is affected by the contents of the tables. The tables are

- Command tables -- There is a command table for each of the Software Modes. The command table lists the commands which are valid in that mode. In general, invalid commands are ignored but an error flag is placed in the Status Table. Other responses to invalid commands are TBD.
- Status Table -- All status collected from the XRT-D is kept in a status table. Selections from the XRT-D status table are transmitted to the MDP by Status Commands from the MDP. Status information from the MDP concerning the MDP and the other instruments is sent to the MCU by Informational Commands and stored in the Status Table.
- Limit Tables -- There are two or more limit tables. Each Software Mode is assigned to a limit table. A special limit table is used for Bakeout Mode; another table is used otherwise. Additional limit tables are TBD. Data from the Status Table is periodically compared to the values in the current limit table. If a limit is exceeded, Safehold Mode is triggered.
- Script Catalog – Scripts are sets of commands which have been loaded prior to or during flight. They can be invoked by Execute commands from the MDP.

5.2.6 Software Environment

The software environment includes the language, real-time operating system and debugging facilities. These will be provided by SwiftX from FORTH, Inc. It is fully supported by them and has been used on several flight software projects. SwiftX is available for all three of the processors being considered. It is the evolutionary successor to PolyFORTH, which was used on Spartan 201/UVCS. If the ESN processor is chosen to be the MCU, the development environment will be copied from that used by Code 740 (Mission Integration & Planning Division, Flight Instrument Development Office) at GSFC and additional support will be available from them.

5.3 Software Management

A software plan will be produced during Phase B. A software management plan will also be developed, consisting of the following documents and sections.

5.3.1 Revision Control

The software revisions will be managed using standard SAO Central Engineering configuration control procedures and facilities.

5.3.2 Interface Control

An interface control document covering the command and data handling interface between the XRT MCU and MDP, and between the XRT MCU and the camera will be produced following the freezing of the software interface, scheduled for December 1999. The command and status interface between the XRT MCU and the Filter/Shutter assembly will be controlled by the specifications for the Filter/Shutter Assembly.

5.4 Hardware and Software EGSE

The EGSE will provide an environment for developing software and testing both hardware and software. The EGSE has both hardware and software components.

5.4.1 Hardware

The EGSE hardware will consist of two PC workstations, an interface board and a power supply.

5.4.1.1 PC workstation

The PC workstations will have the Windows NT operating system, a network interface card for TCP/IP and six asynchronous (COM) ports. The PC configurations will be identical and will provide backup for each other. They will be used for development of the MCU flight software and the MDP simulator software and for control of the MDP simulator. The COM ports will be used for

- Software loads and debugging of MCU.
- Interactive console for MCU.
- Software loads and debugging of MDP simulator.
- Interactive console for MDP simulator.
- Modem
- Spare

5.4.1.2 Interface Board

The interface board will contain the hardware interfaces for simulating the MDP serial synchronous interfaces and discrete interfaces and the camera's discrete digital interface. We are considering using a duplicate of the prototype MCU board as the EGSE interface board.

5.4.1.3 Power supply

The power supply will provide the primary power to the XRT. It will be capable of providing the maximum current which the XRT can draw and will be adjustable over at least the specified voltage range for the power supplied to the XRT by the spacecraft.

5.4.2 Software

5.4.2.1 Development software

The SwiftX FORTH software from FORTH Inc. will be installed on the PC and will be used for compiling, loading and debugging the applications for the XRT MCU and the MDP simulator board.

5.4.2.2 Terminal Emulator

A terminal emulator, such as Hyperterminal or Kermit, will be used as consoles for the MCU and MDP simulator. Telnet server software will allow remote console emulation for the MCU and the MDP simulator.

5.4.2.3 MDP Simulator Software

SwiftFORTH software from FORTH Inc. will be used as part of the MDP simulator, controlling the MDP simulator board.

6. Thermal Design

6.1 Overview

The thermal design of the Solar B XRT has three main objectives: (1) Provide a suitable thermal environment for the major components of the experiment, primarily the optical assembly, the filter assembly, and the electronics, (2) provide sufficient thermal isolation from the camera to allow the focal plane to be cooled to its desired temperature of -60C, and (3) provide sufficient isolation from the spacecraft to be effectively independent thermally of its temperature.

The basic design of the telescope is a tapered tube, with the larger end facing the sun and containing apertures for both the X-ray and small optical telescopes with the XRT experiment. The forward facing surface will be treated with a low solar absorptance/high emittance surface and have blocking filters over the apertures such that the majority of the sun load will be rejected directly at this surface. The outer circumference of the tube will be Multi-Layer Insulation (MLI) covered to minimize heat loss and the effects of the other spacecraft surfaces and the earth. The electronics module will be mounted to the side of the main tube in the shadow of the open front door, and will have integral radiator(s) to reject the heat produced in the electronics.

This design cold-biases the main telescope body such that operational heaters will be used to control temperature in the key areas. It is expected that 2 heater zones of less than

5W each will be utilized in the mirror area to control the optics to better than ±2C. Another zone of similar power will keep the filter wheel assembly within the desired temperature range, and a fourth zone is possible for the electronics box, depending on the variation in power between the highest and lowest operating dissipation. Survival heaters will be placed in these areas as well to prevent damage to the hardware during anomalies, and allow a cold start of the electronics.

6.2 Requirements

It can be seen from the overview above that the majority of the thermal requirements are derived, based on providing an environment for the key telescope components so as to meet their performance requirements. The baseline requirements for the major areas of the XRT are listed in the Table 6-1 below:

Table 6-1 XRT Baseline Temperature Requirements

Component	Control Range	No. of Zones	Control Temperature
Optics Assy.	± 2C	2-3	Epoxy Cure Temp.
CFRP Optical Bench	± 3C	0-2	20 C (TBR)
Filter Assy	±10C	0-1	20 C (TBR)
Electronics	± 10C	0-1	10 C (TBR)

The x-ray optic in the optics assembly will be epoxy-bonded to a set of flexures for its mechanical support. In order to minimize optical distortions resulting from CTE mismatches between the optic, the epoxy, the flexures, and the supporting structure, the temperature setpoint for this assembly will centered at the cure temperature of the epoxy (nominally 20C). The large allowable range for the filter assembly and electronics leave open the possibility of not having active control zones in these areas but instead providing reasonable conductance to controlled areas.

A design goal for the XRT is to minimize the thermal effect of the spacecraft and camera on the control of XRT temperatures. In order to achieve this, SAO has specified low conductance mechanical connections between the XRT and the spacecraft and the XRT and the camera (see Table 6-2). This will be accomplished on the S/C side through the use of relatively long struts of a conductivity material. The camera will be mounted via insulated bolted connections.

Table 6-2 XRT Main Thermal Interface Assumptions

Interface	Conductance	Temperature Range
Spacecraft	< 0.05 W/K	-20 to +50 C
Camera	< 0.03 W/K	-30 to +20 C

In addition, the surfaces of the filter wheel/shutter assembly facing the camera will be treated to be low emittance to minimize the radiative heat transfer to minimize parasitic heat loads on the CCD focal plane.

6.3 Design

6.3.1 Passive Thermal Design

The overall configuration of the XRT, a long tapered tube with the large end sun-facing, allows for a fairly straightforward treatment of the external surfaces of the spacecraft, which are shown in Fig. 6.1. The sunshield will be a metal plate with Z-93 paint applied to all of the surface that is not a telescope aperture. This paint has very high emittance but low solar absorptance, and maintains these properties very well in a full-sun environment. The apertures themselves will be covered with an aluminized kapton or free-standing aluminum pre-filter to reject a large fraction of the solar load at this surface, the baseline thermal design is shown on Foldout 4.

The tube itself will be covered with MLI with a black or natural kapton outer layer. Although higher emittance than a silvered surface, there will be no direct sun load on these surfaces, and the optical properties are more likely to be maintained throughout the full mission life. It is expected that we will be able to achieve an e* of 0.01 or better for the MLI on the telescope tube due to its simple, smooth contours. The relatively small areas around the mounting feet and electronics assembly may have slightly worse MLI performance.

The electronics box will also be MLI covered, but will have part of its space facing area exposed with a high-emittance surface treatment to act as a radiator for the electronics heat dissipation. This radiator area will be made oversized initially, and will be trimmed during thermal vacuum testing to optimum size. Earthshine and albedo will have the most effect on these surfaces, but should easily be accommodated since the electronics have a fairly broad allowable temperature range. If necessary, the radiator surface can have low solar absorptance to reduce the albedo effects.

The sun-facing surface of the electronics will be shaded from most of the direct sun by the open telescope door, which in the current design will have a polished aluminum inner (sun-facing in the open position) surface and a low absorptance, high-e outer surface. These properties and/or amount of treated area will be adjusted to allow the door to run at or slightly below the optics assembly design temperature, and the connection to the telescope will be designed with minimum conductance to further reduce the effect of the door on overall thermal control.

6.3.2 Operational Active Thermal Control

The baseline design of the active thermal control system will utilize solid-state thermostats with the operational temperature fixed and set during design and testing (i.e. no on-orbit adjustment of setpoint). The heaters will be standard resistive tapes with kapton films and will be bonded down. Power for the heaters will come directly from the spacecraft 28V bus. Temperature feedback will be provided by thermistors; housekeeping temperatures will be provided via separate thermistors.

The most critical temperature control zone will be the optics assembly. In the baseline design there is a thin aluminum "thermal shield" between the telescope tube and the optics; it is to this cylindrical surface that we expect to apply some of the heat to control this assembly. The radiative coupling between this surface and the optic itself will be good, and this avoids having to bond heaters directly to the optic. Additional heat may be applied to the central structure supporting the white-light optic.

The baseline optical bench is a Carbon Fiber Reinforced Plastic (CFRP) tube, which has both reasonably high conductivity and high emittance. Our modeling of the internals of the telescope has shown that both the direct and radiative conductances are important in thermal transport within the tube, with the radiative conductance being about twice the direct in the axial direction. This provides a strong mechanism for temperature equilibration within the XRT, such that the heater zones at the optics assembly and one or two near the filter wheel/shutter assembly will produce a reasonably isothermal environment inside the telescope.

If necessary, we also have a heater zone for the electronics. This would come about if different operational modes of the electronics created significantly different heat dissipation. In this case the radiator, sized for the maximum dissipation, rejects too much heat and some make-up heat is needed to keep the XRT-D within its operating range.

6.3.3 Thermal Modeling

SAO has constructed a thermal model of the XRT experiment. The initial purpose of the model was twofold: (1) Provide a model to the spacecraft contractor for their integrated model, and (2) begin modeling some of the overall thermal behavior of the XRT. A wire-frame view of the basic XRT thermal model is shown in Fig x.x.

The model contains both inner and outer surfaces. The tube consists of 12 nodes (4 axial, 3 circumferential, 24 surfaces total). The sunshield, door, and back end are single 2-sided nodes. Thermal mass for the camera and optics assembly are included via lumped arithmetic nodes. The electronics module is a rectangular box with 6 external surfaces, with a 7th surface partially covering the -X box surface that can be of arbitrary size to model the radiator. Linear conductors connect the lumped mass nodes and the electronics module to the tube, and simulate the support rods to the spacecraft.

This model provided supporting data for the design sections above. It was provided to NAOJ and MELCO on September 10, 1999. SAO is currently adding a simplified spacecraft external model based on geometry, optical properties and temperatures provided by

MELCO. This will be used to study the orbital variations in thermal performance of the XRT. We expect to continue to update this model as the design evolves, and create detailed models of critical areas like the optics assembly as needed.

A recent finding using the orbital model (including the spacecraft) shows that there is significant illumination by sunlight of the nominally anti-sun surface and other surfaces due to reflection of direct sunlight by the +Z spacecraft deck. The spacecraft deck has been specified as MLI covered with 50% specularity; normal rippling of the MLI surface may create fairly strong reflections. Early drawings show bulkheads and other structure along the main optical bench and OTA, but these are not indicated in the thermal data from MELCO. This aspect of the on-orbit thermal model will require discussion in the upcoming weeks.

6.3.4 Survival Heaters

Survival heaters, physically similar to the operational heaters, will be placed in approximately the same areas as the operational zones. These will be powered by a separate survival heater bus and each zone will utilize mechanical thermostats (see Foldout 4), possibly in a redundant series/parallel arrangement for maximum reliability. Setpoints will be designed to prevent hardware damage during an anomalous condition where the operational power bus is shut off for an extended period.

It should be noted that the SAO survival heater design is different than the Solar B mission baseline. In the ISAS proposed design, each survival zone is powered by a separate line from their Heater Control Electronics (HCE), and a measurement thermistor line is provided to the HCE. The SAO thermal design team has resisted this approach for several reasons:

(1) It requires many more electrical connections between the XRT and the spacecraft.

(2) The main control of these zones is provided by the spacecraft, presenting many integration and test complications.

(3) It is a less reliable form of temperature control.

We are currently assuming our baseline design approach.

6.4 Impact of Mechanical Design Options

The only design trade that has a potentially large effect on the experiment thermal design is the optical bench material. A thin titanium tube, under consideration for cost reduction reasons, would have a smaller axial (and circumferential) conductance. However, the emittance of titanium is fairly high, and since internal head transfer is dominated by radiation, it would not have a major impact on the thermal design. Since the CTE of titanium is significant, control of the tube may have to be tightened to $\pm$ 1 C to avoid excessive focal plane motion. This is still an achievable control range, although it may be necessary to add more heater zones axially along the bench.

The other area, as yet unstudied, is the impact of the focus mechanism design on the overall thermal design. Both the SAO proposed design and the Meisei design should have minimal impact on the telescope and optical bench. The SAO design places the focus motor outside the tube, which should also have minimal effect on the focal plane temperature. In the Meisei design, where the focus motor is inside the main body of the camera, there is the potential for a significant impact on the operating temperature of the CCD and/or loss of useful viewing time while the temperature equilibrates.

6.5 Testing

Primary thermal cycling and thermal balance testing will be performed at ISAS, on both the Mechanical Test Model/Thermal Test Model (MTM/TTM) and the flight hardware. SAO will also perform T/V and T/B testing on both of these units. Our baseline plan calls for one or two T/V cycles of the TTM followed by a thermal balance test to verify thermal model. We expect to simulate the solar load with heaters during the SAO tests; we would like to have full optical solar simulation during the integrated testing, which is feasible since the sun direction is fixed. This may be important given the complexity of the reflected sunlight from the various S/C surfaces on the externally mounted instruments like the XRT. SAO will also perform a T/V test (4 cycles) and a thermal balance test of the flight hardware prior shipment to Japan.

SAO expects to do some bench testing of heater control units (solid state thermostats) to evaluate their suitability for operational heater control during Phase B.

7. System Interfaces

7.1 Spacecraft

7.1.1 Mechanical

The main mechanical interface between the spacecraft and the XRT is the 3 legged kinematic mount provided by the spacecraft. We have had very little visibility into the spacecraft side of the design of the mechanical interface. The physical layout of the mount points is shown in Foldout 1.

The mount structural design provides restraint in exactly 6 degrees of freedom, supporting the instrument without imposing any unnecessary forces onto the instrument structure. This fact simplifies the details of the XRT mounting considerably. The XRT mounting feet are bolted to mounting plates at the top of each of the 3 mounting legs without intermediate complications such as flexures or ball joints. The mounting pads provide the required alignment to ensure that the instrument can be co-aligned to the other instruments. In addition, the planes of the instrument mounting feet can be aligned with those on the spacecraft mounting pads to ensure that the force of bolting the instrument down does not distort the instrument mounting structure.

Because of the small amount of space between the bottom of the XRT instrument and the surface of the SOT optical bench, it would have been nearly impossible to place a

mounting fastener down though the XRT mounting pad and into the spacecraft mounting pad. Several alternate possibilities were discussed with the spacecraft contractor, MELCO, at design review meetings in Japan, the solution was to simply thread the bolts up through the spacecraft mounting pads into XRT mounting feet.

7.1.2 Electronic

7.1.2.1 Power

Regulated 28V power is provided by the spacecraft to the instrument. This power is unswitched. Power switching is expected to be done inside each instrument. To accomplish this, each instrument must include a latching relay on the input side of the instrument power supply to switch main power, a control line from the spacecraft to actuate the relay on command, and a status line to the spacecraft to indicate the actual state of the relay. In addition, in order to limit switch on surge, it is expected that each instrument will include a relay on the output side of its main power supply that will switch on instrument low voltage, and a control line from the MDP to actuate this relay on another command.

The need for this second switch and the complications it produces is currently under discussion. The preferred configuration from a reliability perspective would be to minimize the number of relays, commands, and status lines. The simplest design would be to have the spacecraft provide switched 28V to each instrument, with switching relays located on the spacecraft and monitored locally by the spacecraft.

7.1.2.2 MDP

The interface for commanding between the instrument and the spacecraft is through the Mission Data Processor (MDP). Commands from the ground are linked up to the spacecraft where they are sent to the MDP. The MDP parses the command to identify the destination of the command and whether the MDP itself must take any action. The commands are then sent over a synchronous RS-422 serial connection to the MCU. A 64 kHz clock from the MDP will be the timing reference. The data link from the MCU to the MDP is also a synchronous RS-422 link operating at 64 kHz. This line carries housekeeping and status information to the MDP.

Additionally, there will be two discrete command lines from the MDP to the MCU. These will be logic level signals that will force a hardware response through a different path than the command channel mentioned above. The two commands are SAFE_HOLD and RESET. The SAFE_HOLD command will make the instrument enter a safe configuration that may require moving mechanisms to predetermined positions. The RESET command forces a system reset. These commands are to be used if the instrument stops responding through the normal command channel.

7.1.2.3 Emergency Heater Control

If instrument power is switched off, the internal heaters and thermistors cannot be used

for thermal management. Spacecraft provided survival heaters and temperature sensors are installed on the instrument for this situation. Survival heaters are powered by a 28V switched bus. Temperature sensors on the instrument are connected to the Heater Control Electronics (HCE) which control the heaters. There will be two (TBD) heater/thermistor circuits.

This issue is currently under negotiation. It is preferred to have survival heaters powered by unswitched 28V, and have heater setpoints maintained by local thermostats, in order to reduce the possibility of a control system error that could put the instrument at risk of exposure to thermal extremes.

7.2 Camera

7.2.1 Mechanical

There are two issues encompassed by the camera mechanical mounting, first the camera itself must be fixed to the back of the telescope, and second the focus actuator must be connected to the focus stage. The camera mounting interface consists of a bolt circle for mounting screws, and a set of alignment pins, and a single, drill at assembly, locking pin. The camera alignment is set by the two alignment pins, one that slides into a close fitting hole, the other that slides into a close fitting slot. Once they are engaged the camera can no longer rotate with respect to the back surface of the XRT. The camera will then be bolted up to the back of the XRT. The first time the camera is mated a drill-at-assembly pin hole will be drilled into the camera mounting flange, and pin will be driven into it. This pin will set the final alignment of the camera, ensure that it won't move, and can be removed and reassembled without losing the final alignment.

The connection between the focus mechanism and the focal stage has to be made once the camera is assembled. Though many different focus mechanism concepts and layouts have been discussed, the baseline focus system splits the actuator and the movable stage between the telescope and the camera. The actuator is mounted on the telescope, while the movable stage comprises the CCD support structure. The interface between the two is a bolted connection. The mounting point is isolated from motion of the actuator in direction that are not parallel to the desired travel of the CCD, and does not support any bending moment. Thus the actuator can only push the stage in the focus adjustment, and misalignments between the travel of the focus stage and the actuator can not cause the actuator to jamb.

7.2.2 Electronic

7.2.2.1 Cable Support

The complete camera interface has not been set yet, however SAO has assumed that several cables will have to go from the camera to the spacecraft. There are two possible routes for these cable to follow. First, the cables can go directly from the camera to the side deck of the spacecraft. This is the shortest route, and the baseline for the signal wires coming from the CCD preamps. The other possible route is less direct. The cables are

routed onto the telescope tube and down the rear foot mount onto the spacecraft deck. Both options raise interface issues.

In an effort to reduce the weight and complexity of the portion of the camera mounted on the back of the telescope, the A/D electronics the convert the charge information to digital values has been placed inside the spacecraft housing. This means that the small, high impedance signals carrying the imaging information must travel from the camera to the inside of the spacecraft housing. In order to reduce the effects of noise and interference these lines must be as short as possible, thus the direct path from the camera to the spacecraft. However, the direct route places and indeterminate load on the camera, and therefore the back of the telescope, in addition this route creates a challenging support problem for the cable itself. These issues are still open.

The XRT interface design has provided nominal connector locations for 2 25-50 pin connectors. This will permit additional camera cables to be carried over the XRT telescope. SAO assumes that required cables will be built by Meisei and supplied to SAO for integration into the telescope wire harness.

7.2.2.2 Status Lines

The primary task of the instrument is taking CCD images. This involves coordinating the operation of the CCD Camera with the operation of the internal mechanisms, primarily the filter wheels and the focal plane shutter. The CCD Camera's main interface is with the MDP. The interface of the rest of the instrument is also with the MDP. Because the MDP is also responsible for two other instruments, as well as other tasks, it is not clear whether it can ensure accurate timing of exposures for high cadence, short exposure length images. A two wire interface between the CCD Camera and the MCU has been proposed and tentatively accepted. A signal from the CCD to the MCU, CCD_BUSY, will indicate when the CCD is ready for an exposure. A signal from the MCU to the CCD, CCD_EXPOSE, will indicate when the shutter is open. On receiving an exposure command from the MDP, the MCU will command the filter wheels to the correct position, and will initialize the shutter. It will then wait until CCD_BUSY indicates that the camera is ready. The MCU will then start the exposure by opening the shutter, which sends the signal CCD_EXPOSE to the camera. The camera waits until CCD_EXPOSE indicates that the exposure is complete, and then transmits the image to the MDP. The signals CCD_BUSY and CCD_EXPOSE will be 5V logic level signals. The signals may be routed through the MDP, but will not be processed by the MDP. The timing of these signals is shown in the figure below.

7.3 Internal Interfaces

Several internal interfaces exist on the XRT, between components designed and/or fabricated by SAO and those fabricated by US collaborates. In all cases these interfaces are either simply mechanical mounting surfaces, or existing designs with previously designed interfaces.

7.3.1 X-ray Mirror

The interface between the x-ray mirror and the telescope is the bond that attaches it to the mirror support flexures. The exact nature of this is interface, both the existence of, and shape for a mounting detail on the mirror, and the nature of the flexure bonding nub will be worked out in detail during Phase B. The mirror itself will be fabricated with a precision front surface. The plane and center of the front surface will define the location and orientation of the optic's figure. This surface will be used as a reference to align the mirror during mounting.

In addition, the rear surface of the mirror will be used to support a system of apertures. The assembly will consist of 2 or 3 apertures that block those light paths that will fail to reflect off both of the elements. These are necessary to improve image contrast and suppress ghost images.

7.3.2 Visible Light Optics

The visible light optics will be mounted in a cell. The cell will be flanged, having a precision mounting surface, aligned to the optical axis, machined into the flange. This mounting surface will be used to align the telescope during mounting.

7.3.3 Main Shutter

The main shutter, provided by Lockheed Martin, is an exact replication of the TRIANA shutter. It mounts to a 4 bolt circular pattern. The mechanism is controlled by an electronics board, also provided by Lockheed Martin. The control board is mounted in the XRT electronics box and connected to the MCU through an RS-422.

7.3.4 Filter Wheels

The filter wheels, provided by Lockheed Martin, are exact replications of the TRIANA filter wheels. They are stackable and mount to a 4 bolt pattern. The wheels are controlled by an electronics board, also provided by Lockheed Martin. The control board, the same one that controls the main shutter, is mounted in the XRT electronics box and connected to the MCU through an RS-422.

8. Contamination Requirements

8.1 Requirements

8.1.1 Particulates

The requirements for particle deposition on the primary mirror are TBD. The issue is an important one since particles on the mirror have two effects on the XRT imaging performance: diffraction, and loss of collecting area. Because of the low angle of incidence, even small particles have a large impact on the effective collecting area. Particulate ac-

cumulation limits on the optical surfaces will be addressed in the contamination control plan to be generated for the preliminary design review.

8.1.2 Condensibles

The requirements for allowable volatile condensible material (VCM) on the x-ray mirror or visible light lenses are TBD. A detailed analysis of this requirement will be performed and documented during Phase B. Similar to the effects of particles, condensed material on the mirror has a larger effect due to the low angle of incidence. The light travels a great distance through the small layer.

8.2 SAO Relevant Experience

SAO has headed up several programs in the past few years that have required similar or more stringent contamination control to what is envisioned for the XRT. These include:

- The High resolution Imager (HRC) instrument on the Chandra Observatory,
- The Transition Region and Coronal Explorer (TRACE) instrument,
- SOHO Ultra Violet Coronal Spectrometer (UVCS) Instrument,
- Spartan Ultra Violet Coronal Spectrometer (UVCS).

Except for HRC, all these instruments image the sun. They all work in a similar spectral region. The result is a deep, institutional understanding of the contamination control issues related to constructing instruments to observe the sun in the far-UV and x-ray.

8.3 Material Selection

Materials will be selected to meet the standard NASA requirement that total mass loss in a vacuum be less than 1%, with a condensible fraction of less that 0.1%. The Goddard database prepared under specification RP-1124 will be used to determine compliance.

8.4 Material Preparation, and Handling

Materials will be processed under standard commercial conditions, and then cleaned per MIL-STD-1246 or similar specification. Once cleaned, all materials or components will be stored in a clean facility.

8.5 Assembly Procedures

All XRT components, once cleaned, will be handled in a cleanroom environment. The structural and electronic components will be stored, and assembled in a class 1000 cleanroom facility. Optical components will be handled and assembled in a class 100 facility. Once the mirror assembly is complete, the inside surface of the mirror will be closed, and pressurized with clean, dry Ni. The mirror assembly will remain closed until as late in the integration flow as possible.

The focal plane and prefilters will be stored in vacuum until as late in the integration flow as possible. This will have the dual affect of keeping them clean, and protecting them.

The major assemblies will be baked out per MSFC-SPEC-1238 prior to final integration; the certification standard will be adjusted accordingly. Once each assembly has been baked out it will be stored under dry N_2 until final integration. The fully assembled XRT will be kept in cleanroom conditions, with the inside purged, or bagged and stored in the pressurized shipping container until it is integrated onto the spacecraft.

The final system bakeout will take place prior to thermal balance. The bakeout will again be per MSFC-SPEC-1238, this time with a certification standard design to ensure that the x-ray optic will remain clean during orbital operations. As a final precaution the mirror assembly will be designed to permit the x-ray optic and the visible light lenses to be cleaned until later in the integration phase of the program.

8.5.1 Facilities

SAO has a number of fixed and flexible contamination control facilities. The most likely assembly area will be the facilities in which the HRC was assembled. The overall instrument will be put together in a large Class 1000 downflow tent that the HRC instrument housing was assembled in. The mirror cell will be assembled in the Class 100 cleanroom built for the assembly of the HRC sensor. A specially designed shipping container will keep the instrument clean while it is in storage or shipment.

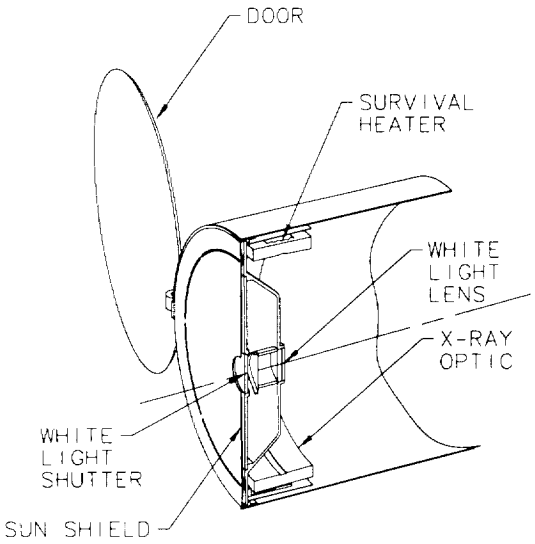
DOOR
SURVIVAL HEATER
WHITE LIGHT LENS
X-RAY OPTIC
WHITE LIGHT SHUTTER
SUN SHIELD

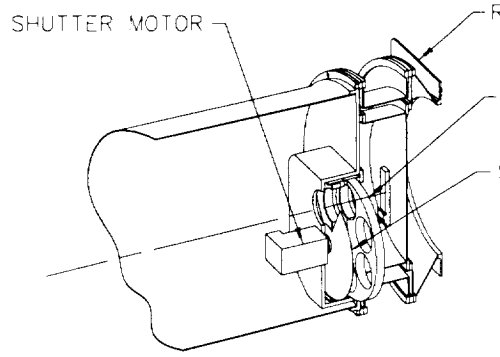
SHUTTER MOTOR

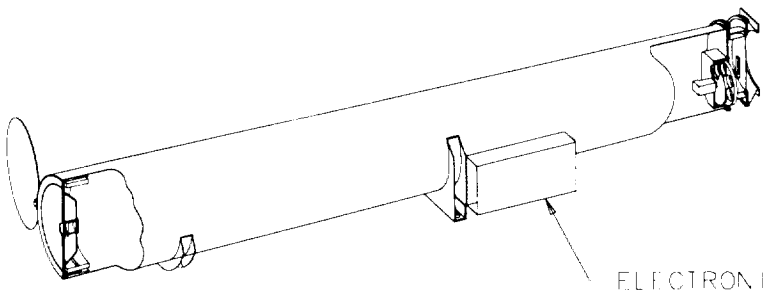
ELECTRONICS

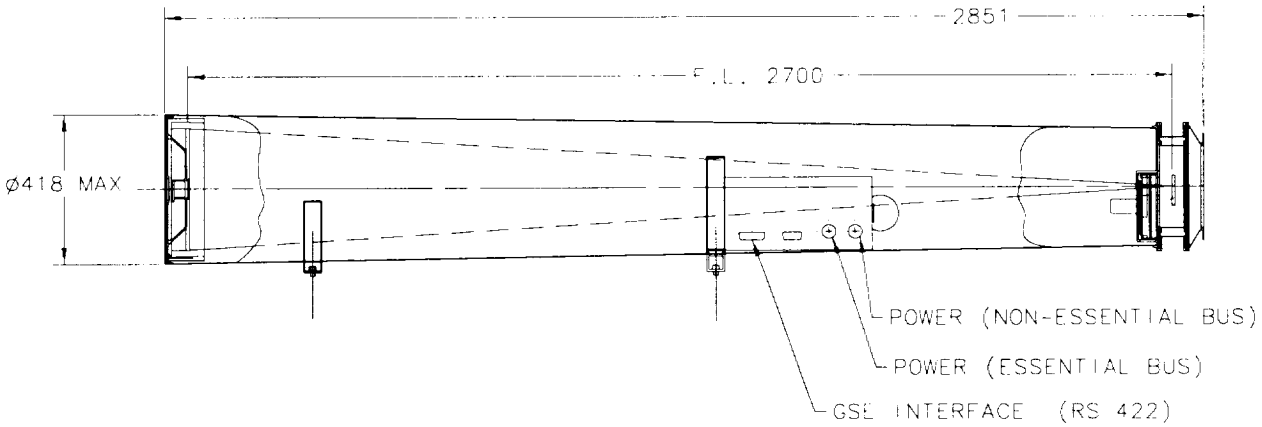
2851
F.L. 2700
ø418 MAX
POWER (NON-ESSENTIAL BUS)
POWER (ESSENTIAL BUS)
GSE INTERFACE (RS 422)

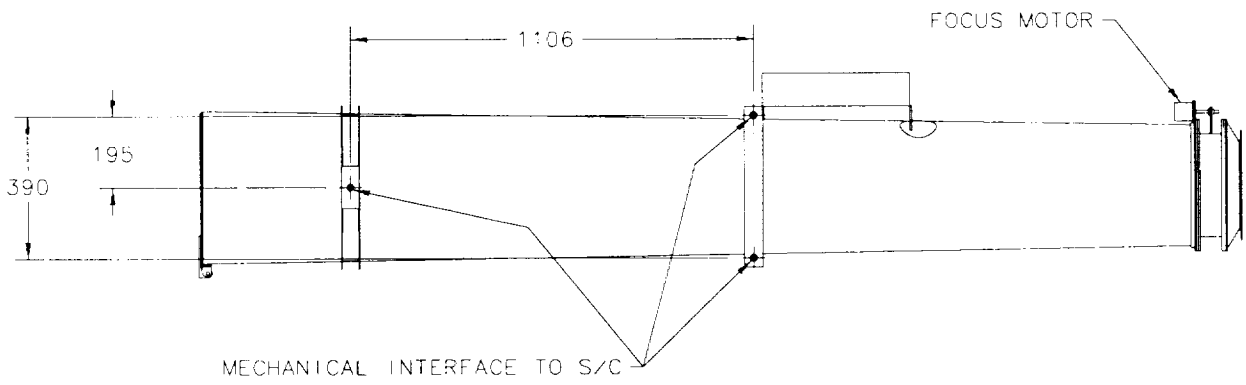
1106
FOCUS MOTOR
195
390
MECHANICAL INTERFACE TO S/C

ADIATOR

FILTER
ASSEMBLY

SHUTTER

XRT MASS TABLE

ITEM	MASS [Kg]
XRT INSTRUMENT (with cont.)	32.4
FRONT ENTRENCE ASSEMBLY	1.6
MIRROR ASSEMBLY	6.5
TUBE ASSEMBLY	12.4
FILTER WHEEL ASSEMBLY	4.1
ELECTRONICS	7.7

XRT INSTRUMENT PARAMETERS

ENERGY RANGE	0.5-6.0 KeV (2-60 ANGSTROMS)
EXPOSURE TIME	.004 - 1.0 SECONDS
GEOMETRIC AREA	6.0 SQ. CM.
EFFECTIVE AREA AT 17 ANGSTROMS	3.5 SQ. CM.

XRT FOLDOUT NO. 1

OPTOMECHANICAL LAYOUT
AND PROPOSED
INTERFACE LOCATIONS

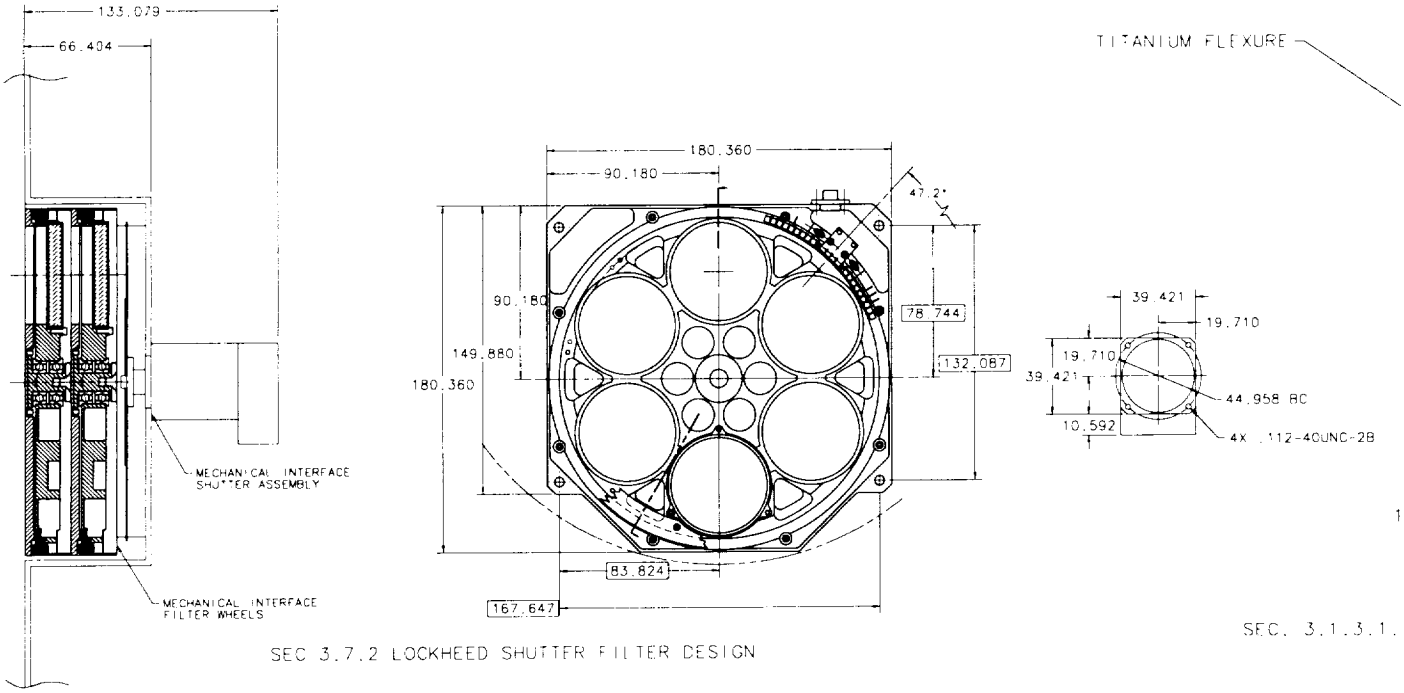

SEC 3.7.2 LOCKHEED SHUTTER FILTER DESIGN

SEC. 3.1.3.1.

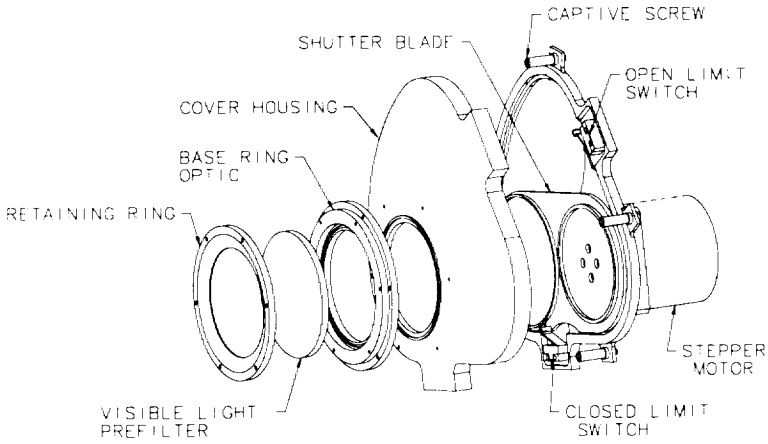

SEC 3.3 VISIBLE LIGHT SHUTTER ASSEMBLY

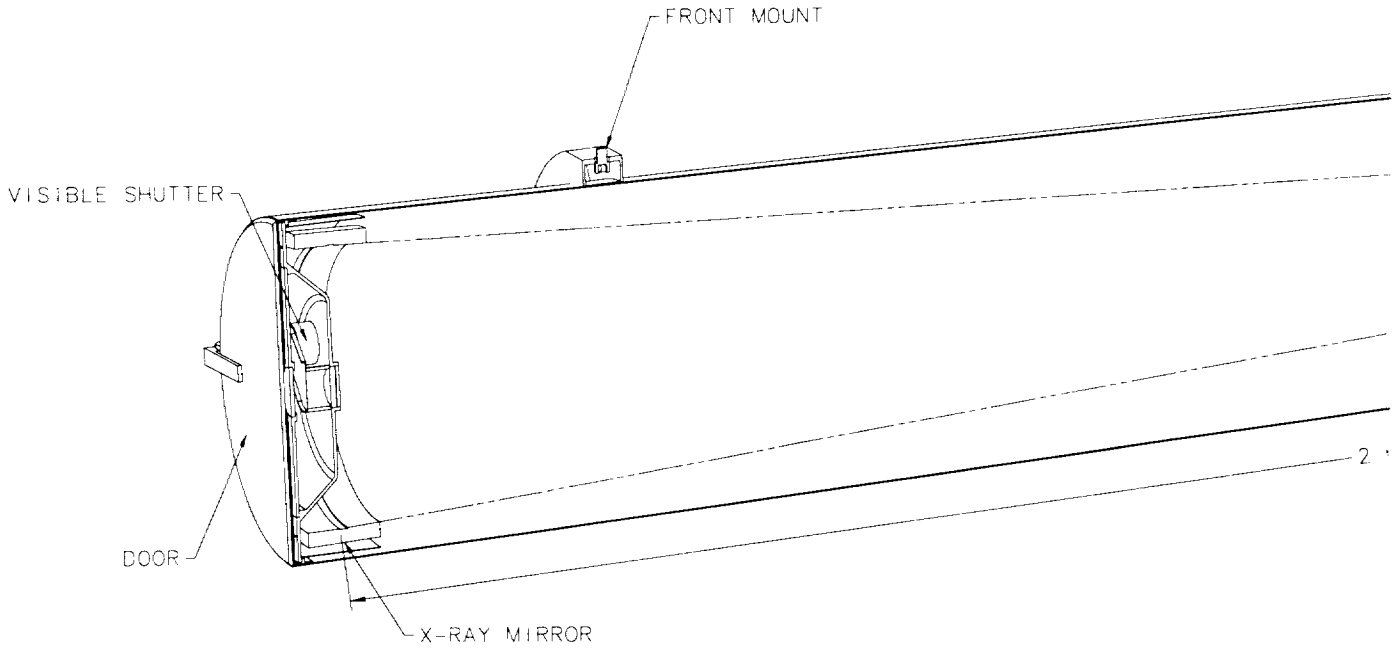

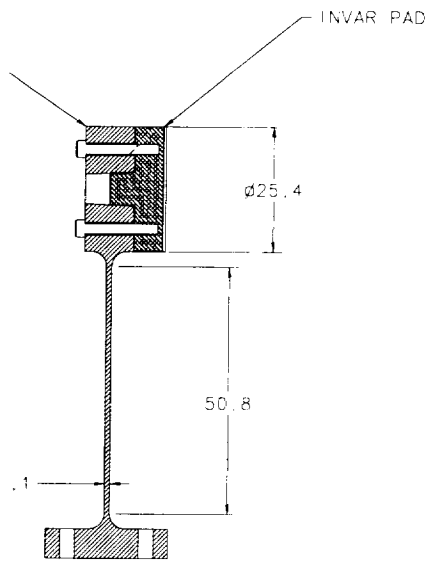

1 TYPICAL FLEXURE DESIGN CASE #3

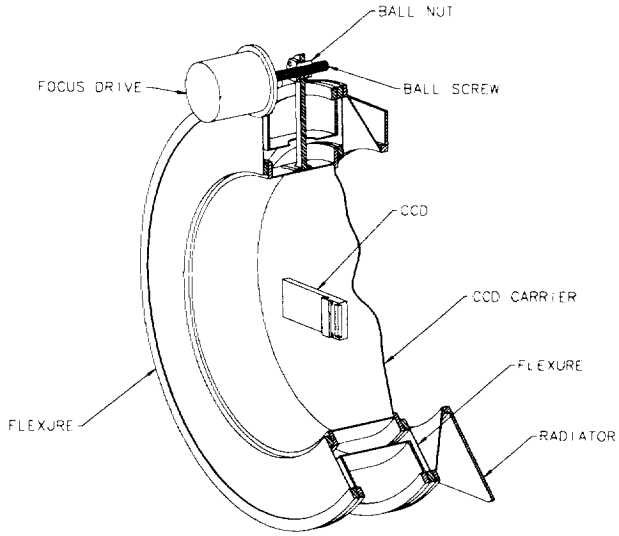

SEC. 3.9 FOCUS MECHANISM

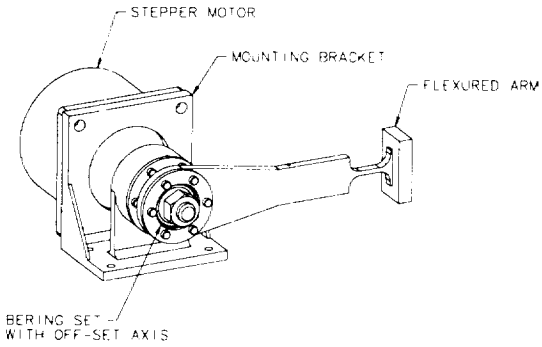

ALTERNATE FOCUS
MECHANISM DESIGN

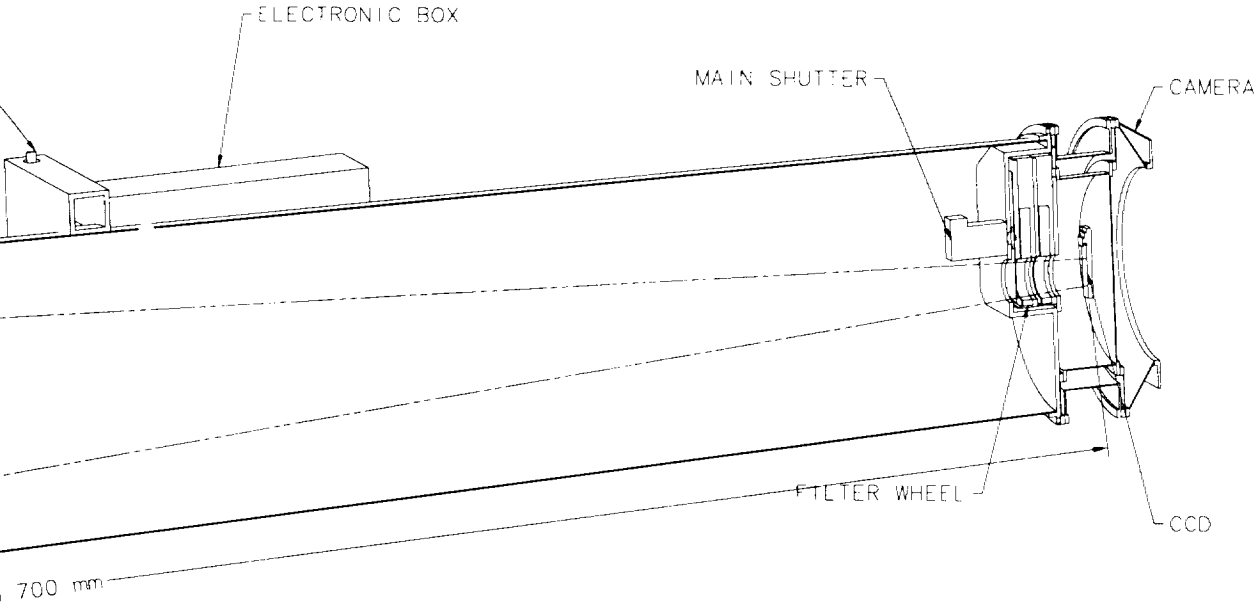

XRT FOLDOUT NO. 2
SOURCE CONTROL DRAWING W/ INTERFACES

Electronic Block Diagram

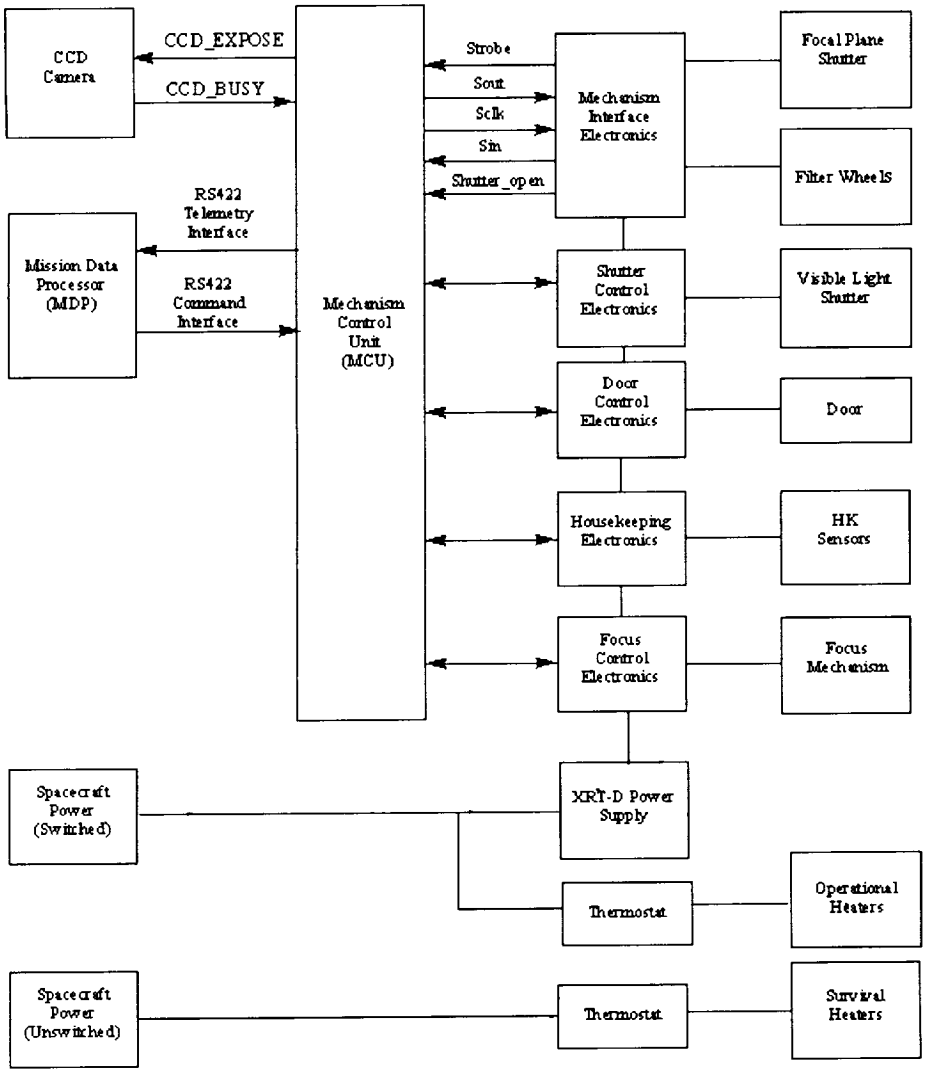

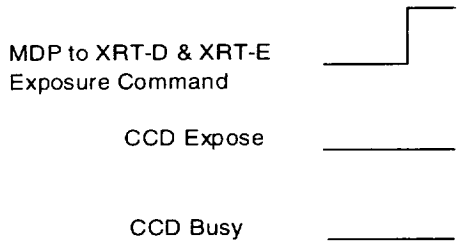

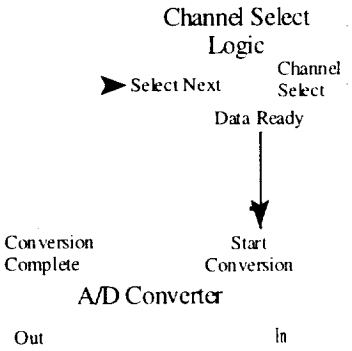

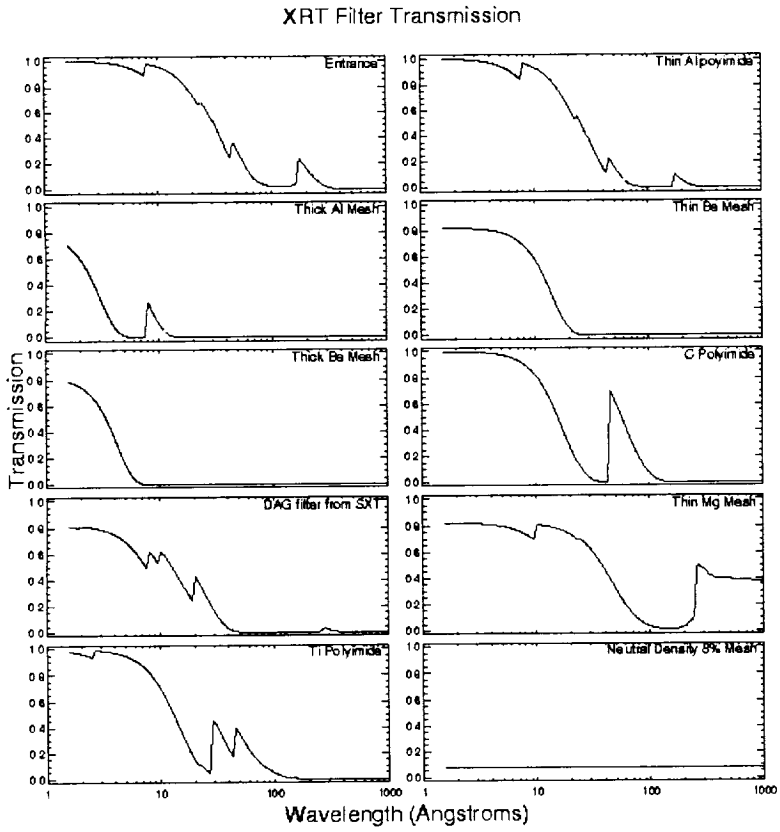

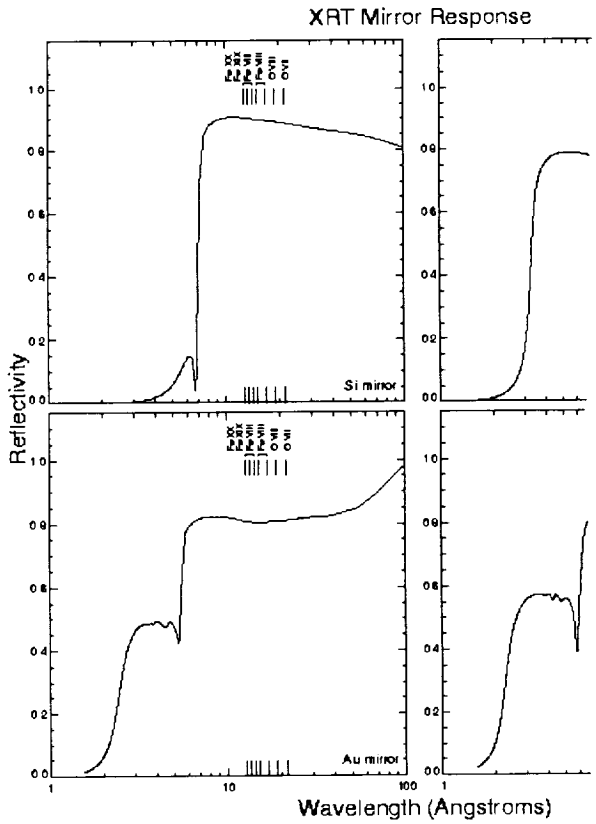

Exposure Timing

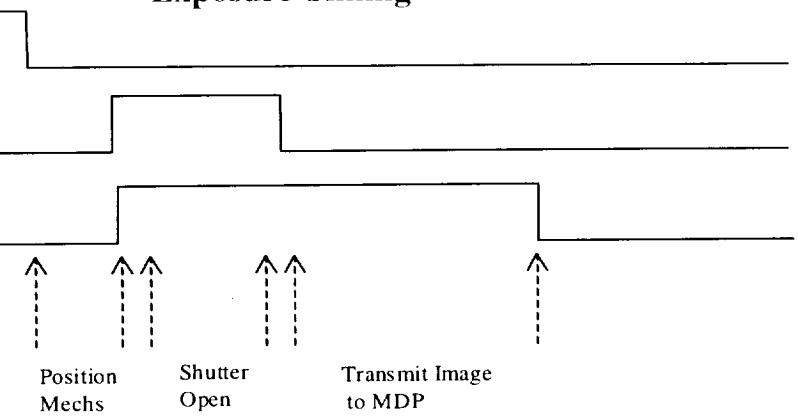

Analog Houskeeping

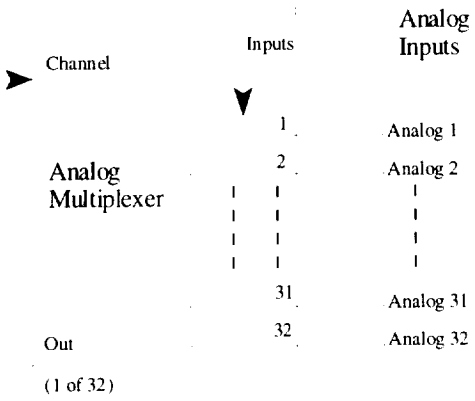

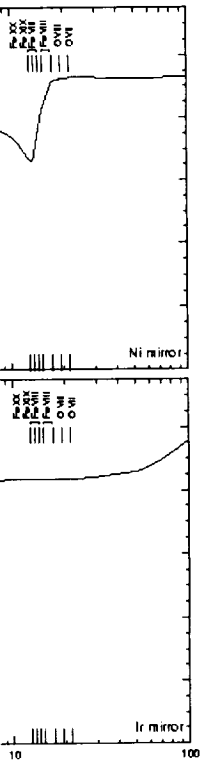

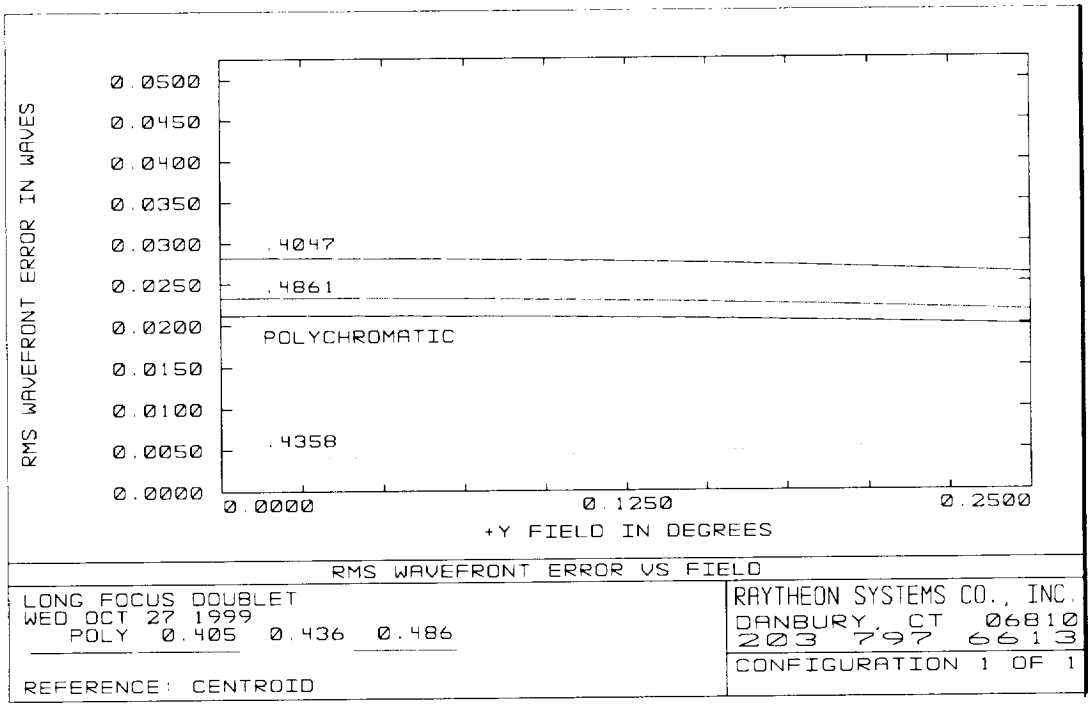

XRT Foldout No. 3

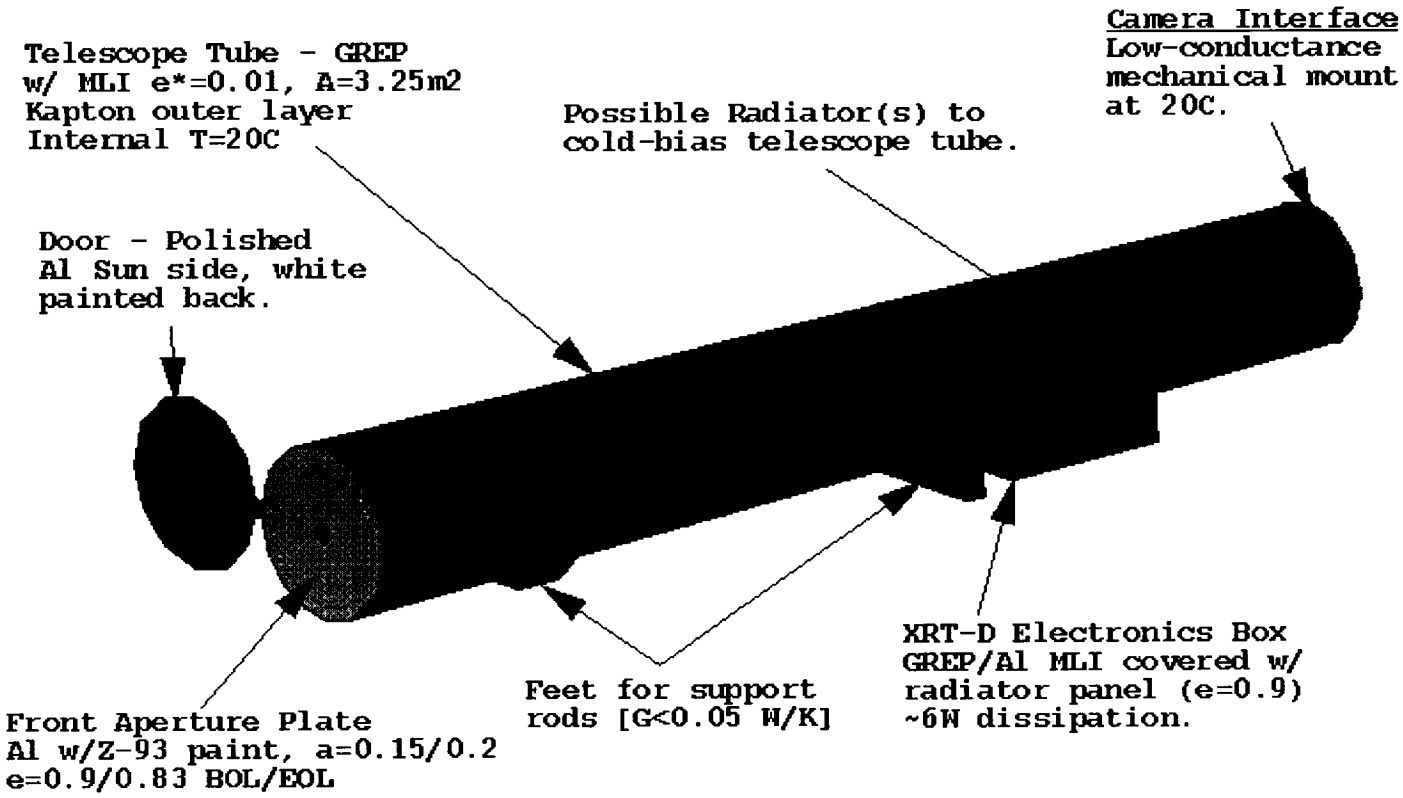

XRT Thermal Model

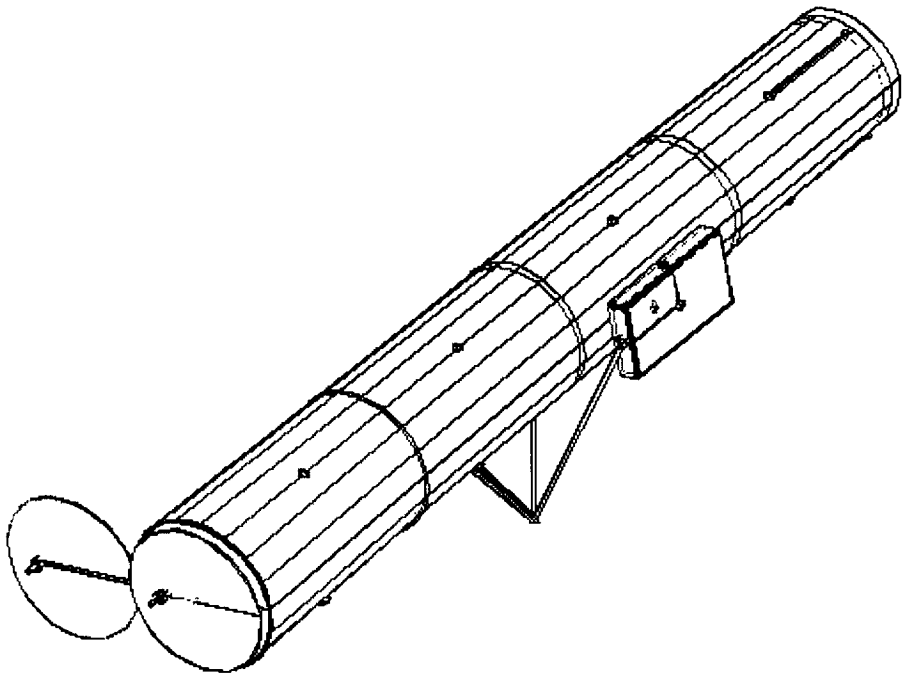

Note: Values are 55% Encircl
at 0.5 keV

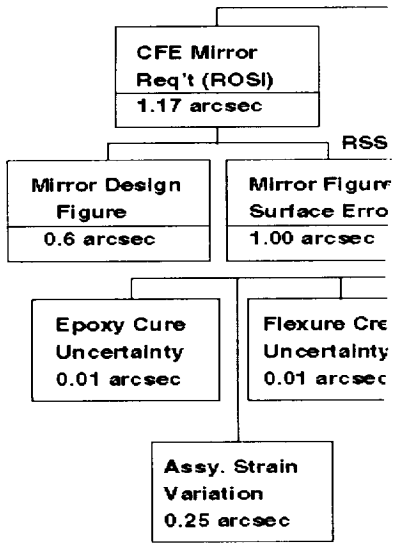

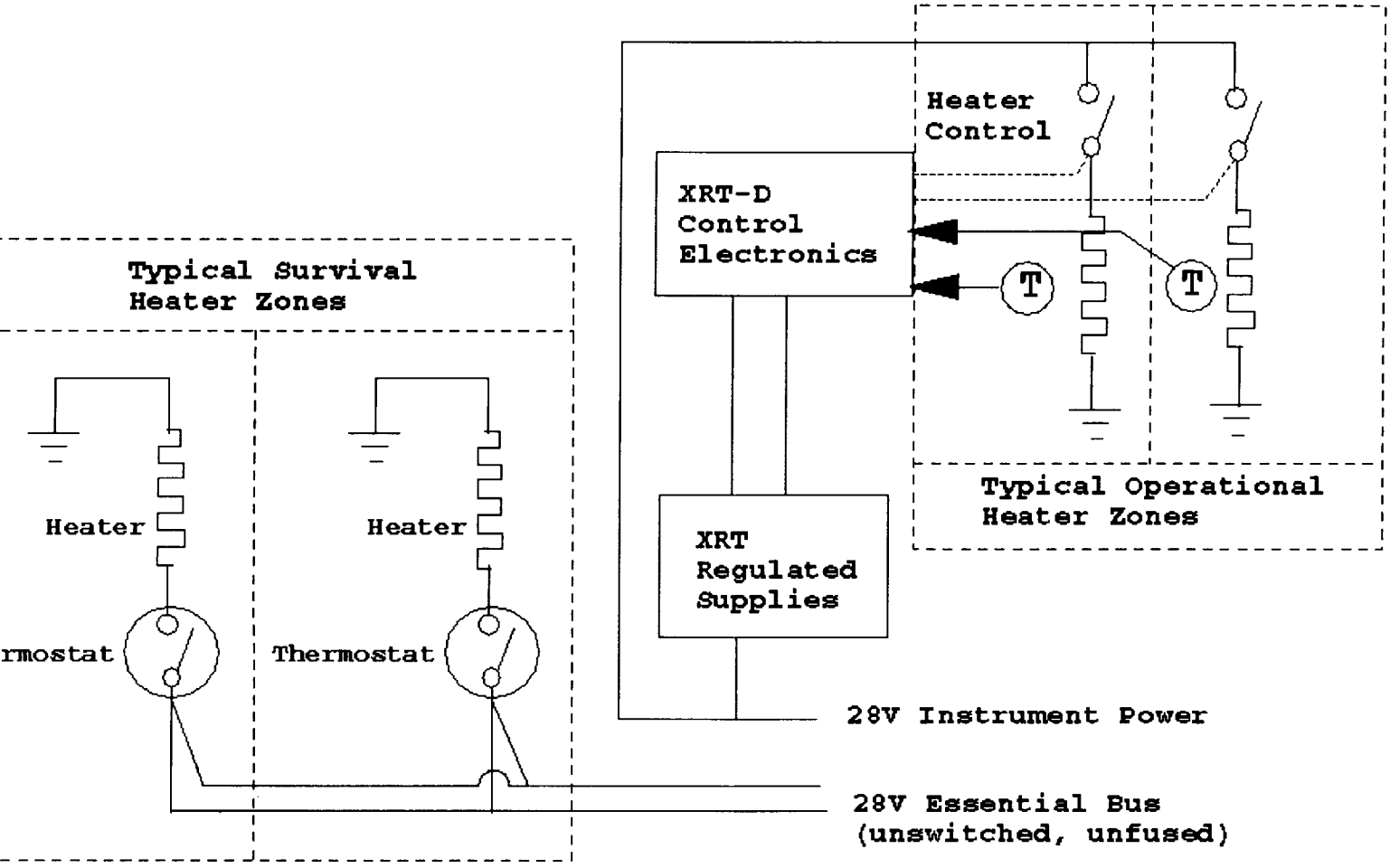

Solar-B XRT On-orbit Imaging Error Budget

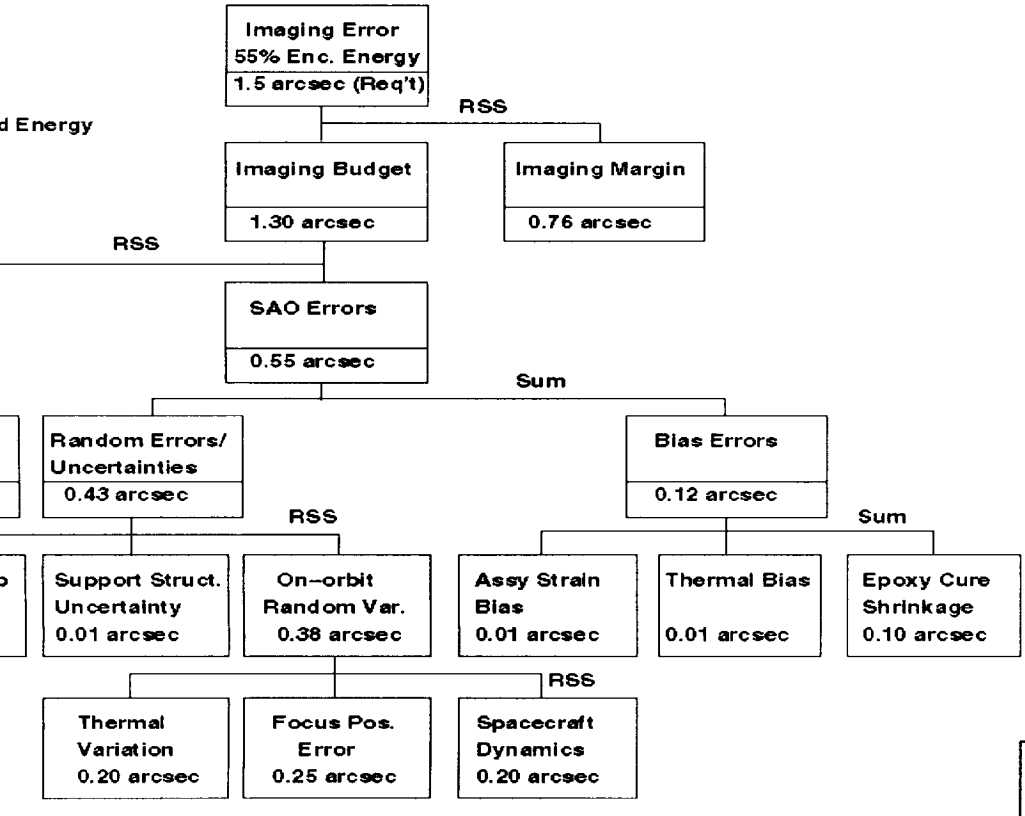

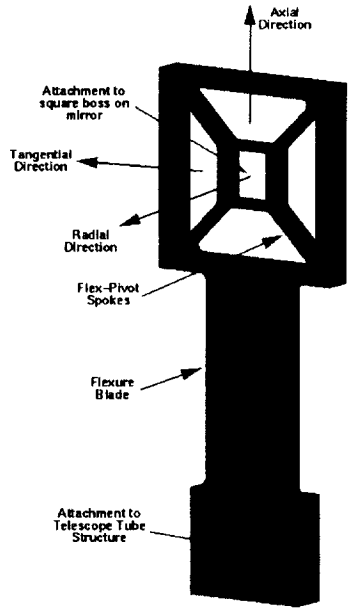

XRT Foldout No. 4

TABLE OF CONTENTS: DATA HANDLING AND DATA ANALYSIS

1. DATA HANDLING AND DATA ANALYSIS 106

1.1 DATA ACQUISITION & ARCHIVING 106
1.2 DATA PROCESSING & CALIBRATION 106
1.3 DATA DISTRIBUTION 107
1.4 DATA ANALYSIS 107

1. Data Handling and Data Analysis

The acquision, archiving and analysis of XRT images is discussed. Current computer technology is sufficient for the reformatting of the data, its long term storage and the scientific analysis. The large CCD format (2048x2048) exceeds the display size of most standard computers, but we expect that by 2004 monitors of this size will be readily available.

1.1 Data Acquisition & Archiving

As with other ISAS science missions, we anticipate that the entire Solar-B telemetry stream will be archived on the Sirius or equivalent system at ISAS. Following the Yohkoh model, we propose that a single reformatting program which resides on an ISAS workstation generate the Level-Zero data for all scientific instruments and Solar-B spacecraft shared data bases. Such a unified system minimizes duplication of effort and telemetry processing, promotes common treatment of the data and greatly facilitates coordinated planning and analysis. While the individual PI teams retain full control of the instrument specific Level-Zero definitions, common attributes in the data sets are exploited and access to Solar-B data such as attitude and ephemeris is provided to all teams in a consistent manner.

As with Yohkoh and consistent with our understanding of the Solar-B telemetry down-links, there will be two types of Level-Zero data sets produced at ISAS. The short term archive consists of the data which is received at KSC. The long term archive includes all available data from KSC and NASA facilities. It is anticipated that the short term Level-Zero data would typically be available to the planners within one hour after a KSC down-link. Based upon Yohkoh experience, we estimate that the long term archive generation can occur 2 to 4 weeks after data acquisition. When all of the available NASA and KSC data for a given day is verified resident on ISAS/Sirius, the reformattor would generate the long term archive. The baseline plan consistent with current ISAS capabilities and infrastructure would be to write two master versions of this long term archive to 4mm tapes.

The same reformattor program generates both short and long term archives, so that both archives and associated data bases have identical formats and only one set of access and analysis tools are required. Quicklook catalogs are automatically replaced (overwritten) by the corresponding long term versions as part of the process.

1.2 Data Processing & Calibration

The lead role in this effort at ISAS will be taken by personnel at Lockheed-Martin, working with SAO, and with the Solar-B Science Team. We propose to develop the data reduction and archival system based upon the successful Yohkoh model currently in place at ISAS. The archival support software will be written using Interactive Data Language (IDL) running under the SolarSoft environment (SSW). The SSW system, which includes full Yohkoh capabilities, is designed with software reuse, software sharing, coordinated solar planning and data analysis as primary goals. Many extensions to the Yohkoh model have evolved during SOHO and the TRACE Data Analysis Center development in areas such as online solar catalogs, WWW interfaces, user data request and

automated distribution. These applications were developed within the SSW environment and large portions of the support software is written in a generic way so it is directly applicable to related Solar-B archival and distribution tasks.

1.3 Data Distribution

Assuming that reasonable cost sharing between ISAS and the Solar-B instrument teams is negotiated, we propose that the long term archive for all of Solar-B is made available on a single DVD per UT-based day. The current pace of evolution, popularity, capacity and apparent reliability of DVD makes that an attractive choice as the Solar-B distribution media. The large capacity of DVDs coupled with the increasing capacity/cost ratio of DVD juke boxes will likely make it an excellent choice for online storage of large Solar-B data sets. A unified distribution , based on time division instead of instrument division, minimizes overhead for each science team and enables Solar-B coordinated data analysis. In this area, the Yohkoh (unified) distribution approach has proven vastly superior to SOHO.

1.4 Data Analysis

Level 1 science data will be generated from the Level-0 archived data via programs in the SSW package. An XRT-PREP procedure will be written to correct the data for hot pixels, radiation noise, dark current and flat fields. The visible light rejection of the front and focal plane filters will be monitored during the mission. If significant light leakage occurs, appropriate software will be written to correct for the errors.

TABLE OF CONTENTS; MANAGEMENT PLAN

1. MANAGEMENT PLAN 109

1.1 TEAM MEMBER RESPONSIBILITIES 109
1.2 INSTITUTIONAL TEAM MEMBERS 111
1.3 MANAGEMENT PROCESSES AND PLANS 112
1.3.1 Technical Performance 112
1.3.2 PLANNING 112
1.3.3 Measurement and Performance 113
1.3.4 Project Controls 113
1.3.5 Communications 113
1.3.6 Implementation & Direction 114
1.3.7 Conflict Resolution 114
1.3.8 Resource Management 114
1.3.9 Configuration Management (CM) and Control 114
1.3.10 Mission Assurance 115
1.4 Schedule & Major Milestones 116
1.5 Risk Management 117
1.6 Government Furnished Property, Services, and Facilities 118
1.7 Reporting 118
1.8 Reviews 118

1. Management Plan

Organizational Structure

The XRT program utilizes a management structure with clear lines of authority, program controls, and well delineated roles and responsibilities. The PI and PM established a management structure for the XRT and implemented it during the Phase A Concept Study. The overall project structure is in place and functioning effectively, and outstanding working relationships have been formed. This implemented structure is based on the highly successful TRACE management organization. All team members have worked previously with both the PI and the PM on the TRACE mission, and are capable of capitalizing on each member's strengths. The overall organization is shown in Figure 1-1 The roles and responsibilities of each of the key personnel are described below. The entire project team is dedicated to the following objectives and operational constraints:

1. Project management by a senior SAO manager with clear linkage to the PI
2. XRT is the first priority of all the key personnel
3. NASA and ISAS visibility into all aspects of the XRT
4. Maintaining a lean and effective organizational structure
5. Maintain clear institutional responsibilities with adequate oversight and review
6. Independent QA functions

1.1 Team Member Responsibilities

The XRT instrument Principal Investigator (PI) is Dr. Leon Golub. Dr. Golub brings over 27 years of experience in x-ray and EUV imaging of the Sun to the XRT program. Dr. Golub was the PI of the SAO TRACE program, and has maintained an active rocket program for the last 15 years. He will have full responsibility for all aspects of the instrument and for ensuring that the XRT instrument meets the mission requirements. The PI has selected a Program Manager (PM) and will select an Operations and Data Analysis Manager (OM) during Phase C. The PI reviews and approves the science objectives, science requirements, the flow-down of the instrument requirements, and the data analysis plan. The PI is the primary scientific interface to NASA and ISAS. The PI is ultimately responsible for the scientific integrity of the investigation, and hence has the ultimate decision-making authority. Dr. Golub will devote 60% of his time to the XRT program, averaged over Phases B-D. References for Dr. Golub are available from Professor Robert Rosner (773-702-0560, Department of Astronomy and Astrophysics, University of Chicago, Chicago, Il.).

Dr. Golub has selected Dr. Jay Bookbinder as the XRT Program Manager (PM). Dr. Bookbinder brings over 14 years of experience in X-ray astrophysics to the XRT program. He recently managed the TRACE hardware effort at SAO, and is currently the PI of the SAO TRACE Mission Operations and Data Analysis program. Dr. Bookbinder

was the scientist/manager for the HTXS Formulation Study (now the Constellation-X mission). Dr. Bookbinder reports to the PI and is delegated the responsibility to design, build, test, and deliver the XRT instrument. The PM is responsible for controlling costs and schedules by efficiently managing the program's assigned financial, material, manpower, and sub-contracted resources, and by identifying, acquiring, and managing the required SAO functional service groups support (e.g., Finance, Contracts, Quality Assurance, Purchasing, Publications, etc.). The PM monitors the program expenses, plans the program budgets, generates the monthly status reports and approves the monthly 533 reports. The PM is responsible for staffing of positions, and for implementing the SDB Plan. Under the PI's direction and council, he is the primary technical and programmatic interface to NASA and ISAS. The PM is responsible for providing status reports, and conducting all reviews, both internal and external. The PM recommends to the PI the need for the use of program reserve if required to preserve contractual commitments. Dr. Bookbinder will devote approximately 75% of his time to the XRT program, averaged over Phases B-D. References for Dr. Bookbinder are available from Mr. Bob Rasche (PM NICMOS, PM Constellation-X, 617 496-7774, 60 Garden Street, Cambridge, MA 02138).

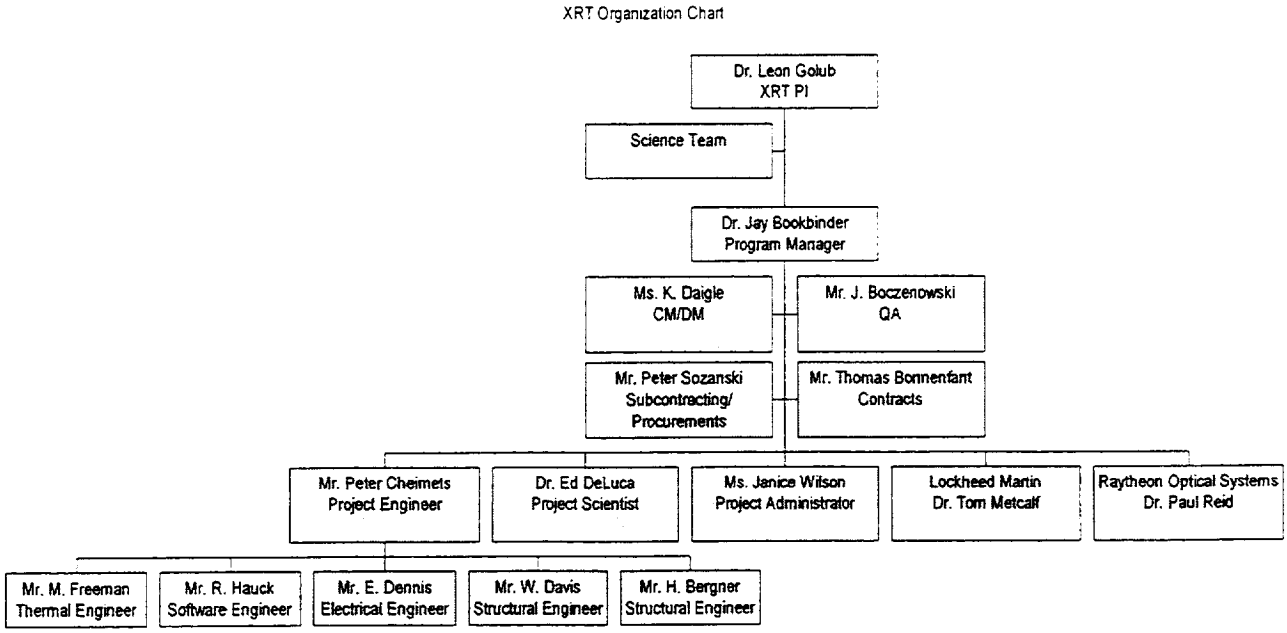

Figure 1-1

The Project Scientist (PS), Dr. Edward DeLuca, reports to the PM, and is delegated the responsibility for chairing the science team meeting. Dr. DeLuca brings over 13 years of experience in solar physics theory and modelling to the XRT program. He is currently the SAO Project Scientist on the TRACE mission. The PS shall assist the PM in developing the Program Plan and program schedules. The PS will help in organizing the mission operations of the XRT. He will function as the day-to-day science arm on the Program Manager's team. Dr. DeLuca will devote approximately 50% of his time to the XRT program, averaged over Phases B-D. References for Dr. DeLuca are available from Professor Robert Rosner (773-702-0560, Department of Astronomy and Astrophysics, University of Chicago, Chicago, Il.).

The PM is supported by a Project Engineer (PE), Mr. Peter Cheimets, who is delegated the full authority for all technical matters (including sub-contractor's technical performance) within the schedule and cost constraints of the Program Plan. The PE is responsible for the end-to-end system design; the definition of system, subsystem, and subcontractor interfaces and interface control parameters; and cross-system design verifications. He will identify and direct Lead Engineers for each subsystem as required. Mr. Peter Cheimets will devote approximately 60% of his time to the XRT program averaged over Phases B-D. References for Mr. Cheimets are available from Mr. Bob Rasche (PM NICMOS, PM Constellation-X, 617 496-7774, 60 Garden Street, Cambridge, MA 02138).

1.2 Institutional Team Members

The SAO Central Engineering (CE) department will carry out the engineering activities for the XRT. SAO/CE has extensive experience in a wide variety of space flight experiments, including the complete design and development of the Chandra/HRC, UVCS/Spartan, and major responsibilities on UVCS/SOHO, ROSAT, SWAS, TRACE and many other missions. SAO/CE provides a complete range of engineering and technical resources and facilities including groups in structural analysis, mechanical engineering, electrical engineering, drafting, thermal and systems engineering, and product assurance. Facilities include bonded storage areas, electronic and mechanical instruments, and computational facilities.

Considered part of the core team are Lockheed Martin (LM) and Raytheon Optical Systems, Inc. (ROSI). These team members provide expertise in key areas that enhance our ability to deliver the XRT on schedule and within budget.

Lockheed Martin (LM) holds several key responsibilities, including areas of hardware, software, and operations. LM's first obligation is the fabrication and testing of the filter wheels and shutter. Based on the existing TRIANA mechanisms ensures meeting the tight schedule and budgetary requirements of the program. LM also draws on extensive experience in working closely with ISAS on the *Yohkoh* mission, and will provide key manpower developing the mission operations scenario and during the Mission Operations phase. The principal contact at LM for the XRT program is Dr. Thomas Metcalf. Note that Dr Alan Title, PI for the FPP, is a Co-Investigator on the XRT.

Raytheon Optical Systems (formerly Hughes Danbury Optical Systems) is teamed with SAO to provide the (grazing incidence and white light) optics for the XRT. In particular, the grazing incidence optic utilizes ROSI's recent experience with designing, fabricating, and testing the SXI grazing incidence optics, as well as their extensive work on the *Chandra* optics. The principal technical contact at ROSI for the XRT program is Dr. Paul Reid.

The Science Team is responsible for establishing detailed scientific objectives and instrumentation requirements for the XRT by conducting science/cost trades, carrying out

data analyses, and reporting the results in engineering usable format. The Science Team is also responsible for defining the data reduction and analysis architecture, developing the software, and coordinating the post-launch data reduction and analyses. In turn, the Project Engineer (PE) supports the Science Team by providing them with engineering analyses and trade studies.

1.3 Management Processes and Plans

The overall XRT project structure is in place and functioning effectively. The PM will manage and refine the structure as necessary to ensure that the project is responsive and functional throughout all project phases. The management process includes project reporting, assignment of work tasks, independent hardware and software reviews, configuration management, acquisition planning, insight/oversight of vendors, tracking requirements and verification, conflict resolution procedures, logistics, lessons-learned activities, performance feedback to project staff and organizations. The PM shall establish metrics linked to major project milestones and ongoing processes to ensure adequate visibility to effectively manage the entire project. These metrics will be developed in a collaborative process with the project staff.

1.3.1 Technical Performance

The Level 1 Science Requirements Document and the flow-down of these requirements to the various subsystems will be used to document the technical system performance against the science requirements. These documents will track the effect of engineering changes on the science performance of the XRT. These documents also form the basis of the XRT Test and Verification plan. The PI and PS will evaluate the science impact of any change to the system.

1.3.2 Planning

The key to good planning is an accurate definition of the tasks to be accomplished to reach plan goals: a detailed Work Breakdown Structure (WBS) derived from these tasks, and a task-based schedule structure identifying key measurable milestones, deliverables, task dependencies, and program slack (schedule reserves) based on risk assessments. The proposed Program Management Team has the required experience and skill to generate a high-confidence Program Plan.

The management approach that SAO will utilize ensures that the program goals will be met on schedule and within budget. The two key elements of our approach are (1) maintaining a detailed requirements flow down document that is well understood by all the participants, including subcontractors, and (2) clear, effective, and traceable communications between the scientific and engineering staffs. SAO also maintains a Performance Specification and Flow-down document that forms the basis for all engineering decisions. This living document will be available on the web. Changes to this document will automatically be e-mailed to all XRT staff. This document is maintained

by the SAO Systems Engineer, and contains the requirements flow-downs to each subsystem.

1.3.3 Measurement and Performance

The XRT Project will have a set of measurement metrics that track project performance. These measurements will be tracked monthly or weekly as necessary. The following items will be measured: schedule performance, staffing per WBS element, drawings percent released, expenditures vs. baseline profile, contract actions, subcontract actions, subcontract performance, anomaly reports, fabrication started, software lines per day, software percent completed, action items issued/accepted, action items closed. Frequent monitoring of items of high risk or in the critical path will occur. A program operating plan has been developed, and detailed spending profiles will be further refined in Phase B.

1.3.4 Project Controls

The PM shall establish and manage project controls, including budget, schedule, and procurement items. Budget controls take the form of milestone payment authorizations to organizations and subcontractors, and signature authority for configuration management. The PM's schedule controls are signature authority on all project schedules, authority to manage the use of slack and the initiation of all requirement/funding/schedule trade efforts.

1.3.5 Communications

With an established Program Plan, the next driver to successful Program Management is timely and accurate communication among all members of the XRT Team and subcontractors, as well as among the Team, SAO's Associate Director for the High Energy Division, and NASA, so that effective and timely decisions can be made at each appropriate management level.

Communications between the scientists and engineers at SAO and our collaborators is characterized as *continuous* and detailed, with interactions taking place several times a day. Email serves to provide rapid and *traceable* communications without mis-understandings. Mail exploders ensure that all engineering and scientific staff are cognizant of requirements changes in all areas, and that all communications are archived on a weekly, monthly, and yearly basis. The Program Manager and PI having an "open-door" policy that allow all concerns to be aired quickly.

To facilitate communications, the Program Manager meets on a day-to-day basis with his technical team (the Project Scientist and the Project Engineer) to assess progress, identify potential problems, and to provide direction. Subsequent technical interchange meetings are held as often as required to resolve open technical issues. Formal action item lists are created and maintained.

To ensure progress is made consistent with the program schedule, a weekly engineering status meeting is held. This meeting, chaired by the PM, allows management insight into all aspects of the engineering. These meetings also ensure that systems-wide concerns and issues are identified and dealt with in a timely fashion.

On a more formal basis, bi-weekly project status reviews are held with the PI covering projected cost and schedule data as well as technical performance. Management concerns are identified and corrective actions are recommended by the PM and approved by the PI. Bi-monthly internal program reviews are also held for the Associate Director of the High Energy Division, to provide SAO management with a snapshot of program health and a working knowledge of program status.

SAO traditionally maintains extremely close communications with team members and subcontractors. As with TRACE, we will hold a weekly, one-hour telecon with our corporate partners: Lockheed-Martin and Raytheon Optical Systems. During these telecons, each member of the team provides a brief status report of the past week's work, plans for the coming week, and any problems. Particular attention is paid to interfaces.

During Phase A, we developed a preliminary approach to a bi-weekly telecon between the J-side XRT program manager (Sakao-san). These discussions were primarily concerned with interfaces, beginning in Phase B we expect that operational and science issues will also be part of the content of these telecons

1.3.6 Implementation & Direction

Day to day decisions and directions concerning managing the resources of the program are in the province of the Program Manager provided these decisions or directions do not compromise obligated bottom line costs or schedules or science performance. Decisions or directions regarding the use of program reserves can only be made with the approval of the PI.

1.3.7 Conflict Resolution

The PM has the responsibility to coordinate the activities of the program participants, and resolve conflicts according to agreements between ISAS, NASA, and other team members. If necessary, matters can be referred to the PI for resolution.

1.3.8 Resource Management

Resources (mass, power, envelope) will be allocated to the various subsystems by the PM and PE. These resources will be tracked by the PE. Resource contingencies are held by the PM, allocated by the PM, and documented as required.

1.3.9 Configuration Management (CM) and Control

SAO maintains a Configuration Management System that meets the requirements of NASA standards as well as those of ISO 9000 and is involved in all phases of the project. CM is responsible for the review and release of all contractually required data for a project. CM manages the data via interpretation and definition of contractual requirements; develops schedules for the timely generation and review of such documentation; and manages the review and incorporation of all changes to said deliverable data.

CM exercises change control via the Configuration Control Board (CCB) and provides traceability of the design via a Configuration Status Accounting (CSA) database with reports generated daily, if appropriate. These reports are utilized by Quality Assurance, production control, expediting, drafting room personnel, design engineering, and project management as the definitive source for current design status of the end item during all phases of the project. The PM chairs the Configuration Control Board (CCB) and has signature authority on all baseline and change actions. Examples of items under configuration control include the various requirements documents, ICDs, test plans, verification plans, integration procedures, and hardware drawings.

CM coordinates preparation and maintainence of the hardware family tree; the preliminary design review data package; the critical design review data package; the release, revision control and submission of deliverable documentation to customer; and participation in all design and acceptance reviews and audits.

CM is responsible for the preparation of the As-Designed vs the As-Built document and provides an analyses of the design release records versus QA build records to verify that the End Item was built to the most current design.

CM coordinates preparation of the Acceptance Data Package (ADP) for the deliverable item. As such, all data for the project must be accounted for. Any open items are identified, waivers and deviations as well as engineering change proposals (ECPs) are identified and status provided. This support is ongoing until the end item is accepted by the customer.

1.3.10 Mission Assurance

The XRT instrument will be designed to Class C standards, and mission assurance will follow the ISO 9001 guidelines. The mission assurance program will incorporate all necessary plans and reviews, and will be implemented in parallel with the design activities. SAO's product assurance program includes reliability analysis and component testing, and is aimed at selecting components in advance to minimize schedule and cost impact. SAO mission assurance emphasizes verification by test, and includes a failure reporting procedure that ensures that management has immediate insight into potential problems. Past "lessons learned" from other missions will be incorporated to ensure that flight hardware with heritage from other designs will avoid flight hardware failures.

1.4 Schedule & Major Milestones

Figure 1.4-1 represents the major milestones of the proposed XRT program. This schedule has been based on a detailed set of task schedules with all currently known dependencies, slack time requirements, and alternate risk mitigation concepts considered; over 200 tasks are in the detailed schedule.The current critical path is the optics development and qualification. The structure of this schedule is a result of the maturity of the instrument designs and analyses. The project schedule will be maintained in Microsoft Project software and a monthly update will be available on the XRT website. Figure 1.4-1 the schedule ensures that all personnel are cognizant of due dates and schedule interdependencies.

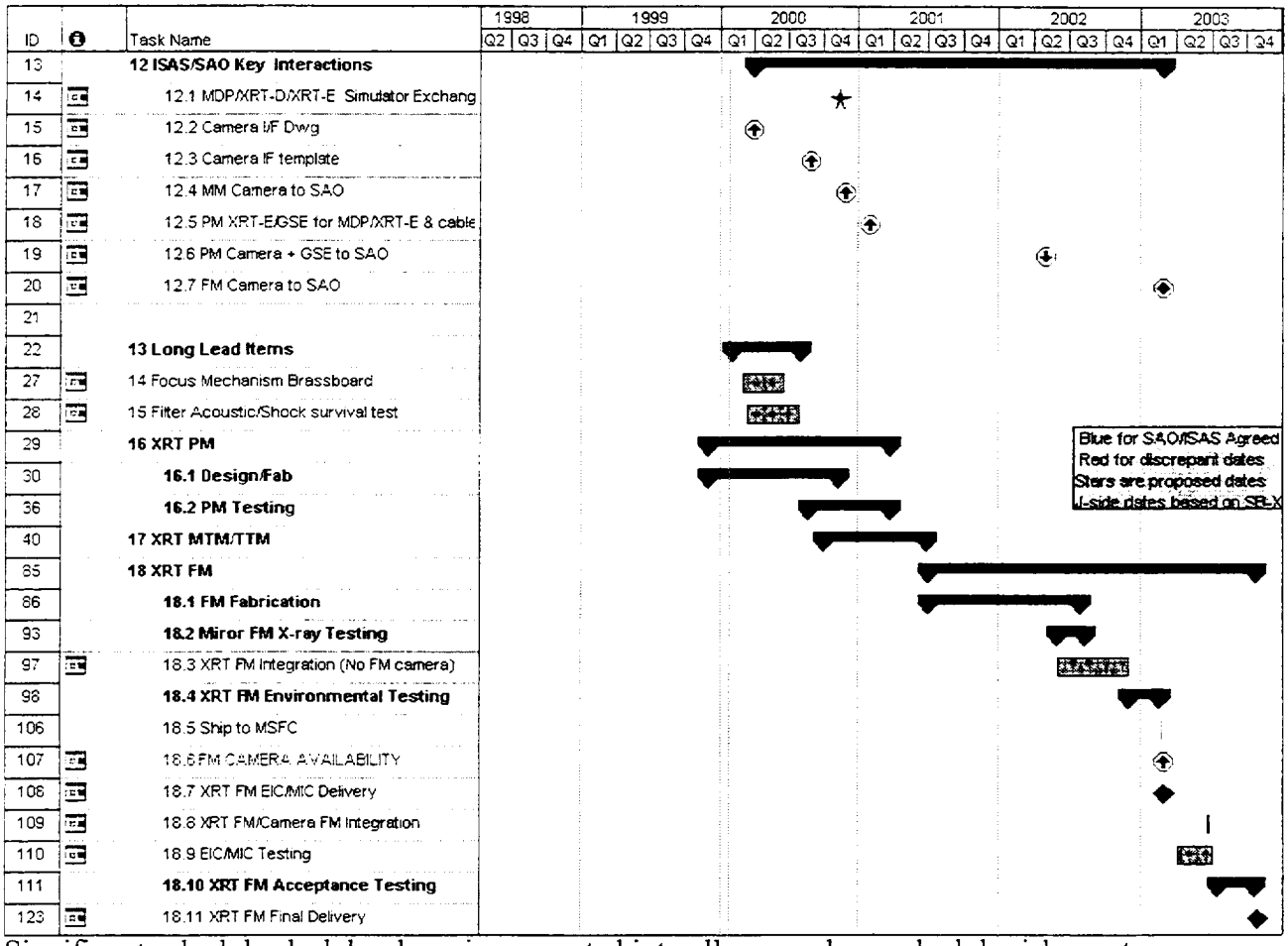

Significant schedule slack has been incorporated into all areas where schedule risk must be minimized. Slack is carried for all hardware deliverables to ISAS. In addition, slack is carried at lower levels of the schedule for all long lead items, major subcontract deliveries, and major testing activities. See table 1.4-2 below.

Table 1.4-2

Deliverables Slack	
Electrical Proto-model Delivery	5 weeks
MTM/TTM Delivery	4 weeks
Flight Model Delivery for EIC/MIC	3 weeks
Flight Model Delivery for I&T	5 weeks

1.5 Risk Management

The identification and assessment of potential risks (cost, schedule, technical, and scientific) has been of high priority during Phase A. During the Phase A Study, low-risk alternatives have been developed for areas that were deemed high risk by the PM or PE. Continuing the effort of identifying and managing risk will continue to be high priority during Phases B-D.

The XRT instrument has followed a design philosophy that avoids or minimizes risk in all areas, including the spacecraft interfaces. Risk avoidance encompasses technical, schedule, cost, and programmatic risks. Technical risks are minimized by the extremely simple instrument design. Interfaces have been defined that result in simple mechanical, electrical, and thermal interface definitions. Programmatic risks are minimized through (a) design base maturity and a thorough understanding of the mission's technical requirements and engineering approaches, (b) a proven system of planning, scheduling, reviews, and configuration management, and (c) a strong product assurance program and procurement expediting. Cost risks are minimized by use of the Requirements Flow-down document, a detailed WBS, and an extremely simple instrument design that minimizes mechanisms. Schedule risks are managed by holding a significant schedule reserves (approximately 4 months for the hardware deliverables, with additional slack at lower levels in the schedule as discussed above) that assures that the final delivery will be made on time.

SAO will continue to pursue risk-mitigation strategies in Phase B. In particular, two key engineering activities will take place in Phase B to minimize overall programmatic risks. First, we will execute a high-fidelity test of the ability of the focal plane filters to survive the acoustic loads present at launch. Second, we will be developing a brass-board model of the proposed focus mechanism. We view both of these items of high priority, and hence they are specifically called out in the overall program schedule shown above.

SAO identifies as risk two additional areas: the stringent weight and power limitations imposed on the X-ray instrument. These risk areas also impact costs and schedules. SAO will work closely with ISAS to manage the weight and power budgets, but notes that to a large extent the proposed costs for the XRT instrument are driven by the need to design, analyze, fabricate and test extremely lightweight components. Allocation of approximately 8 kg additional mass to the XRT would reduce cost, as well as reducing overall schedule risks. Allocation of approximately 5 watts additional power would also reduce programmatic risks.

1.6 Government Furnished Property, Services, and Facilities

Table 1.6-1 is a list of potential GFP/GFF for the XRT program. All listed facilities can be used wihtout modification. Some facilities may not be required (i.e., some tests may be performed at alternate locations including at other team member or subcontractor facilities) or may be substituted for each other (ie., the MSFC XRCF and the NIST beamline are both listed, but at most one would be utilized).

Table 1.6-1

GSFC Bldg 7	Mass Properties Measurement Facility. Large EMI facility. Thermal vac chambers.
GSFC Bldg 10	Acoustic Test Facility; 27'x40' Solar Vacuum Chamber
MSFC Bldg 4619	Structural Dynamics and Thermal Vac. Facility
MSFC	XRCF (X-ray Calibration Facility)
NIST	X-ray beamline

1.7 Reporting

A monthly narrative progress report will be generated by the PM and distributed to NASA, SAO management, and all team members. The content of this report includes a current status vs. the baseline schedule, plans for the next month, and areas of concern and suggested solutions if needed. Monthly financial reports (Forms 533) are generated and provided to NASA.

1.8 Reviews

The XRT team will support the independent reviews including: Requirements Review, Preliminary and Critical Design Reviews,Flight Confirmation Review, Pre-ship Review, and Flight Readiness Review. Actions assigned from these reviews will be entered into our online database and tracked until resolved.

TABLE OF CONTENT: TECHNICAL DEFINITION PLAN

1. TECHNICAL DEFINITION PLAN 120

1. Technical Definition Plan

The Technical Definition Phase is the final activity in the Mission Design Process. This phase will begin when an Authorization To Proceed (ATP) is given on November 1, 1999 and will culminate the last week of April 2000 with the Flight Confirmation Review. During this phase, the instrument architecture and design established in Phase A will be refined and become the baseline design to be presented at the Preliminary Design Review. The baseline design will be utilized to generate all data required for the start of the Implementation Phase (Phase C/D). Formalization of interfaces and subsystem specifications will begin. Firm costs and schedules will be prepared in Phase B that will be the baseline for the remaining mission phases.

The XRT science and engineering teams established during Phase A will transition in their entirety to Phase B. Maintaining the team ensures continuity of the design process and avoids inefficiencies associated with personnel changes. The core team will be supplemented by additional support in the various engineering disciplines as well as in areas such as procurements, subcontracting, and configuration management. As in Phase A, this team will meet weekly to assess progress against the baseline schedules.

The first task for the XRT science and engineering teams will be to review and update the instrument requirements, and to review and update the various system error budgets. With these in hand, external interfaces will be formalized and internal interfaces frozen.

Subsystem functional and performance specifications will be developed, and subsystem designs will be generated and subsystem performance and margin analysis will be conducted. Resources allocated at the subsystem level will be validated. Emphasis is placed on specification and design of the long lead items.

The short development time required by the program to meet the first set of hardware deliveries (the electrical Proto-model and the Mechanical Test Model/Thermal Test Model (MTM/TTM)) impose requirements on long lead item purchases and early testing of critical components. Long lead item purchases that will occur in Phase B include the telescope main tube and the optics blanks. The major component level tets to take place in Phase B is the high fidelity acoustic test of the focal plane filters, items at risk because of the unusually high acoustic loads present at launch. A set of engineering filters will be ordered and a high fidelity test will be performed to determine filter survival.

Programmatic efforts will include the development of the Risk Mitigation Plan, the Configuration Management Plan, the Cleanliness Plan, the Verification Plan, various ICDs, and the Phase C/D Implementation Plan. Phase B subcontracts will be issued, and discussions begun on the terms and conditions for the Phase C/D subcontracts. The CEI will be finalized and presented at the time of the PDR.

The preliminary program schedules developed in Phase A will be reviewed, revised and used to generate the baseline development schedule for Phase C/D taking into account the results of the Phase B testing. The critical path will be identified. The WBS will be revised as necessary, and the associated Phase C/D cost estimate will be reviewed, revised as necessary and a baseline cost plan for Phase C/D will be generated in conjunction with the schedule development. Efforts will continue to identify potential cost savings for the instrument.

TABLE OF CONTENT; COST PLAN

1. COST PLAN 123

1.1 COST ESTIMATING TECHNIQUES 123
1.2 PHASE B COST ESTIMATE 124
1.3 PHASE C/D COST ESTIMATE 124
1.4 PHASE E COST ESTIMATE 125
1.5 TOTAL NASA INVESTIGATION (TIC) ESTIMATE 125

1. Cost Plan

1.1 Cost Estimating Techniques

The costs for XRT were estimated by using two independent estimating methods: (a) grass-roots (or bottoms-up) and (b) analogy to similar work performed at SAO. By restricting comparisons to work at SAO, we ensure a more accurate estimate of actual costs. We did not make use of cost models for these estimates. We consider the grass-roots estimates to be the more accurate method, and these costs are the ones we present. This estimate was prepared with inputs from all of the scientists, engineers and managers responsible for delivering instrumentation and scientific data for the XRT. All estimates are in real year dollars, with NASA-approved inflation rates applied.

The bottoms-up estimates were produced by the members of the proposal team who will be responsible for the actual work. These estimates are based on the WBS provided in the Phase B proposal.Workforce, procurements, services, facilities, and travel were estimated down to Level 5 of the WBS, depending on the complexity of the WBS element, by the appropriate individuals at each institution. The extensive preliminary design work and a careful evaluation of the interface requirements for each WBS element ensure that these bottoms-up costs accurately reflect the labor involved in developing the XRT.

In addition to labor costs, vendor quotes have been obtained for major hardware, software, and service procurements. To obtain these costs, RFIs were issued, and the responses are used to cost major purchases and subcontracts. Such items include the optics, the main structural support tube (a composite material), and the shutter and filter wheel mechanisms.

Following the bottoms up estimate, costs are reviewed by the PI, Program Manager, Project Engineer, and systems engineers to ensure that all interfaces are accounted for. SAO draws on extensive space engineering experience to verify the various assembly and subassembly estimates that comprise the space portion of the XRT instrument. The resulting hardware estimates include amortized amounts for management, systems engineering, configuration management, data management, and product assurance.

In addition to the bottoms-up cost estimation methodology, all costs at the system and subsystem level have been "reality checked" by analogy with similar work done by SAO on a variety of other space programs, including the High Resolution Camera (HRC) on AXAF, the TRACE mission, ROSAT, and the Einstein mission.

1.2 Phase B cost Estimate

The Phase B cost by WBS element is:

WBS 1	Management	$422,848
WBS 2	X-ray Telescope Flight System	$148,811
WBS 3	GSE & Proto-models	$1,058,173
WBS 4	Systems Engineering & Integration	$93,506
WBS 5	Operations	$0
WBS 6	Product Assurance	$16,042

Phase B Workforce Staffing Plan

Table 1.1-1below provides the SAO (including LM) Phase B workforce staffing plan by discipline:

Table 1.1-1

	FTE
Science.	1.3
Management	1.2
Engineering.	4.4
QA/CM	0.4

The SAO Phase B workforce staffing plan by WBS is (note that CM is carried as management in table 1.1-2 below):

Table 1.1-2

		FTE
WBS 1	Management .	2.3
WBS 2	X-ray Telescope Flight System	0.9
WBS 3	GSE & Proto-models	3.0
WBS 4	Systems Engineering & Integration	0.5
WBS 5	Operations	0.3
WBS 6	Product Assurance	0.2

1.3 Phase C/D Cost Estimate

A Phase C/D ROM cost estimate has been developed by SAO to assist MSFC for planning purposes. Phase C/D costs will continue to evolve until the Phase C/D proposal is submitted to MSFC. The current Phase C/D costs are estimated to be approximately $12.8M in real year dollars.

The SAO Phase C/D preliminary staffing plan by discipline is seen in table 1.1-3.

Table 1.1-3

	FTE				
	FY 00	FY 01	FY 02	FY 03	FY 04
Science + EPO	0.8	2.1	2.2	2.2	2.4
Management	0.8	1.8	1.8	1.6	1.5
Engineering	4.1	5.6	7.1	2.2	1.8
QA/CM	0.4	1.3	1.3	1.3	1.2

The SAO Phase C/D preliminary staffing plan by WBS is provided in table 1.1-4. As above, note that CM is carried as management. Also, mission operations preparations are carried in WBS 1 and as part of the subcontract effort from Lockheed-Martin, that manpower effort is not shown below.

Table 1.1-4

		FTE				
		FY 00	FY 01	FY 02	FY 03	FY 04
WBS 1	Management	1.7	4.2	4.4	4.2	4.2
WBS 2	X-ray Telescope Flight System	0.7	2.5	5.7	1.7	0.8
WBS 3	GSE & Proto-models	3.3	3.2	0.6	0.1	0.1
WBS 4	Systems Engineering & Integration	0.1	0.9	0.9	0.7	1.0
WBS 5	Operations	0	0	0	0	0
WBS 6	Product Assurance	0.3	0.9	1.0	1.0	1.0

1.4 Phase E Cost Estimate

A Phase E ROM cost estimate has been developed by SAO to assist MSFC for planning purposes. The current estimate of the Phase E costs are estimated to be approximately $9M in real year dollars.

1.5 Total NASA Investigation (TIC) Estimate

SAO estimates that the total NASA cost for the XRT instrument will be $15.4M in real year dollars.

While SAO's current cost estimates meet the NASA mandated cost caps, we have had to assume a fully success-oriented program. Manpower loadings are less than optimal in several support areas, Including configuration management, schedule development and contingency planning, integration manpower, and education and public outreach. Procurements are also based on a success-oriented basis, with the number of spares at a minimum.

1. Appendices

1.1 Resumes

1.2 Phase B SOW

1.3 Phase C/D SOW

1.4 Phase E SOW

1.5 References

LEON GOLUB VITA

Smithsonian Astrophysical Observatory
60 Garden Street
Cambridge, MA 02138
(617) 495-7177 Fax: 496-7577 e-mail: golub@corona.harvard.edu

Education:

Ph. D., Physics, M. I. T. (1972)
B. S., Physics, Cum Laude, C. C. N. Y. (1967)

Positions Held:

1980- : Astrophysicist, Smithsonian Astrophysical Observatory
1977- : Lecturer on Astronomy, Harvard University
1977-80: Research Associate, Harvard College Observatory
1975-77: Staff Scientist, Solar Physics Group, A. S. E.
1972-75: Senior Scientist, "
1967-72: Research Associate, Experimental High Energy Physics, M.I.T.

Professional Societies:

American Astronomical Society
American Physical Society
International Astronomical Union
Optical Society of America
American Geophysical Union
Society of Photo-Optical Instrumentation Engineers
Phi Beta Kappa

Committee Memberships and Awards:

Geophysical Research Letters (AGU) On-line Reviewer
Executive Committee Councillor, DAP, American Physical Society
Councillor, SPD, American Astronomical Society
NASA Solar Physics MOWG (Management Operations Working Group)
NASA SPS (Space Physics Advisory Subcommittee)
NASA Solar Probe Science Working Group
NASA Solar-B Science Working Group
NASA Space Physics Connections Working Group
NASA Sounding Rocket Working Group
NASA OSL Non-advocacy Review Board
Conference Chairman, "X-ray Instrumentation in Astronomy II"
Space Station Users' Working Group
SAMEX Science Working Group
Max '91 Science Working Group
NRC/Space Science Board Space Physics Task Group
NASA Solar Mgmt. Operations Working Group
NASA Skylab Achievement Award

SELECTED PUBLICATIONS

"The Solar Corona", (1997) **Textbook**, Cambridge University Press.

"Difficulties in Observing Coronal Structure," (1997) Sol. Phys., **174**, 99.

"Reflections on the Business of Space", **Keynote Address**, Space Horizons Conference, Cambridge MA, May, 1996.

"Sub-Arcsecond Observations of the Solar X-ray Corona", (1990) Nature **344**, 842.

"Rocket Astronomy", (1990, 1995) McGraw-Hill Science Encyclopedia

"X-ray Instrumentation in Astronomy II", SPIE Conf. No. 982, (1990) L. Golub, Editor and Conference Chairman.

"On Stellar X-ray Emission", (1985) *Ann. Rev. Astron. Astrophys.*, **23**, 41.

"X-ray Bright Points and the Solar Cycle", (1980) Phil. Trans. Royal Soc. London A **297**, 595; Invited Talk.

VITA AND BIBLIOGRAPHY -- ADRIAAN A. VAN BALLEGOOIJEN

Born: [redacted]

Citizenship: The Netherlands

Education:

1973 - University of Utrecht, The Netherlands, Bachelor's degree ("Candidaats") in Physics and Mathematics
1978 - University of Utrecht, Master's degree ("Doctoraal") in Astronomy and Physics
1982 - University of Utrecht, Ph.D. in Astronomy, thesis on "Sunspots and the Physics of Magnetic Flux Tubes in the Sun"

Positions held:

1978 - 1982: Graduate student fellowship, Netherlands Organization for Pure Research (ZWO), The Hague, The Netherlands
1983 - 1986: Consultant, Lockheed Palo Alto Research Laboratory, Solar and Optical Physics Branch, Palo Alto, CA
1986 - 1991: Astrophysicist, Smithsonian Institution (Trust Fund), Smithsonian Astrophysical Observatory, Cambridge, MA
1991 - : Astrophysicist, Smithsonian Institution (Federal), Smithsonian Astrophysical Observatory, Cambridge, MA
1988 - : Lecturer, Harvard University, Cambridge, MA

Professional Associations: American Astronomical Society
Solar Physics Division of AAS

Research Interests: Solar magnetic fields, nonthermal heating of the solar atmosphere, convection, radiative transfer, filaments and prominences, sunspot structure, magnetic fields in accretion disks.

Publications relevant to the proposal:

van Ballegooijen, A.A. 1984, On the Temperature Structure of Sunspot Umbrae, Solar Phys., 91, 195

van Ballegooijen, A.A. 1985, Electric Currents in the Solar Corona and the Existence of Magnetostatic Equilibrium, ApJ, 298, 421

van Ballegooijen, A.A. 1985, Contribution Functions for Zeeman-Split Lines, and Line Formation in Photospheric Faculae, in Measurements of Solar Vector Magnetic Fields, ed. M.J. Hagyard (NASA CP-2374), p. 322

van Ballegooijen, A.A. 1985, Transport of Polarized Light in Small Flux Tubes, in Theoretical Problems in High Resolution Solar Physics, ed. H.U. Schmidt (Muenchen: Max-Planck-Institut fuer Astrophysik), p. 167

van Ballegooijen, A.A. 1986, Cascade of Magnetic Energy as a Mechanism of Coronal Heating, ApJ, 311, 1001

Spruit, H.C., Title, A.M., and van Ballegooijen, A.A. 1987, Is there a weak mixed polarity background field? Theoretical Arguments, Solar Phys., 110, 115

van Ballegooijen, A.A. 1988, Magnetic fine structure of solar coronal loops, in Solar and Stellar Coronal Structure and Dynamics, ed. R. Altrock (Sunspot: National Solar Observatory), p. 115

van Ballegooijen, A.A., and Martens, P.C.H. 1989, Formation and Eruption of Solar Prominences, ApJ, 343, 971

van Ballegooijen, A.A. 1989, Magnetic Heating of Stellar Chromospheres and Coronae, in Proc. Sixth Cambridge Workshop on Cool Stars, Stellar systems, and the Sun, ed. G. Wallerstein, ASP Conf. Series, Vol. 9, p. 15

van Ballegooijen, A.A., and Martens, P.C.H. 1990, Magnetic Fields in Quiescent Prominences, ApJ, 361, 283

van Ballegooijen, A.A. 1990, Structure and Equilibrium of Coronal Magnetic Fields, in Proc. IAU Symp. 142, Basic Plasma Processes on the Sun, eds. E.R. Priest and V. Krishan, p. 303

van Ballegooijen, A.A. 1994, Magnetic Fine Structures in Coronal Loops, in Proc. Second SOHO Workshop on Mass Supply and Flows in the Solar Corona, eds. B. Fleck, G. Noci and G. Poletto, Space Science Reviews, 70, 31

Priest, E.R., van Ballegooijen, A.A., and Mackay, D.H. 1996, A Model for Dextral and Sinistral Prominences, ApJ, 460, 530

Schrijver, C.J., Title, A.M., van Ballegooijen, A.A., Hagenaar, H.J., and Shine, R.A. 1997, Sustaining the Quiet Photospheric Network: The Balance of Flux Emergence, Fragmentation, Merging, and Cancellation, ApJ, 487, 424

Title, A.M., Schrijver, C.J., van Ballegooijen, A.A., Hagenaar, H.J., and Shine, R.A. 1997, The Dynamic Nature of the Supergranular Network, BAAS, SPD meeting No. 29 (Bozeman, MT, June 1997), 02.42

van Ballegooijen, A.A. 1998, Understanding the Solar Cycle, in Synoptic Solar Physics -- 18th NSO Sacramento Peak Summer Workshop, Sunspot, NM, 8-12 Sept. 1997, eds. Jack Harvey, K.S. Balasubramaniam \& D. Rabin, ASP Conf. Series, Vol. 140, 17

van Ballegooijen, A.A., Cartledge, N.P., and Priest, E.R. 1998, Magnetic Flux Transport and the Formation of Filament Channels on the Sun, ApJ, 501, 866

van Ballegooijen, A.A., Nisenson, P., Noyes, R.W., Lofdahl, M.G., Stein, R.F., Nordlund, A., and Krishnakumar, V. 1998, Dynamics of Magnetic Flux Elements in the Solar Photosphere, ApJ, in press

CURRICULUM VITAE

Jay A. Bookbinder

Address: Smithsonian Astrophysical Observatory
60 Garden Street
Cambridge, MA 02138
(617) 495-7058

Date of Birth: December 30, 1957

Education:	1985		Ph.D., Harvard University Department of Astronomy
	1979		B.A., Princeton University Cum Laude in Physics
Academic Awards:	1987		NATO Fellowship
	1983		Certificate for Excellence in Teaching Harvard University
	1979 -	1981	Smithsonian Fellowship
Positions Held:	8/97 -	present	Mission Scientist Constellation X-ray Mission (CXM)
	1/96 -	present	Adjunct Professor of Physics and Astronomy Denver University
	8/95 -	present	SAO Program Manager, TRACE
	6/93 -	1/97	Program Manager, SWATH
	12/92 - 1/97	present	Project Scientist, SWATH Smithsonian Astrophysical Observatory
	6/91 -	present	Lecturer, Harvard University
	6/88 -	present	Astrophysicist Smithsonian Astrophysical Observatory
	10/85 -	6/88	Research Associate Joint Institute for Laboratory Astrophysics
	1981 -	1985	Research Fellow, Harvard University
	1980 -	1983	Teaching Fellow, Harvard University

CURRICULUM VITAE

Jay A. Bookbinder

cont'd

Committee Memberships:

1997	Science Organizing Committee 10th Cambridge Cool Stars Workshop
1997	Science Organizing Committee High Resolution Solar Atmospheric Dynamics Workshop
1996 - 1998	CfA Library Committee
1991	Science Organizing Committee 7th Cambridge Cool Stars Workshop
1988 - 1991	Arecibo Science Advisory Comm.(Chair 1991)
1987 - 1990	NRAO User's Committee
1987	Local Organizing Committee 5th Cambridge Cool Stars Workshop

Misc. Committee Memberships:

1996	NASA (ADP, ASCA) Peer Reviews
1995	NASA (ADP, ASCA) Peer Reviews
1994	NASA (ADP, ASCA) Peer Reviews
1993	NASA (ROSAT,ASCA) Peer Reviews
1993	NSF (Stellar) Peer Review
1992	NASA (ADP,IUE) Peer Reviews
1991	NASA (ROSAT) Peer Review
1988 - 1992	NRAO Peer Review

Professional Societies:

American Astronomical Society
American Mathematical Association
SPIE
AAAS
Sigma Xi

General Fields of Investigation: High resolution Solar X-ray imaging; high resolution stellar X-ray spectroscopy; non-thermal heating of stellar coronae. Current observational programs include HST studies of Lyman-alpha emission from late-type stars as a probe of both the ISM and stellar atmospheric heating, HST and ASCA studies of eclipsing binaries to determine the spatial structures in stellar chromospheres and coronae, and magnetic field measurements on late-type stars utilizing the CSHELL instrument on the IRTF.

Peter Cheimets
Project Engineer

June 1981: **M.S. Mechanical Engineering from Stanford University**
Degree in Mechanical Dynamics and Control Systems Design.

June 1978: **B.S. Mechanical Engineering from MIT**
Concentration in Mechanical Design.

1983 - Date: **Mechanical Engineer with Smithsonian Astrophysical Observatory**

- **TRACE Project Engineer:** Design, fabrication and testing of TRACE mirrors, primary mirror mounts and front aperture filters. Responsibility for the overall project, as well as the design and fabrication of the TRACE mirrors, primary mirror mount, pre-filter design and filter chamber design and construction. This project included full ECO control on all documentation, full procedural control on all flight operations and a full battery of NASA-required testing all proto-type and flight hardware.
- **SMA Project Engineer:** Design, fabrication and testing of the SubMillimeter Array (SMA) chopping subreflector and manipulator. Project involved designing, fabricating and testing a fully operational prototype, followed by 5 built to print copies. I had overall team management, budget and schedule oversight, overall design and fabrication management throughout the project. Project successfully concluded 20% under budget.
- **Mark III Interferometer Project Engineer** Design and fabrication of the Mark III Interferometer. I designed, coordinated the fabrication and assembly of the Mark III interferometer. The design involved placing two 7 meter linear stages in separate vacuum chambers. Constructing numerous complex electro-optical and opto-mechanical systems and installing a 40 meter variable baseline under extreme schedule and budget pressure. The project was the result of a cooperative effort across many institutions requiring interaction with as many as 4 separate organizations to accomplish a single task. Project included many short and emergency turn around efforts, all met within imposed schedule and budget.
- **Design and Analysis:** Work on numerous other ground, balloon and space based astrophysical instruments including:
  - **Advanced X-ray Astrophysical Facility (AXAF):** A space telescope class high energy stellar telescope.
  - **EXITE**: Balloon based Extreme x-ray telescope.
  - **Normal Incident X-ray Telescope (NIXT):** Normal Incident telescope for viewing the Sun from a sounding rocket.
  - **MMT Spectrometer Design:** Design of a number of spectrometers for use at the Multiple Mirror Telescope and other telescopes on Mt. Hopkins.
- **Review and Oversight:** I have conducted many reviews of the space hardware design projects as part of SAO compliance with NASA requirements.
- **Teaching**: I have taught CAD/CAM and electromechanical design at Harvard University and MIT. I have taught manufacturing techniques at Stanford University.

EDWARD E. DeLUCA

Institutional Address:

Smithsonian Astrophysical Observatory

60 Graden Street

Cambridge, MA 02138

(617) 496-7725

Education:

Wesleyan University, B.A. (cl), Astronomy (1979).

Wesleyan University, M.A., Astronomy (1980).

University of Colorado, Ph.D., Astrophysics (1986).

Positions Held:

1980-81	Teaching Assistant, Dept. of APAS, University of Colorado
1981-82	Research Assistant, Dept. of APAS, University of Colorado
1982-86	Research Assistant, High Altitude Observatory, NCAR
1986-87	Postdoctoral Research Fellow, Advanced Study Program, NCAR
1987-88	Astrophysicist, Smithsonian Astrophysical Observatory
1987-88	Visiting Scholar, Dept. of Astronomy and Astrophysics, The University of Chicago
1988-90	Research Associate, Dept. of Astronomy and Astrophysics, The University of Chicago
1990-93	Assistant Astronomer, Institute for Astronomy, University of Hawaii
1993-	Astrophysicist, Smithsonian Astrophysical Observatory

Honors:

Compton Lecturer Spring 1989: University of Chicago

Professional Societies:

American Physical Society, American Astronomical Society, American Geophysical Union, The New York Academy of Sciences.

Research Interests

MHD simulations of coronal heating and reconnection.

Two and three dimensional simulations of dynamo action in compressible fluids.

Coronal temperature diagnostics and fine structure.

ALAN M. TITLE

Consulting Physicist and Senior Member of the Research Laboratory
Advance Technology Center Lockheed Martin Corporation
(650) 424 4034
FAX (650) 424 3994
e-mail title@nice.lmsal.com

Consulting Professor
Co-Director Stanford-Lockheed Institute for Space Research
Stanford University
Stanford, CA

Education

Ph.D., Physics, 1966, California Institute of Technology
B. S., Physics, 1961, Columbia University
B. A., Mathematics, 1960, University of California, Los Angeles

Professional Society Memberships

American Association for Advancement of Science
American Astronomical Society
Optical Society of America
Solar Division, AAS

Awards, Honors and Professional Activities

Robert E. Gross Award, 1983, Scientist of the Year, Lockheed Corporation
Space Science Metal, American Institute Aeronautics and Astronautics, 1990
James Arthur Lectureship Harvard University 1991

Member, Solar Probe Science Definition Team for NASA, 1996-present
Member, Solar B Science Definition Team for NASA, 1996-present
Member, Solar Stereo Science Definition Team for NASA, 1996-present
Member, National Academy of Sciences Committee on Small Explorers, 1996
Member, National Academy of Sciences Task Force on Solar Physics, 1996-Present
Member, Sun-Earth Connection Advisory Committee to NASA Administrator, 1998
Member, Space Science Board of the National Research Council, 1998-2001
Member, Executive Committee Space Science Board, 1998-2001

Principal Investigator, SOUP on Spacelab 2, 1974-1987
Principal Investigator, CIP on OSL, 1980-present
Principal Investigator, TRACE Small Explorer Mission 1993 - present

Co-Investigator responsible of Science Instrument, MDI for SOHO, 1988-present

CURRICULUM VITAE

Terry Gene Forbes

Education:

BS: Physics, 1968, Purdue University, Lafayette, Indiana.

MS: Astro-Geophysics, 1970, University of Colorado, Boulder, Colorado.

PhD: Astro-Geophysics, 1978, University of Colorado, Boulder, Colorado

Employment History:

Research Professor (1990-present) Department of Physics, and The Institute for the Study of Earth, Oceans and Space, University of New Hampshire, Durham, New Hampshire, 03824.

Associate Research Professor (1986-1990) Department of Physics, and The Institute for the Study of Earth, Oceans and Space, University of New Hampshire, Durham, New Hampshire, 03824.

Research Scientist II (1984-1986) Space Science Center, University of New Hampshire, Durham, New Hampshire, 03824.

Research Fellow (1980-1984) Department of Applied Mathematics, University of St. Andrews, St. Andrews, Scotland, KY16 9SS.

Post-Doctoral Appointment (1978-1980) Los Alamos National Laboratory, Los Alamos, New Mexico, 87545.

Physical Scientist Specialist (1971-1973), US Army Electronics Command (ECOM), Ft. Monmouth, NJ, 07703, (Compulsory Military Service).

Research Engineer I (1968-1969) Amphenol Division, Bunker-Ramo Corporation, Commerce Drive, Oak Brook, Illinois, 60521.

Relevant Publications:

Implosion of a Uniform Current Sheet in a Low Beta Plasma, T.G. Forbes, *J. Plasma Phys.*, *27*, 491, 1982.

Numerical Study of Line-tied Magnetic Reconnection, T.G. Forbes and E.R. Priest, *Solar Phys.*, *81*, 303, 1982.

Numerical Experiment Relevant to Line-tied Magnetic reconnection in Two-Ribbon Flares, T.G. Forbes and E.R. Priest, *Solar Phys.*, *84*, 169, 1983.

Mass Upflows in 'Post'-Flare Loops, T.G. Forbes and E.R. Priest, *Solar Physics*, *88*, 211, 1983.

Reconnection in the Solar Atmosphere, T.G. Forbes and E.R. Priest, in *Solar Terrestrial Physics: Present and Future*, (eds. D.M. Butler and K. Papadopoulous) NASA RP-1120, p. 1-35, 1984.

Shock-Condensation Mechanism for Loop Prominences, T.G. Forbes and J.M. Malherbe, *Astrophys. J. Lett.*, *302*, L67-L70, 1986.

Fast-Shock Formation in Line-tied Magnetic Reconnection Models of Solar Flares, T.G. Forbes, *Astrophys. J.*, *305*, 553, 1986.

New Models for Fast Steady-State Magnetic Reconnection, E.R. Priest and T.G. Forbes, *J. Geophys. Res.*, *91*, 5579, 1986.

Comparison of Analytical and Numerical Models for Steadily-Driven Magnetic Reconnection, T.G. Forbes and E.R. Priest, *Revs. Geophys.*, *25*, 1583, 1987.

Magnetohydrodynamic Boundary Conditions for Global Models, T.G. Forbes, in *Modeling Magnetospheric Plasma*, (eds. T.E. Moore and J.H. Waite, Jr.), invited paper, *AGU Monograph 44*, p. 319, 1988.

Shocks Produced by Impulsively Driven Reconnection, T.G. Forbes, *Solar Phys.*, *117*, 97, 1988.

Steady Magnetic Reconnection in Three Dimensions, E.R. Priest and T.G. Forbes, *Solar Phys.*, *119*, 211, 1989.

The Formation of Flare Loops by Magnetic Reconnection and Chromospheric Ablation, T.G. Forbes, J.M. Malherbe, and E.R. Priest, *Solar Phys.*, *120*, 285-307, 1989

Magnetic Field Evolution During Prominence Eruptions and Two-Ribbon Flares, E.R. Priest and T.G. Forbes, *Solar Phys.*, *126*, 319, 1990.

Numerical Simulation of a Catastrophe Model for Coronal Mass Ejections, T.G. Forbes, *J. Geophys. Res.*, *95*, 11919-11931, 1990.

Flare Loops and Giant Arches, G.M. Simnett and T.G. Forbes, in *Dynamics of Solar Flares*, proceedings of the Flare 22 Workshop held in Chantilly, France October 16-19, 1990 (eds. B. Schmieder and E.R. Priest), L'Observatoire de Paris Press, Paris, p. 121, 1991.

Catastrophe Mechanism for Coronal Mass Ejections, T.G. Forbes and P.A. Isenberg, *Astrophys. J.*, *373*, 294-307, 1991.

Numerical Simulation of Magnetic Reconnection and Radiative Cooling in Line-Tied Current Sheets, T.G. Forbes, and J.M. Malherbe, *Solar Phys.*, *135*, 361-391, 1991.

Magnetic Reconnection in Solar Flares, T.G. Forbes, *Geophysical and Astrophysical Fluid Dynamics*, *62*, 15-36, 1991.

The Structure of Radiative Slow-Mode Shocks, P. Xu and T.G. Forbes, *Solar Phys.*, *139*, 315-342, 1992.

Does Fast Magnetic Reconnection Exist?, E.R. Priest and T.G. Forbes, *J. Geophys. Res., 97*, 16757-16772, 1992.

Catastrophic Evolution of a Force-Free Flux Rope: A Model for Eruptive Flares, P. Isenberg, T.G. Forbes, and P. Démoulin, *Astrophys. J., 417*, 368-386, 1993.

On Current Sheet Approximations in Models of Eruptive Flares, T.N. Bungey, and T.G. Forbes, *Solar Phys., 149*, 205-208, 1994.

On the Maximum Energy Release in Flux-Rope Models of Eruptive Flares, T.G. Forbes, E.R. Priest, and P.A. Isenberg, *Solar Phys., 150*, 245-266, 1994.

Photospheric Magnetic Field Evolution and Eruptive Flares, T.G. Forbes and E.R. Priest, *Astrophys. J., 446*, 377-389, 1995.

Models for the Motions of Flare Loops and Ribbons, J. Lin, T.G. Forbes, E.R. Priest, and T.N. Bungey, *Solar Phys., 159*, 275-299, 1995.

Magnetic Reconnection and Field Line Shrinkage in Solar Flares, T.G. Forbes and L.W. Acton, *Astrophys. J., 459*, 330-341 1996.

Reconnection Dynamics in Cusp-Shaped Flare Loops, T.G. Forbes, in *High Energy Solar Physics* (eds. R. Ramaty, N. Mandzhavidze, and X.-M. Hua), AIP Press, New York, pp. 275-284, 1996.

Arcade Models of Flares, T.G. Forbes, in *Magnetodynamic Phenomena in the Solar Atmosphere–Prototypes of Stellar Magnetic Activity, Proceedings of IAU Colloq. 153*, (eds. Y. Uchida, T. Kosugi, and H.S. Hudson), Kluwer, Dordrecht, 287-294, 1996.

Reconnection Theory for Flares, T.G. Forbes, in *Observations of Magnetic Reconnection in the Solar Atmosphere* (eds. R.D. Bentley and J.T. Mariska), *Astron. Soc. Pac. Conf. Series*, ASP, Provo, Utah, pp. 259-267, 1996.

The Effect of Curvature on Flux-Rope Models of Coronal Mass Ejections, J. Lin, T.G. Forbes, P.A. Isenberg, and P. Démoulin, *Astrophys. J., 505*, 1006-1019, 1998.

Solar and Stellar Flares, T.G. Forbes, *Phil. Trans. Royal Soc. A*, in press, 1999.

Magnetic Reconnection – MHD Theory and Applications, E.R. Priest and T.G. Forbes, Cambridge University Press, in press, 1999.

The Effects of Reconnection on the CME Process, J. Lin and T.G. Forbes, *J. Geophys. Res.*, submitted, 1999.

1. Appendices

1.2 Statement Of Work;

ATTACHMENT J-1

PHASE B
STATEMENT OF WORK

FOR THE

SOLAR-B
X-RAY TELESCOPE

July 21, 1999

SOLAR-B
X-RAY TELESCOPE
STATEMENT OF WORK
TABLE OF CONTENTS

SECT.	SUBJECT	Page No.
1.0	Introduction	J-1-4
2.0	Scope and Major Milestones	J-1-5
2.1	Scope	J-1-5
2.2	Solar-B Major Milestones	J-1-5
3.0	Contractor Tasks	J-1-5
3.1	Management	J-1-5
3.1.1	Project Management	J-1-6
3.1.2	Project Planning and Control	J-1-6
3.1.3	Procurement Management	J-1-8
3.1.4	Configuration Management	J-1-8
3.1.5	Science Support	J-1-8
3.2	X-ray Telescope Flight System	J-1-9
3.3	Ground Support Equipment and Proto Models	J-1-9
3.3.1	Electrical Proto Model	J-1-10
3.3.2	Mechanical/Thermal Proto Model	J-1-10
3.3.3	Electrical Ground Support Equipment (EGSE)	J-1-10
3.3.4	Mechanical Ground Support Equipment (MGSE)	J-1-10
3.3.5	Mockups and Simulators	J-1-10
3.4	Systems Engineering and Integration	J-1-11
3.4.1	Systems Engineering	J-1-11
3.4.2	Instrument Testing and Verification	J-1-11
3.4.3	Observatory Level Integration and Test	J-1-12

TABLE OF CONTENTS

(Continued)

3.5	Operations	J-1-12
3.5.1	Mission Operations Definition and Planning	J-1-12
3.5.2	Mission Operations Support	J-1-12
3.6	Product Assurance	J-1-12
4.0	General Requirements	J-1-13
4.1	Information Technology Security	J-1-13
4.2	Documentation	J-1-13
4.3	Technical Direction	J-1-13
5.0	Government Furnished Property	J-1-13
6.0	Deliverables	J-1-13

Solar-B X-ray Telescope
Phase B
Statement of Work (SOW)

1.0 Introduction

The X-ray Telescope (XRT) instrument has been selected for development by the Smithsonian Astrophysical Observatory as an experiment to be flown on the Japanese Solar-B satellite. The Solar-B Mission, which includes the Solar-B satellite, is a program of the Japanese Institute of Space and Astronautical Science (ISAS) with collaboration by the National Aeronautics and Space Administration (NASA) and the United Kingdom (UK) Particle Physics and Astronomy Research Council (PPARC). The Solar-B development is divided into five phases: Phase A - concept study and requirements definition; Phase B - hardware definition and preliminary design; Phase C/D - detailed design and development through launch plus 30 days; and Phase E - mission operations and data analysis. This Statement of Work (SOW) is for the Phase B hardware definition and preliminary design effort. The subsequent Phase C/D and Phase E efforts will be implemented under separate contract instruments.

The overall science objectives and requirements for the Solar-B Mission and the X-ray Telescope instrument were defined in NASA Announcement of Opportunity (AO98-OSS-05), dated May 1, 1998. Smithsonian Astrophysical Observatory (SAO), with Dr. Leon Golub as Principal Investigator (PI), was selected in response to the competitive AO to further define, design, develop, test, and integrate the X-ray Telescope (XRT) instrument. In addition, the PI and his team of Co-Investigators (Co-I's), will conduct, in collaboration with the Solar-B International Partners, the Solar-B science mission.

The Phase A development effort was initiated under NASA contract NAS8-99099 and will conclude on October 31, 1999. Upon completion of the Phase A activities, the Phase B development effort will commence and is expected to be six (6) months in duration. The Phase C/D development phase will be initiated, pending further approvals by NASA, at the conclusion of Phase B.

NASA has approved the Solar-B collaborative effort as part of the Sun Earth Connection Theme within the Office of Space Science. Organizationally, Solar-B is part of the Solar Terrestrial Probes Program managed by Goddard Space Flight Center (GSFC). Project management responsibility for Solar-B has been delegated to the Marshall Space Flight Center (MSFC). NASA will provide minimal technical oversight into the XRT development activities. Smithsonian Astrophysical Observatory will provide project and resources management, including establishment of an overall schedule consistent with the program milestones stated in Section 2.2 and establishment of guidelines to assure adequate implementation of the essential management and technical processes for the X-ray Telescope effort. SAO is permitted maximum latitude in the experiment implementation in order to assure mission success.

2.0 Scope and Major Milestones

2.1 Scope

Smithsonian Astrophysical Observatory, henceforth referred to as the contractor, shall supply the necessary skills, services, materials, equipment, documentation, software, and facilities to perform the tasks in this SOW and The X-ray Telescope for Solar-B proposal number P4446-7-98 dated July 31, 1998.

2.2 Solar-B Major Milestones

The contractor shall develop an overall X-ray Telescope schedule that supports the following milestones:

Preliminary Design Review	March 2000
Phase C/D	May 1, 2000 – September 2004
Electrical Proto Model Delivery	December 31, 2000
Mechanical/Thermal Proto Model Delivery	April 1, 2001
Critical Design Review	March 2001
Flight Model Delivery	December 1, 2002
Launch	August 2004

3.0 Contractor Tasks

The contractor shall provide the labor, material, and services necessary to accomplish the effort described in the following paragraphs.

3.1 Management

The contractor shall provide an overall management activity which achieves cost-effective planning, organizing, staffing, budgeting, directing, controlling, procuring, and reporting of technical and programmatic achievements, schedules, and time relationships to attain project objectives. As part of this management activity, the contractor shall continually evaluate, monitor, and take action to minimize the overall technical, cost, and schedule risk to the project.

3.1.1 Project Management

The contractor shall define, establish, and implement a management system to monitor, report, and manage the X-ray Telescope cost, schedule, and technical aspects of the project. The management system shall be described and documented in accordance with DRD 873MA-001.

The contractor shall develop a continuous risk management process that will identify risks to the success of the XRT instrument from the standpoint of cost, schedule, and technical capability. The process will include the mechanisms of risk analysis, planning, tracking, and control. The Risk Management Plan shall be prepared in accordance with DRD 873MA-005.

3.1.2 Project Planning and Control

The contractor shall define and document a Work Breakdown Structure (WBS) at a level sufficient to efficiently manage the total Solar-B X-ray Telescope Phase B/C/D effort. The WBS shall be traceable to the deliverable end item level delineating all hardware, services, materials, subcontracts, and other tasks necessary to define the project. The WBS shall be consistent with the Solar-B Project WBS (PWBS) and Contract Work Breakdown Structure (CWBS) documented in Attachment J-3. The WBS and dictionary shall be prepared in accordance with DRD 873MA-004.

The contractor shall establish, implement, maintain, and deliver the XRT master and detailed activity schedules that delineate all primary activities for the Solar-B XRT instrument and that supports the overall Solar-B Milestones (reference Section 2.2). Project schedules will be established for each level consistent with the WBS. Schedules shall be provided in accordance with DRD's 873MA-001 and 873MA-002. These schedules shall be prepared and maintained such that critical paths are readily visible, changes to planned implementation processes can be easily described, and schedule trends can be evaluated. Schedules shall integrate reference schedules from subcontractors and other supporting entities. The scheduling system will be part of the management system used by the contractor for internal management and shall be used for reporting to NASA.

The contractor shall establish plans and allocate resources based upon the work packages delineated in the Work Breakdown Structure (WBS). The plans shall address cost, schedule, and technical performance, and shall serve as the basis for evaluating overall contract performance, progress, and variances from the project baseline. Overall contract performance, progress, and variances from the project baselines shall be measured using performance measurement criteria (PMC) documented in accordance with the Project Management Plan (DRD 873MA-001). The PMC shall show the relationship between cost, work planned, work accomplished, and schedule. The contractor shall provide performance reports in accordance with DRD 873MA-001 and DRD 873MA-002. The contractor shall provide traceability from the baseline to the current status, as reported in the monthly performance reports, for the duration of the contract.

The contractor shall conduct budget studies and provide inputs to NASA's Program Operating Plans (POP's). Financial Management Reports shall be submitted in accordance with DRD 873MA-003.

The contractor shall conduct and/or support the following project reviews to determine and communicate the overall project progress.

a. Monthly Status Review – The Monthly Progress Report, prepared per DRD 873MA-002, will provide the basis for the Monthly Status Review. This review will be conducted either via teleconference or at the contractor's facility.
b. Non-Advocate Review (NAR) – The contractor shall support the Non-Advocate Review process. Support will entail providing documentation to support the scientific justification for the XRT and the Solar-B mission. The contractor should plan to support the final NAR meeting in Washington DC.
c. Independent Assessment (IA) – The contractor shall support the Independent Assessment process. This process will evaluate the project's cost, schedule, technical specifications, management processes, and status. Support will consist of providing documentation, submitting the key XRT managers to interviews from the Independent Assessment Committee (at the contractor's site), and support to the findings meeting at either Marshall Space Flight Center or Goddard Space Flight Center.
d. Confirmation Review (CR) – The contractor shall support the Confirmation Review. This review grants approval to proceed with the Solar-B project into the Phase C/D or Implementation Phase. Support will consist of attendance at the CR meeting in Washington DC and the timely closure of any actions resulting from the review.

In addition, the contractor shall provide for informal conferences, as needed, with the technical monitor or Project Manager and/or his designated representatives for the purpose of reviewing progress, issues, and technical and management problems. These conferences may be held by telephone or at the contractor's facility.

3.1.3 Procurement Management

The contractor shall establish and implement a procurement function that performs the required activities in compliance with applicable procurement regulation, policies and procedures. The procurement activities include, but are not limited to, timely initiation of procurements, selection of appropriate subcontracting or purchasing methods, preparation of procurement packages, coordination of Government approval or consent as required, and placement of orders. Competition in subcontracting shall be the preferred method of source selection.

Effective management and control shall be exercised over intradivisional work, subcontractors, and vendors. The contractor shall provide in-depth technical and business management of first tier procurements.

3.1.4 Configuration Management

The contractor shall establish, maintain, and implement a configuration management system that will provide configuration control and traceability. The configuration management system shall include the contractor's approach to specifying, documenting, controlling, and maintaining visibility of the hardware and software design. The system must be capable of providing the necessary documentation and data to define the final XRT hardware for acceptance by the Government. In addition, it must provide for the expedient submission, approval, and implementation of changes and modifications to the XRT specification (DRD 873CM-002) and Interface Control Document (DRD 873CM-004), and provide status reporting. All change proposals, revision notices, and deviations shall be comprehensive, accurate, and clearly traceable from requirements through implementation. The configuration management system shall be described and documented in the Configuration Management Plan per DRD 873CM-001. The system shall be described and documented to span the contractor activities starting with Phase B and extending through Phase C/D.

3.1.5 Science Support

The contractor shall continue the effort initiated in Phase A to establish a Public Outreach program consistent with the effort defined in the contractor proposal. In addition, Co-Investigator support shall be maintained at a level necessary to sustain cohesive scientific support for the Solar-B X-ray Telescope.

3.2 X-ray Telescope Flight System

The contractor shall continue the effort initiated in Phase A to define the XRT instrument. The contractor shall also conduct the preliminary design effort to support the overall design, development, test, and evaluation of the flight hardware, support equipment, engineering models, and software for the Solar-B X-ray Telescope.

Specifically, the contractor shall allocate the requirements to the appropriate subassembly and component level. Consistent with the requirement allocation, the contractor shall establish and control design concepts including materials, parts, and processes for each element. The contractor shall document and present the proposed concepts for evaluation during the Preliminary Design Review (PDR) process. The purpose of the PDR is to assure compliance with the overall requirements, review the element functional allocation, and its producibility. The contractor shall support the Preliminary Design Review (PDR) meeting to be conducted at the Marshall Space Flight Center. As a result of the PDR, the XRT Specification (DRD 873CM-002) and the Interface Control Document (DRD 873CM-004) will be baselined and subject to the formal configuration control requirements of the Configuration Management Plan (DRD 873CM-001). The documentation requirements for the Preliminary Design Review are delineated in DRD 873CM-003.

The contractor shall develop and document a Software Management Plan per DRD 873SW-001. The Software Management Plan will document the entire software development process including organizational responsibilities, requirements and interface definition, testing, validation, verification, configuration management, documentation, and software quality assurance.

The contractor shall conduct the necessary testing to evaluate the design features, operability, and useful life of the candidate mechanism design and other components. The contractor shall document the progress of this testing effort in the Preliminary Design Review Data Package per DRD 873CM-003.

3.3 Ground Support Equipment and Proto Models

The contractor shall initiate the design and development effort to support the engineering model testing in Japan in CY2001. In addition, the contractor shall initiate the design and development of required test and support equipment to support the XRT Phase C/D effort.

3.3.1 Electrical Proto Model

The contractor shall initiate efforts to design, develop, fabricate, assemble, and test an Electrical Proto Model to validate the XRT electrical interfaces as defined in the XRT Specification (DRD 873CM-002) and the Interface Control Document (DRD 873CM-004). The status of this effort and the specifics of the design shall be documented in the Preliminary Design Review Package (DRD 873CM-003) and presented at the PDR meeting.

3.3.2 Mechanical/Thermal Proto Model

The contractor shall initiate efforts to design, develop, fabricate, assemble, and test a Mechanical/Thermal Proto Model to validate the XRT mechanical and thermal interfaces as defined in the XRT Specification (DRD 873CM-002) and the Interface Control Document (DRD 873CM-004). The status of this effort and the specifics of the design shall be documented in the Preliminary Design Review Package (DRD 873CM-003) and presented at the PDR meeting.

3.3.3 Electrical Ground Support Equipment (EGSE)

The contractor shall initiate efforts to design, develop, fabricate, assemble, and test all EGSE for the XRT flight instrument development effort. The status of this effort shall be documented in the Preliminary Design Review Package (DRD 873CM-003) and presented at the PDR meeting.

3.3.4 Mechanical Ground Support Equipment (MGSE)

The contractor shall initiate efforts to design, develop, fabricate, assemble, and test all MGSE for the XRT flight instrument development effort. The status of this effort shall be documented in the Preliminary Design Review Package (DRD 873CM-003) and presented at the PDR meeting.

3.3.5 Mockups and Simulators

The contractor shall initiate efforts to design, develop, fabricate, assemble, and test all Mockups and Simulators for the XRT flight instrument development effort. The status of this effort shall be documented in the Preliminary Design Review Package (DRD 873CM-003) and presented at the PDR meeting.

3.4 Systems Engineering and Integration

The contractor shall perform all necessary system engineering functions to ensure that the X-ray Telescope meets the requirements of the XRT Specification (DRD 873CM-002).

3.4.1 Systems Engineering

The contractor shall continue the efforts initiated during Phase A to further define the instrument requirements and interface definition. In addition, the contractor shall support Technical Interchange Meetings with the Solar-B Government and International Partners as required. The scope of the meetings will be to address issues with the Solar-B mission definition, spacecraft and instrument design, and interface definition. The meetings will be at various locations including the contractor's facility and in Japan. The contractor should plan to support one meeting per month. The instrument requirements shall be documented in the XRT Specification (DRD 873CM-002) and the interface requirements in the Interface Control Document (DRD 873CM-004).

The contractor shall perform systems analysis to support the overall XRT design, development, test, and integration activities. Trade studies and analyses shall be conducted to evaluate the design sensitivities to the various manufacturing, assembly, and environmental factors. The contractor shall establish and maintain a systems error budget that reflects the error allocation given for each of the various error sources. The error budget will be documented in accordance with DRD 873SE-001.

The contractor shall derive contamination control requirements consistent with the mission scientific objectives. These requirements shall be documented in the XRT Specification DRD 873CM-002. The contractor shall prepare and document a contamination control program to ensure the contamination requirements can be met. The program will entail material selection criteria, material testing requirements, fabrication and assembly considerations, and assembly cleanliness certification. The Contamination Control and Implementation Plan shall be documented in accordance with DRD 873MP-001.

3.4.2 Instrument Testing and Verification

The contractor shall develop and document the XRT verification approach, planned overall testing and verification activities, and organizations necessary to execute the project's verification program to show compliance with all XRT requirements. The Verification Plan shall be prepared per DRD 873VR-001.

3.4.3 Observatory Level Integration and Test

The contractor shall support the Observatory Level integration and test planning activities with the Solar-B International Partners. This effort includes planning activities associated with launch site integration and support. Documentation of the Observatory Level integration and test activities shall be as specified in the Verification Plan (DRD 873VR-001).

3.5 Operations

The contractor shall provide support to all mission operations planning, definition, and operations support activities with the Government and the Solar-B International Partners.

3.5.1 Mission Operations Definition and Planning

The contractor shall provide support to all mission operations planning and definition efforts with the Government and the Solar-B International Partners. This effort includes defining overall mission objectives, reference timelines, launch and orbit transfer operations planning, and orbital checkout operations definition.

3.5.2 Mission Operations Support

The contractor shall support the activities to define the mission operation support requirements. This effort includes planning and defining hardware, software, training, and personnel requirements to support the Mission Operations and Data Analysis operations.

3.6 Product Assurance

The contractor shall establish, implement, and maintain a product assurance program that will assure that the quality, safety, and reliability requirements of the project are met. The plans for the quality, safety, and reliability efforts shall be documented in the Product Assurance Plan per DRD 873QE-001.

4.0 General Requirements

4.1 Information Technology Security

The contractor will incorporate appropriate safeguards to ensure the availability, integrity, and confidentiality of information technology resources utilized in support of this contract. Safeguards will be commensurate with the sensitivity or criticality of the resources and will be sufficient to minimize the risk to NASA's mission and reputation.

4.2 Documentation

All presentations and documentation under this contract shall be prepared in English. The contractor shall use electronic mail to transfer preliminary data and meeting notes. The contractor shall publish meeting minutes by electronic mail to a set list of Solar-B participants coordinated by the Contracting Officer's Technical Representative (COTR) and to all parties represented at Solar-B meetings. In general, project documentation should be produced in a Microsoft® Office compatible format for ease of dissemination.

4.3 Technical Direction

The contractor shall keep the technical monitor informed of technical interchanges with the International Partners, document any technical or programmatic requirements, and copy the technical monitor on the transmittal letters for written data transfers. Direction from the International Partners that impacts the Phase B contract cost or schedule must be approved by the Contracting Officer prior to acceptance by the contractor. Direction that increases the X-ray Telescope instrument project run-out cost must be approved by the Solar-B Project Manager prior to acceptance.

5.0 Government Furnished Property

There is no Government Furnished Property provided for the Phase B effort.

6.0 Deliverables

No hardware will be delivered under this contract. The contractor shall deliver the documentation defined in Attachment J-2, Data Procurement Document (DPD 873).

ATTACHMENT J-1

Phase C/D
STATEMENT OF WORK

FOR THE

SOLAR-B
X-RAY TELESCOPE

September 15, 1999

SOLAR-B
X-RAY TELESCOPE
STATEMENT OF WORK
TABLE OF CONTENTS

SECT.	SUBJECT	Page No.
1.0	Introduction	J-1-4
2.0	Scope and Major Milestones	J-1-5
2.1	Scope	J-1-5
2.2	Solar-B Major Milestones	J-1-5
3.0	Contractor Tasks	J-1-5
3.1	Management	J-1-5
3.1.1	Project Management	J-1-6
3.1.2	Project Planning and Control	J-1-6
3.1.3	Procurement Management	J-1-8
3.1.4	Configuration Management	J-1-8
3.1.5	Science Support	J-1-8
3.2	X-ray Telescope Flight System	J-1-9
3.3	Ground Support Equipment and Proto Models	J-1-9
3.3.1	Electrical Proto Model	J-1-10
3.3.2	Mechanical/Thermal Proto Model	J-1-10
3.3.3	Electrical Ground Support Equipment (EGSE)	J-1-10
3.3.4	Mechanical Ground Support Equipment (MGSE)	J-1-10
3.3.5	Mockups and Simulators	J-1-10

TABLE OF CONTENTS

(Continued)

3.4	Systems Engineering and Integration	J-1-11
3.4.1	Systems Engineering	J-1-11
3.4.2	Instrument Testing and Verification	J-1-11
3.4.3	Observatory Level Integration and Test	J-1-12
3.5	Operations	J-1-12
3.5.1	Mission Operations Definition and Planning	J-1-12
3.5.2	Mission Operations Support	J-1-12
3.6	Product Assurance	J-1-12
4.0	General Requirements	J-1-13
4.1	Information Technology Security	J-1-13
4.2	Documentation	J-1-13
4.3	Technical Direction	J-1-13
5.0	Government Furnished Property	J-1-13
6.0	Deliverables	J-1-13

Solar-B X-ray Telescope
Phase B
Statement of Work (SOW)

1.0 Introduction

The X-ray Telescope (XRT) instrument has been selected for development by the Smithsonian Astrophysical Observatory as an experiment to be flown on the Japanese Solar-B satellite. The Solar-B Mission, which includes the Solar-B satellite, is a program of the Japanese Institute of Space and Astronautical Science (ISAS) with collaboration by the National Aeronautics and Space Administration (NASA) and the United Kingdom (UK) Particle Physics and Astronomy Research Council (PPARC). The Solar-B development is divided into five phases: Phase A - concept study and requirements definition; Phase B - hardware definition and preliminary design; Phase C/D - detailed design and development through launch plus 30 days; and Phase E - mission operations and data analysis. This Statement of Work (SOW) is for the Phase B hardware definition and preliminary design effort. The subsequent Phase C/D and Phase E efforts will be implemented under separate contract instruments.

The overall science objectives and requirements for the Solar-B Mission and the X-ray Telescope instrument were defined in NASA Announcement of Opportunity (AO98-OSS-05), dated May 1, 1998. Smithsonian Astrophysical Observatory (SAO), with Dr. Leon Golub as Principal Investigator (PI), was selected in response to the competitive AO to further define, design, develop, test, and integrate the X-ray Telescope (XRT) instrument. In addition, the PI and his team of Co-Investigators (Co-I's), will conduct, in collaboration with the Solar-B International Partners, the Solar-B science mission.

The Phase A development effort was initiated under NASA contract NAS8-99099 and will conclude on October 31, 1999. Upon completion of the Phase A activities, the Phase B development effort will commence and is expected to be six (6) months in duration. The Phase C/D development phase will be initiated, pending further approvals by NASA, at the conclusion of Phase B.

NASA has approved the Solar-B collaborative effort as part of the Sun Earth Connection Theme within the Office of Space Science. Organizationally, Solar-B is part of the Solar Terrestrial Probes Program managed by Goddard Space Flight Center (GSFC). Project management responsibility for Solar-B has been delegated to the Marshall Space Flight Center (MSFC). NASA will provide minimal technical oversight into the XRT development activities. Smithsonian Astrophysical Observatory will provide project and resources management, including establishment of an overall schedule consistent with the program milestones stated in Section 2.2 and establishment of guidelines to assure adequate implementation of the essential management and technical processes for the X-ray Telescope effort. SAO is permitted maximum latitude in the experiment implementation in order to assure mission success.

2.0 Scope and Major Milestones

2.1 Scope

Smithsonian Astrophysical Observatory, henceforth referred to as the contractor, shall supply the necessary skills, services, materials, equipment, documentation, software, and facilities to perform the tasks in this SOW and The X-ray Telescope for Solar-B proposal number P4446-7-98 dated July 31, 1998.

2.2 Solar-B Major Milestones

The contractor shall develop an overall X-ray Telescope schedule that supports the following milestones:

Preliminary Design Review	March 2000
Phase C/D	May 1, 2000 – September 2004
Electrical Proto Model Delivery	December 31, 2000
Mechanical/Thermal Proto Model Delivery	April 1, 2001
Critical Design Review	March 2001
Flight Model Delivery	December 1, 2002
Launch	August 2004

3.0 Contractor Tasks

The contractor shall provide the labor, material, and services necessary to accomplish the effort described in the following paragraphs.

3.1 Management

The contractor shall provide an overall management activity which achieves cost-effective planning, organizing, staffing, budgeting, directing, controlling, procuring, and reporting of technical and programmatic achievements, schedules, and time relationships to attain project objectives. As part of this management activity, the contractor shall continually evaluate, monitor, and take action to minimize the overall technical, cost, and schedule risk to the project.

3.1.1 Project Management

The contractor shall further define as needed and implement the management system to monitor, report, and manage the X-ray Telescope cost, schedule, and technical aspects of the project established in Phase B, in accordance with DRD 873MA-001.

The contractor shall implement the continuous risk management process, including the mechanisms of risk analysis, planning, tracking, and control, prepared during Phase B in accordance with DRD 873MA-005.

3.1.2 Project Planning and Control

The contractor shall maintain the Work Breakdown Structure (WBS) prepared during Phase B at a level sufficient to efficiently manage the total Solar-B X-ray Telescope Phase C/D effort. The WBS shall be traceable to the deliverable end item level delineating all hardware, services, materials, subcontracts, and other tasks necessary to define the project. The WBS shall remain consistent with the Solar-B Project WBS (PWBS) and Contract Work Breakdown Structure (CWBS) documented in Attachment J-3. The WBS and dictionary shall remain in accordance with DRD 873MA-004.

The contractor shall maintain, and deliver up dates to, the XRT master and detailed activity schedules that delineate all primary activities for the Solar-B XRT instrument and that supports the overall Solar-B Milestones (reference Section 2.2). Project schedules will be maintained for each level consistent with the WBS. Schedules shall be provided in accordance with DRD's 873MA-001 and 873MA-002. These schedules shall be maintained such that critical paths are readily visible, changes to planned implementation processes can be easily described, and schedule trends can be evaluated. Schedules shall integrate reference schedules from subcontractors and other supporting entities. The scheduling system will be part of the management system used by the contractor for internal management and shall be used for reporting to NASA.

The contractor shall maintain plans and allocate resources based upon the work packages delineated in the Work Breakdown Structure (WBS). The plans shall address cost, schedule, and technical performance, and shall serve as the basis for evaluating overall contract performance, progress, and variances from the project baseline. Overall contract performance, progress, and variances from the project baselines shall be measured using performance measurement criteria (PMC) documented in accordance with the Project Management Plan (DRD 873MA-001). The PMC shall show the relationship between cost, work planned, work accomplished, and schedule. The contractor shall provide performance reports in accordance with DRD 873MA-001 and DRD 873MA-002. The contractor shall provide traceability from the baseline to the current status, as reported in the monthly performance reports, for the duration of the contract.

The contractor shall conduct budget studies and provide inputs to NASA's Program Operating Plans (POP's). Financial Management Reports shall be submitted in accordance with DRD 873MA-003.

The contractor shall conduct and/or support the following project reviews to determine and communicate the overall project progress.

a. Monthly Status Review – The Monthly Progress Report, prepared per DRD 873MA-002, will provide the basis for the Monthly Status Review. This review will be conducted either via teleconference or at the contractor's facility.
b. Critical Design Review: The support the critical design review. Support will entail preparing a detailed set of documentation establishing the status of the XRT design and implementation. The documentation will be prepared in accordance with DRD 873XX-XXX.

In addition, the contractor shall provide for informal conferences, as needed, with the technical monitor or Project Manager and/or his designated representatives for the purpose of reviewing progress, issues, and technical and management problems. These conferences may be held by telephone or at the contractor's facility.

3.1.3 Procurement Management

The contractor shall implement a procurement function that performs the required activities in compliance with applicable procurement regulation, policies and procedures. The procurement activities include, but are not limited to, timely initiation of procurements, selection of appropriate subcontracting or purchasing methods, preparation of procurement packages, coordination of Government approval or consent as required, and placement of orders. Competition in subcontracting shall be the preferred method of source selection.

Effective management and control shall be exercised over intradivisional work, subcontractors, and vendors. The contractor shall provide in-depth technical and business management of first tier procurements.

3.1.4 Configuration Management

The contractor shall implement, and maintain a configuration management system that will provide configuration control and traceability. The configuration management system shall include the contractor's approach to specifying, documenting, controlling, and maintaining visibility of the hardware and software design. The system must be capable of providing the necessary documentation and data to define the final XRT hardware for acceptance by the Government. In addition, it must provide for the expedient submission, approval, and implementation of changes and modifications to the XRT specification (DRD 873CM-002) and Interface Control Document (DRD 873CM-004), and provide status reporting. All change proposals, revision notices, and deviations shall be comprehensive, accurate, and clearly traceable from requirements through implementation. The configuration management system shall be described and documented in the Configuration Management Plan per DRD 873CM-001. The system shall be described and documented to span the contractor activities starting with Phase B and extending through Phase C/D.

3.1.5 Science Support

The contractor shall continue the effort initiated in Phase A to establish a Public Outreach program consistent with the effort defined in the contractor proposal. In addition, Co-Investigator support shall be maintained at a level necessary to sustain cohesive scientific support for the Solar-B X-ray Telescope.

3.2 X-ray Telescope Flight System

The contractor shall continue the effort initiated in Phase A and B to define the XRT instrument. The contractor shall also conduct the design effort to specify the overall final design, development, test, and evaluation of the flight hardware, support equipment, engineering models, and software for the Solar-B X-ray Telescope. After the Critical Design Review, the contractor will complete the design, fabrication, and test the flight system.

Consistent with the requirement allocations made in Phase A and B, the contractor shall establish and control design details including materials, parts, and processes for each element. The contractor shall document and present the proposed detailed design for evaluation during the Critical Design Review (CDR) process. The purpose of the CDR is to assure compliance with the overall requirements, review the element functional allocation, and its readiness for production. The contractor shall support the Critical Design Review (CDR) meeting to be conducted at the Marshall Space Flight Center. (As a result of the CDR, the XRT Specification (DRD 873CM-002) and the Interface Control Document (DRD 873CM-004) will be baselined and subject to the formal configuration control requirements of the Configuration Management Plan (DRD 873CM-001)<Determine which documents are affected at this point>). The documentation requirements for the Critical Design Review are delineated in DRD 873CM-00X.

The contractor shall maintain the Software Management Plan per DRD 873SW-001. The Software Management Plan shall document the entire software development process including organizational responsibilities, requirements and interface definition, testing, validation, verification, configuration management, documentation, and software quality assurance.

The contractor shall conclude the necessary testing to evaluate the design features, operability, and useful life of the candidate mechanism design and other components. The contractor shall document the progress of this testing effort in the Critical Design Review Data Package per DRD 873CM-00X.

3.3 Ground Support Equipment and Proto Models

The contractor shall complete the design and development effort to support the engineering model testing in Japan in CY2001. In addition, the contractor shall complete the design and development of required test and support equipment to support the remainder of the XRT Phase C/D effort. The contractor will complete, and test the protomodel, mechanical test model.

3.3.1 Electrical Proto Model

The contractor shall complete efforts to design, develop, fabricate, assemble, and test an Electrical Proto Model to validate the XRT electrical interfaces as defined in the XRT Specification (DRD 873CM-002) and the Interface Control Document (DRD 873CM-004). The status of this effort and the specifics of the design shall be documented in the Critical Design Review Package (DRD 873CM-00X) and presented at the CDR meeting.

3.3.2 Mechanical/Thermal Proto Model

The contractor shall complete efforts to design, develop, fabricate, assemble, and test a Mechanical/Thermal Proto Model to validate the XRT mechanical and thermal interfaces as defined in the XRT Specification (DRD 873CM-002) and the Interface Control Document (DRD 873CM-004). The results of this effort and the specifics of the design shall be documented in the Critical Design Review Package (DRD 873CM-00X) and presented at the CDR meeting.

3.3.3 Electrical Ground Support Equipment (EGSE)

The contractor shall complete efforts to design, develop, fabricate, assemble, and test all EGSE for the XRT flight instrument development effort. The results of this effort shall be documented in the Critical Design Review Package (DRD 873CM-003) and presented at the CDR meeting.

3.3.4 Mechanical Ground Support Equipment (MGSE)

The contractor shall complete efforts to design, develop, fabricate, assemble, and test all MGSE for the XRT flight instrument development effort. The results of this effort shall be documented in the Critical Design Review Package (DRD 873CM-00X) and presented at the CDR meeting.

3.3.5 Mockups and Simulators

The contractor shall continue efforts to design, develop, fabricate, assemble, and test all Mockups and Simulators for the XRT flight instrument development effort. The status of this effort shall be documented in the Critical Design Review Package (DRD 873CM-00X) and presented at the CDR meeting.

3.4 Systems Engineering and Integration

The contractor shall perform all necessary system engineering functions to ensure that the X-ray Telescope meets the requirements of the XRT Specification (DRD 873CM-002).

3.4.1 Systems Engineering

The contractor shall continue the efforts initiated during Phase A and B to finalize the instrument requirements and interface definition. In addition, the contractor shall support Technical Interchange Meetings with the Solar-B Government and International Partners as required. The scope of the meetings will be to address issues with the Solar-B mission definition, spacecraft and instrument design, and interface definition. The meetings will be at various locations including the contractor's facility and in Japan. The contractor should plan to support one meeting per month. The instrument requirements shall be documented in the XRT Specification (DRD 873CM-002) and the interface requirements in the Interface Control Document (DRD 873CM-004).

The contractor shall perform systems analysis to support the overall XRT design, development, test, and integration activities. Trade studies and analyses shall be conducted to evaluate the design sensitivities to the various manufacturing, assembly, and environmental factors. The contractor shall maintain a systems error budget that reflects the error allocation given for each of the various error sources. The error budget shall be documented in accordance with DRD 873SE-001.

The contractor shall implement contamination control requirements as documented in the XRT Specification DRD 873CM-002. The contractor shall implement the contamination control program to ensure the contamination requirements are met. The program shall entail material selection criteria, material testing requirements, fabrication and assembly considerations, and assembly cleanliness certification. The Contamination Control and Implementation Plan shall be documented in accordance with DRD 873MP-001.

3.4.2 Instrument Testing and Verification

The contractor shall implement the XRT verification approach, and conduct the overall testing and verification activities necessary to execute the project's verification program to show compliance with all XRT requirements.

3.4.3 Observatory Level Integration and Test

The contractor shall support the Observatory Level integration and test planning activities with the Solar-B International Partners. This effort includes planning activities associated with launch site integration and support. Documentation of the Observatory Level integration and test activities shall be as specified in the Verification Plan (DRD 873VR-001).

3.5 Operations

The contractor shall provide support to all mission operations planning, definition, and operations support activities with the Government and the Solar-B International Partners.

3.5.1 Mission Operations Definition and Planning

The contractor shall provide support to all mission operations planning and definition efforts with the Government and the Solar-B International Partners. This effort includes defining overall mission objectives, reference timelines, launch and orbit transfer operations planning, and orbital checkout operations definition.

3.5.2 Mission Operations Support

The contractor shall support the activities to define the mission operation support requirements. This effort includes planning and defining hardware, software, training, and personnel requirements to support the Mission Operations and Data Analysis operations.

3.6 Product Assurance

The contractor shall establish, implement, and maintain a product assurance program that will assure that the quality, safety, and reliability requirements of the project are met. The plans for the quality, safety, and reliability efforts shall be documented in the Product Assurance Plan per DRD 873QE-001.

4.0 General Requirements

4.1 Information Technology Security

The contractor will incorporate appropriate safeguards to ensure the availability, integrity, and confidentiality of information technology resources utilized in support of this contract. Safeguards will be commensurate with the sensitivity or criticality of the resources and will be sufficient to minimize the risk to NASA's mission and reputation.

4.2 Documentation

All presentations and documentation under this contract shall be prepared in English. The contractor shall use electronic mail to transfer preliminary data and meeting notes. The contractor shall publish meeting minutes by electronic mail to a set list of Solar-B participants coordinated by the Contracting Officer's Technical Representative (COTR) and to all parties represented at Solar-B meetings. In general, project documentation should be produced in a Microsoft® Office compatible format for ease of dissemination.

4.3 Technical Direction

The contractor shall keep the technical monitor informed of technical interchanges with the International Partners, document any technical or programmatic requirements, and copy the technical monitor on the transmittal letters for written data transfers. Direction from the International Partners that impacts the Phase B contract cost or schedule must be approved by the Contracting Officer prior to acceptance by the contractor. Direction that increases the X-ray Telescope instrument project run-out cost must be approved by the Solar-B Project Manager prior to acceptance.

5.0 Government Furnished Property

<There is no Government Furnished Property provided for the Phase B effort.>
<Exact requirements will have to wait until Jay gets back>

6.0 Deliverables

During Phase C/D the following items are deliverable:

Item	Delivery Date
Protomodel	29 December 2000

Mechanical/thermal test model (MTM/TTM)	2 April 2001
Flight XRT for EIC/MIC	2 December 2002
Final Flight XRT	31 July 2003

The contractor shall deliver the documentation defined in Attachment J-2, Data Procurement Document (DPD 873).

Phase E SOW

1. SAO shall support XRT science planning and science observations both in Japan and locally.
2. SAO shall maintain and update software for science planning and operations as necessary.
3. SAO shall support mission operations and maintain a mission operations interface facility at SAO.
4. SAO will maintain and update relevant XRT instrument calibrations as necessary.
5. SAO will develop and implement a data archiving and distribution system.
6. SAO shall receive, process, and analyze data from the Solar-B mission.
7. SAO will prepare scientific results for publication in oral and written form, using commonly accepted scientific practices and procedures.
8. SAO will implement its Phase E Education and Outreach activities.
9. SAO shall prepare quarterly and annual narrative reports to NASA summarizing recent activities.
10. SAO shall prepare and submit to NASA monthly and quarterly 533 reports.

1. Appendices

1.3 SAO Relevant Experience

HRC

SAO designed, built, and now operates the High Resolution Camera (HRC) on the Chandra Observatory (AXAF). The successful instrument builds on 30 years of resident and institutional experience in the field of stellar x-ray astrophysics. The camera is based on a system of multichannel plates and operates in the imaging focal of the observatory.

TRACE

SAO, in collaboration with Lockheed Palo Alto Labs, produced the highly successful TRACE instrument. TRACE, stands for Transition Region And Coronal Explorer, was launched in sun synchronous orbit on April 1, 1998. It has photographed the sun's surface in the UV and extended UV continually from late April 1998 until now. The TRACE telescope design is different from the XRT optical system in that it is based on normal incident optics and utilizes multilayer coatings to achieve the desired reflectivity. However, there are many similarities between the two systems. First and foremost is the fact that they are both solar pointed instruments. Second, the spectrums are similar enough that our approaches to contamination control that we developed under TRACE will be applicable in to XRT.

SAO was responsible for 4 systems in the TRACE instrument, the mirrors, the primary mirror mount, the x-ray pre-filters, and the chamber in which the x-ray pre-filters were launched. The experience gave us valuable insight into the issues of mirror design and mounting, as well as issues that surround the handling and mounting of x-ray pre-filters.

SOHO UVCS

SAO oversaw the construction, and now operates the UVCS instrument on the SOHO satellite. The solar coronagraph operates in the ultraviolet recording the sun's corona out to 10 solar radii.

Spartan UVCS

SAO designed and built the Spartan UVCS. It has flown several times in the on the Spartan free flying platform. All mission have been very successful.

1 Appendices

1.4 Reference List

Acton, L.W., Tsuneta, S., Ogawara, Y., *et al.* 1992. *Science* 258, 618
Amari T., Luciani J.F., Aly J.J., Tagger M. 1996. *Astrophys. J.* 446, L39--L42
Amari T., Aly J.J., Luciani J.F., Boulmezaoud T., Mikić Z 1997. *Solar Phys.* 174, 129-149
Antiochos, S.K. & Sturrock, P.A.,1982, *ApJ*, 254, 343.
Berger, M.A., and Field, G.B.: 1984, *J. Fluid Mech.*, 147, 133
Berger, T.E. de Pontiue, B., Schrijver, C.J. & Title, A..M. 1999 *ApJ.*, 519 L97
Brosius, J.W., Davila, J.M., Thomas, R.J., & Thompson, W.T. 1994. *ApJ* 425, 343
Cane, H.V.: 1984, *Astron. Astrophys.*, 140, 205
Canfield, R.C., & Pevtsov, A.A. 1998, in Proc. NSO Workshop on Synoptic Solar Physics, eds. K.S. Balasubramaniam, J.W. Harvey & D. Rabin, ASP Conf. Series
Cargill, P.J. 1994, *ApJ*, 422, 381
Cargill, P.J., Mariska, J.T., & Antiochos, S.K. 1995, *ApJ*, 439, 1034
Cargill, P.J., & Klimchuk, J.A. 1997, *ApJ*, 478, 799
Carmichael, H. 1964, in *The Physics of Solar Flares*, Hess, W.N. (ed.) NASA SP-50, p. 451. Cheng, C.-C. 1983, *ApJ*, 265, 1090.
Cliver, E., and Kahler, S. 1991, *ApJ*, 366, L91.
Davila, J.M. 1994. *ApJ* 423, 871
Démoulin P., Bagalá L.G., Mandrini C.H., Hénoux J.C., Rovira M.G. 1997. *A & A* 325, 305
Démoulin P. & Priest, E.R., 1997, *Solar Physics*, 175, 123
Doschek, G.A., Boris, J.P., Cheng, C.-C., Mariska, J.T., & Oran, E.S. 1982, *ApJ*, 258, 373
Doschek, G.A., Cheng, C.C., Oran, E.S., Boris, J.P., and Mariska, J.T. 1983, *Ap J.*, 265, 1103.
Falconer, D.A., Moore, R.L., Porter, J.G., Gary, G.A., Shimizu, T. 1997, *ApJ*, 482, 519
Fisher, G.H., Canfield, R.C., and McClymont, A.N. 1985, *ApJ*, 289, 414
Forbes, T.G., and Malherbe, J.M.: 1991, *Solar Phys.*, 135, 361.
Gosling, J.T. 1997, in Solar Wind Eight, Winterhalter, D., J.T. Gosling, S.R. Habbal, W.S. Kurth and M. Neugebauer (eds.), AIP, NY.
Heyvaerts, J., & Priest, E.R. 1983. *A & A* 117, 220.
Hiei, E., and Hundhausen, A.J.: 1997, in New Perspectives on Solar Prominences, IAU Colloq. 167, Rust, D.M. and B. Schmieder (eds.), Astron. Soc. Pacific, San Francisco, p. in press.
Hirayama, T.: 1974, *Solar Phys.*, 34, 323.
Hollweg, J. V. 1987. *ApJ* 312, 880
Hudson, H., 1991, *Solar Phys.* 133, 357.
Hudson, H.S. & Webb, D., 1997, in Coronal Mass Ejections, eds. Crooker, Joselyn & Feynman, AGU, 27
Judge, P., Wikstol, O., and Hansteen, V. (1997) *BAAS SPD Meeting #29* #05.05
Kano, R., 1997, Ph.D. thesis, Univ. Tokyo

Kano, R. & Tsuneta, S. 1996 *PASJ* 48 535.
Kopp, R.A., and Pneuman, G.W.: 1976, *Solar Phys.*, 50, 85.
Kopp, R.A., & Polleto, G. 1993, *ApJ*, 418, 496
Lepping, R.P.: 1997, Trans. Amer. Geophys. Union, 78, S239
Lin, R.P., Schwartz, R.A., Kane, S.R., Pelling, R.M., & Hurley, K.C. 1984, *ApJ*, 283, 421
Low B.C. 1996. *Solar Phys.* 167, 217--265
Lu, E.T., & Hamilton, R.J. 1991, *ApJ*, 380, L89
Mandrini C.H., Démoulin P., Van Driel-Gesztelyi L., Schmieder B., Cauzzi G., Hofmann A. 1996. *Solar Phys.* 168, 115
Mariska, J.T. 1988, *ApJ*, 334, 489
Mc Clymont A.N., Jiao L., Mikic Z. 1997. *Solar Phys.* 174, 191
Nagai, F.: 1980, *Solar Phys.*, 68, 351
Parker, E. N. 1972. *ApJ* 174, 499
Parker, E. N. 1983. *ApJ* 264, 635
Parker, E. N. 1988. *ApJ* 330, 474
Pevtsov, A.A., Canfield, R.C., & Metcalf, T.R. 1995, *ApJ*, 440, L109
Pevtsov, A.A., Canfield, R.C., & McClymont, A.N. 1997, *ApJ*, 481, 973
Porter, J.G., & Klimchuk, J.A. 1995, *ApJ*, 454, 499
Porter, J.G., Moore, R.L., Reichman, E.J., Engvold, O., & Harvey, K.L. 1987, *ApJ*, 323, 380
Porter, J.G., Toomre, J., & Gebbie, K.B. 1984, *ApJ*, 283, 879
Priest, E.R. 1997. Proc. Fifth *SOHO* Workshop on ``The Corona and Solar Wind near Minimum Activity'' (eds. A. Wilson and O. Kjeldseth-Moe), ESA SP-404, p. 93-102
Priest E.R. and Démoulin P. 1995. J. *Geophys. Res.* 100, 23,443
Priest, E.R., Foley, C.R., Heyvaerts, J., Arber, T., Culhane, J.L. & Acton, L.W. 1997. *ApJ* (subm.)
Reames, D.V. 1990, *ApJ*, 358, L63
Rust, D.M.: 1983, *Space Sci. Rev.*, 34, 21.
Rust, D.M., & Kumar, A. 1996, *ApJ*, 464, L199
Schmieder, B., Forbes, T.G., Malherbe, J.M., and Machado, M.E.: 1987, *ApJ*, 317, 956
Schmieder B., Aulanier G., Démoulin P., van Driel-Gesztelyi L., Roudier T., Nitta N., Cauzzi G. 1997. *A & A* 325, 1213
Serio, S., Reale, F., Jakimiec, J., Sylwester, B., & Sylwester, J. 1991, *A & A*, 241, 197
Sheeley, N.R., Jr. and Golub, L. 1979. *Solar Phys.* 63, 119
Shimizu, T., & Tsuneta, S., 1997, *ApJ*, 486, 1045
Shimizu, T., & Tsuneta, S., Acton, L.W., Lemen, J.R., Ogawara, Y., & Uchida, Y. 1992, *PASJ*, 44, L147
Shimizu, T., & Tsuneta, S., Acton, L.W., Lemen, J.R., Ogawara, Y., & Uchida, Y. 1994, *ApJ*, 422, 906
Similon, P.L., & Sudan, R.N. 1989. *ApJ* 336, 442SolarB 1999a: Solar-B Japan/UAS?UK 1st Design Meting, 03/08/1999, SLB-M-E99002SolarB 1999b: Environmental Conditions for Soalr-B (draft), 03/1992SolarB 1999c: Fax from Taro Sakao to Leon Golub 03/29/1999Sterling, A.C., Mariska, J.T., Shibata, K., & Suematsu, Y. 1991, *ApJ*, 381, 313
Sturrock, P.A.: 1968, in Structure and Development of Solar Active Regions, Kiepenheuer, K. (ed.) IAU, Paris, p. 471

Appendicies

Sturrock, P.A., Dixon, W.W., Klimchuk, J.A., & Antiochos, S.K. 1990, *ApJ*, 356, L1
Suematsu, Y., Wang, H., & Zirin, H. 1995, *ApJ*, 450, 411
Tarbell, T.D., Bruner, M., Jurcevich, B., Lemen, J., Strong, K., Title, A., Wolfson, J., Golub, L., and Fisher, R. 1994. Proc. 3rd *SOHO* Workshop, ESA SP-373, Dec. 1994
Taylor, J.B.: 1986, *Revs. Modern Phys.*, 58, 741
Thompson, B.J., Plunkett, S.P., Gurman, J.B., Newmark, J.S., St. Cyr, O.C. & Michels, D.J., 1997, *Geophys. Res Letters*, in press.
van Ballegooijen, A. A. 1985. *ApJ* 298, 421.
van Ballegooijen, A. A. 1986. *ApJ* 311, 1001
Webb, D.F., and Cliver, E.W., 1995. J. Geophys. Res., 100, 5853
Wikstol, O., Judge, P.G., and Hansteen, V.H., 1997. *ApJ* 483, 972.
Wolter, H. 1952a. Ann. Physik 10, 94
Yokoyama, T. & Shibata, K., 1998. *ApJ* Lett., 494, L113
Yoshida, T., Tsuneta, S., Golub, L., Strong, K., & Ogawara, Y., 1995. Pub. Astr. Soc. Japan, 47, L15
Yoshida, T., & Tsuneta, S., 1996. *ApJ*, 459, 342
Zirker, J.B., & Cleveland, F.M., 1993a. *Solar Phys.*, 144, 341
Zirker, J.B., & Cleveland, F.M., 1993b. *Solar Phys.*, 145, 119
Zirker, J.B., Martin, S.F., Harvey, K., & Gaizauskas, V., 1997. *Solar Phys.*, 175, 27

Appendicies